

**MECHANICAL PROPERTIES AND DURABILITY  
OF QUATERNARY CEMENT CONCRETES**

BY

**MOHAMMED KHAJA MOINUDDIN**

A Thesis Presented to the  
DEANSHIP OF GRADUATE STUDIES

**KING FAHD UNIVERSITY OF PETROLEUM & MINERALS**

DHAHRAN, SAUDI ARABIA

In Partial Fulfillment of the  
Requirements for the Degree of

**MASTER OF SCIENCE**

In

**CIVIL ENGINEERING**

**May, 2012**

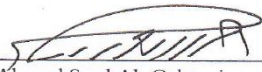
**KING FAHD UNIVERSITY OF PETROLEUM & MINERALS**

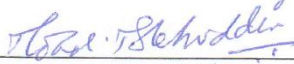
**DHAHRAN 31261, SAUDI ARABIA**


**DEANSHIP OF GRADUATE STUDIES**

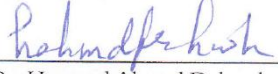
This thesis, written by **MOHAMMED KHAJA MOINUDDIN** under the supervision of his thesis advisors and approved by his thesis committee, has been presented to and accepted by the Dean of Graduate Studies, in partial fulfillment of the requirements for the degree of **MASTER OF SCIENCE IN CIVIL ENGINEERING**.


**Thesis Committee**


  
Dr. Ahmad Saad Al-Gahtani (Advisor)

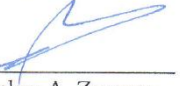
  
Dr. Mohammed Maslehuddin (Co-advisor)

  
Dr. Shamshad Ahmad (Member)

  
Dr. Hamoud Ahmad Dehwah (Member)

  
Dr. Salah U. Al-Dulaijan (Member)

  
16 JUL 2012 Dr. Nedal T. Ratrouf  
Departmental Chairman

  
Dr. Salam A. Zummo  
Dean of Graduate Studies

18/7/12  
Date





حَدَّثَنَا يَحْيَى بْنُ إِسْرَاهِيمَ، قَالَ حَدَّثَنَا ابْنُ عُثَيْمٍ، عَنْ عَبْدِ الْعَزِيزِ بْنِ صُهَيْبٍ،  
عَنْ أَنَسٍ، عَنِ النَّبِيِّ صَلَّى اللَّهُ عَلَيْهِ وَسَلَّمَ  
ح وَحَدَّثَنَا آدَمُ، قَالَ حَدَّثَنَا شُعْبَةُ، عَنْ قَتَادَةَ، عَنْ أَنَسٍ، قَالَ قَالَ النَّبِيُّ صَلَّى اللَّهُ عَلَيْهِ وَسَلَّمَ

" لَا يُؤْمِنُ أَحَدُكُمْ حَتَّى أَكُونَ أَحَبَّ إِلَيْهِ

مِنْ وَالِدِهِ وَوَلَدِهِ وَالنَّاسِ أَجْمَعِينَ "

*"None of you will have faith untill he loves me*

*more than his father, his children, and all mankind"*

(Source: Sahih al-Bukhari, Vol. 1: #15)

**DEDICATED**

**TO**

**HUMANS**

## ACKNOWLEDGEMENTS

All praise is suitable to ALLAH (subhana wa ta'la), the creator and the sustainer of the worlds, for bestowing me the era of science and technology, which is cherished to Prophet MUHAMMAD (sallallahu alaihi wasallam).

I would like to thank King Fahd University of Petroleum and Minerals for providing terrific research facilities and financial assistance for pursuing my MS.

It's a great privilege to have worked under the experienced, excellent and gentle supervision of my Thesis committee. I acknowledge sincere appreciation and thanks to my advisor Dr. Ahmad Saad Al-Gahtani for his handy leadership throughout this research. I am greatly indebted and very fortunate to have worked under the supervision of my co-advisor Dr. Mohammad Maslehuddin who bestowed his precious time for me. Their inspiration, unreserved cooperation and constant encouragement helped me in completing this research successfully. I am also grateful to my committee members Dr. Shamshad Ahmad, Dr. Hamoud Ahmad Dehwah, and Dr. Salah Uthman Al-Dulaijan for their support during this research. I would like to thank Dean, Chairman, Graduate Advisor, Graduate Coordinator and other faculty members for their concerns.

I owe ample credit to Mr. Mohammed Shameem for his technical guidance during the research work. I would also like to extend owes to Mr. Mohammed Ibrahim, Mr. Mohamed Salihu Barry, Mr. Mohammed Rizwan Ali, Mr. Mohammed Mukarram Khan, Mr. Syed Imran Ali, colleagues and society of KFUPM for their support.

My thanks are also due to Mr. Mohammed Shuwaikat, Mr. Aalimm Pasha and Mr. Hussein Khuwait, for helping me during laborious casting work.

Finally, I thank brother Ghufraan Ahmed who helped with his software's skills and with his precious time to bring this thesis in the present form.

**In all, throughout my life I will be totally indebted to the unmentioned and invisible hands of my parents for their incredible blending, concreting and reinforcement.**

## TABLE OF CONTENTS

TABLE OF CONTENTS .....	vi
LIST OF TABLES .....	viii
LIST OF FIGURES.....	ix
THESIS ABSTRACT .....	xii
CHAPTER 1: INTRODUCTION .....	1
1.1 Concrete Durability in the Arabian Gulf.....	1
1.2 Need for Research.....	6
1.3 Objective .....	9
CHAPTER 2: LITERATURE REVIEW .....	10
2.1 Multi-Component Cement .....	10
2.2 Early Work on Multi-Component Cements .....	13
2.3 Effect of Multi-Component Cement on Compressive Strength.....	20
2.4 Effect of Multi-Component Cements on Durability .....	22
CHAPTER 3: RESEARCH METHODOLOGY .....	27
3.1 Experimental Program .....	27
3.2 Materials.....	29
3.2.1 Cement .....	29
3.2.2 Coarse Aggregates.....	30
3.2.3 Fine Aggregates .....	30
3.2.4 Superplasticizer.....	30
3.2.5 Water .....	30
3.3 Waste Products .....	31
3.3.1 Bag House Dust (BHD).....	31
3.3.2 Cement Kiln Dust (CKD).....	32
3.3.3 Clay .....	33
3.3.4 Limestone Powder (LSP) .....	33

3.3.5	Natural Pozzolan (NP) .....	33
3.3.6	Pulverized Steel Slag (PSS).....	34
3.4	Supplementary Cementitious Materials (SCMs) or Mineral Admixtures .....	35
3.4.1	Fly Ash (FA) .....	35
3.4.2	Silica Fume (SF) .....	36
3.5	Concrete Mixture Design .....	36
3.6	Preparation and Curing of Concrete Specimens.....	39
3.7	Testing of Concrete Specimens .....	42
3.7.1	Compressive Strength.....	42
3.7.2	Drying Shrinkage .....	43
3.7.3	Rapid Chloride Permeability .....	44
3.7.4	Reinforcement Corrosion .....	46
3.7.5	Setting Time .....	52
3.7.6	Water Absorption .....	53
CHAPTER 4: RESULTS AND DISCUSSION .....		55
4.1	Compressive Strength .....	55
4.2	Chloride Permeability .....	67
4.3	Corrosion Potentials .....	78
4.4	Corrosion Current Density .....	89
4.5	Drying Shrinkage .....	101
4.6	Water Absorption .....	114
4.7	Setting Time .....	122
CHAPTER 5: CONCLUSIONS AND RECOMMENDATIONS.....		125
5.1	Conclusions .....	125
5.2	Recommendations .....	127
REFERENCES .....		128
<b>VITAE</b> .....		129

## LIST OF TABLES

Table 2-1 : Ternary and Quaternary Blends Used in Offshore Structures.....	25
Table 2-2 : Ternary and Quaternary Blends .....	26
Table 3-1: Chemical Composition of Cement.....	29
Table 3-2: Grading of coarse aggregates.....	30
Table 3-3: Chemical Composition of BHD. ....	31
Table 3-4: Chemical Composition of CKD. ....	32
Table 3-5: Chemical Composition of Clay.....	33
Table 3-6: Chemical Composition of LSP. ....	33
Table 3-7: Chemical Composition of NP. ....	34
Table 3-8: Chemical Composition of PSS.....	34
Table 3-9: Chemical Composition of FA.....	35
Table 3-10: Chemical Composition of SF.....	36
Table 3-11: Details of control and quaternary cement Concrete mixtures. ....	37
Table 3-12: Weights of materials in the mixtures investigated. ....	38
Table 3-13: Weights of aggregates in each mix used in this investigation. ....	39
Table 3-14: Details of concrete specimens and tests. ....	41
Table 3-15: Chloride Permeability and its Classification.....	46
Table 3-16: Probability of Occurrence of Reinforcement Corrosion. ....	47
Table 4-1: Average Compressive Strength of Plain and five Control mixes. ....	56
Table 4-2: Average Compressive Strength of Group-I QCC mixes. ....	56
Table 4-3: Average Compressive Strength of Group-II QCC mixes.....	56
Table 4-4: Average Chloride Permeability of Plain and five Control mixes.....	67
Table 4-5: Average Chloride Permeability of Group-I QCC mixes.....	67
Table 4-6: Average Chloride Permeability of Group-II QCC mixes.....	67
Table 4-7: Average Corrosion Current Density ( $I_{corr}$ ) of Plain and five Control mixes.....	89
Table 4-8: Average Corrosion Current Density ( $I_{corr}$ ) of Group-I QCC mixes. ....	90
Table 4-9: Average Corrosion Current Density ( $I_{corr}$ ) of Group-II QCC mixes. ....	90
Table 4-10: Average Drying Shrinkage of Plain and Five Control mixes. ....	101
Table 4-11: Average Drying Shrinkage of Group-I QCC mixes. ....	102
Table 4-12: Average Drying Shrinkage of Group-II QCC mixes. ....	103
Table 4-13: Average Water Absorption of Plain and Five Control mixes.....	114
Table 4-14: Average Water Absorption of Group-I QCC mixes.....	114
Table 4-15: Average Water Absorption of Group-II QCC mixes.....	114
Table 4-16: Setting Time of Group-I QCC mixes.....	123
Table 4-17: Setting Time of Group-II QCC mixes.....	123



## LIST OF FIGURES

Figure 3-1: Flow Chart of the Experimental Program for QCC <sup>S</sup> only. ....	28
Figure 3-2: Set of concrete specimens from each concrete mixture. ....	40
Figure 3-3: Compression Testing Machine. ....	42
Figure 3-4: Drying Shrinkage Specimens and dial gauge. ....	43
Figure 3-5: Specimens and cells utilized for determining the Rapid Chloride Permeability.....	45
Figure 3-6: Rapid Chloride Permeability Test Setup. ....	45
Figure 3-7: Reinforcement Corrosion Specimen. ....	47
Figure 3-8: Corrosion Potential Measurement Setup. ....	48
Figure 3-9: Specimens utilized for corrosion potentials and corrosion rate measurements. ....	48
Figure 3-10: Schematic Representation of the Corrosion Current Density Measurements. ....	50
Figure 3-11: Corrosion Current Density Measurement Setup. ....	51
Figure 3-12: A close-up view of the concrete specimen with counter and reference electrodes. ...	51
Figure 3-13: Vicat Apparatus. ....	52
Figure 3-14: Equipment Used to Determine Water Absorption. ....	54
Figure 4-1: Compressive Strength Development of QCC Specimens Prepared with 15% BHD... 57	57
Figure 4-2: Compressive Strength Development of QCC Specimens Prepared with 15% CKD... 58	58
Figure 4-3: Compressive Strength Development of QCC Specimens Prepared with 20% Clay.... 59	59
Figure 4-4: Compressive Strength Development of QCC Specimens Prepared with 20% LSP..... 60	60
Figure 4-5: Compressive Strength Development of QCC Specimens Prepared with 20% PSS. .... 61	61
Figure 4-6: Compressive Strength Development of QCC Specimens Prepared with 15% BHD... 62	62
Figure 4-7: Compressive Strength Development of QCC Specimens Prepared with 15% CKD... 63	63
Figure 4-8: Compressive Strength Development of QCC Specimens Prepared with 20% Clay.... 64	64
Figure 4-9: Compressive Strength Development of QCC Specimens Prepared with 20% LSP..... 65	65
Figure 4-10: Compressive Strength Development of QCC Specimens Prepared with 20% PSS. ... 66	66
Figure 4-11: Chloride permeability of QCC specimens with 15% BHD after 28 days of curing. ... 68	68
Figure 4-12: Chloride permeability of QCC specimens with 15% CKD after 28 days of curing. ... 69	69
Figure 4-13: Chloride permeability of QCC specimens with 20% Clay after 28 days of curing. ... 70	70
Figure 4-14: Chloride permeability of QCC specimens with 20% LSP after 28 days of curing. .... 71	71
Figure 4-15: Chloride permeability of QCC specimens with 20% PSS after 28 days of curing. .... 72	72
Figure 4-16: Chloride permeability of QCC specimens with 15% BHD after 28 days of curing. .. 73	73
Figure 4-17: Chloride permeability of QCC specimens with 15% CKD after 28 days of curing. .. 74	74
Figure 4-18: Chloride permeability of QCC specimens with 20% Clay after 28 days of curing. ... 75	75
Figure 4-19: Chloride permeability of QCC specimens with 20% LSP after 28 days of curing. .... 76	76
Figure 4-20: Chloride permeability of QCC specimens with 20% PSS after 28 days of curing. .... 77	77

Figure 4-21: Corrosion Potentials on Steel in the QCC Specimens Prepared with 15% BHD.....	79
Figure 4-22: Corrosion Potentials on Steel in the QCC Specimens Prepared with 15% CKD.....	80
Figure 4-23: Corrosion Potentials on Steel in the QCC Specimens Prepared with 20% Clay.....	81
Figure 4-24: Corrosion Potentials on Steel in the QCC Specimens Prepared with 20% LSP.....	82
Figure 4-25: Corrosion Potentials on Steel in the QCC Specimens Prepared with 20% PSS.....	83
Figure 4-26: Corrosion Potentials on Steel in the QCC Specimens Prepared with 15% BHD.....	84
Figure 4-27: Corrosion Potentials on Steel in the QCC Specimens Prepared with 15% CKD.....	85
Figure 4-28: Corrosion Potentials on Steel in the QCC Specimens Prepared with 20% Clay.....	86
Figure 4-29: Corrosion Potentials on Steel in the QCC Specimens Prepared with 20% LSP.....	87
Figure 4-30: Corrosion Potentials on Steel in the QCC Specimens Prepared with 20% PSS.....	88
Figure 4-31: Corrosion Current Density on Steel in QCC specimens prepared with 15% BHD. .	91
Figure 4-32: Corrosion Current Density on Steel in QCC specimens prepared with 15% CKD. .	92
Figure 4-33: Corrosion Current Density on Steel in QCC specimens prepared with 20% Clay....	93
Figure 4-34: Corrosion Current Density on Steel in QCC specimens prepared with 20% LSP. ...	94
Figure 4-35: Corrosion Current Density on Steel in QCC specimens prepared with 20% PSS.....	95
Figure 4-36: Corrosion Current Density on Steel in QCC specimens prepared with 15% BHD. .	96
Figure 4-37: Corrosion Current Density on Steel in QCC specimens prepared with 15% CKD. .	97
Figure 4-38: Corrosion Current Density on Steel in QCC specimens prepared with 20% Clay....	98
Figure 4-39: Corrosion Current Density on Steel in QCC specimens prepared with 20% LSP. ...	99
Figure 4-40: Corrosion Current Density on Steel in QCC specimens prepared with 20% PSS...	100
Figure 4-41: Drying Shrinkage Strain in QCC Specimens Prepared with 15% BHD.....	104
Figure 4-42: Drying Shrinkage Strain in QCC Specimens Prepared with 15% CKD.....	105
Figure 4-43: Drying Shrinkage Strain in QCC Specimens Prepared with 20% Clay. ....	106
Figure 4-44: Drying Shrinkage Strain in QCC Specimens Prepared with 20% LSP.....	107
Figure 4-45: Drying Shrinkage Strain in QCC Specimens Prepared with 20% PSS. ....	108
Figure 4-46: Drying Shrinkage Strain in QCC Specimens Prepared with 15% BHD.....	109
Figure 4-47: Drying Shrinkage Strain in QCC Specimens Prepared with 15% CKD.....	110
Figure 4-48: Drying Shrinkage Strain in QCC Specimens Prepared with 20% Clay. ....	111
Figure 4-49: Drying Shrinkage Strain in QCC Specimens Prepared with 20% LSP.....	112
Figure 4-50: Drying Shrinkage Strain in QCC Specimens Prepared with 20% PSS. ....	113
Figure 4-51: Water Absorption of QCC specimens with 15% BHD after 28 days of curing.....	115
Figure 4-52: Water Absorption of QCC specimens with 15% CKD after 28 days of curing.....	116
Figure 4-53: Water Absorption of QCC specimens with 20% Clay after 28 days of curing.....	117
Figure 4-54: Water Absorption of QCC specimens with 20% LSP after 28 days of curing.....	117
Figure 4-55: Water Absorption of QCC specimens with 20% PSS after 28 days of curing. ....	118

Figure 4-56: Water Absorption of QCC specimens with 15% BHD after 28 days of curing.....	119
Figure 4-57: Water Absorption of QCC specimens with 15% CKD after 28 days of curing.....	120
Figure 4-58: Water Absorption of QCC specimens with 20% Clay after 28 days of curing. ....	120
Figure 4-59: Water Absorption of QCC specimens with 20% LSP after 28 days of curing.....	121
Figure 4-60: Water Absorption of QCC specimens with 20% PSS after 28 days of curing. ....	122
Figure 4-61: Setting Time of Group-I QCC specimens. ....	123
Figure 4-62: Setting Time of Group-I QCC specimens. ....	124

## **THESIS ABSTRACT (ENGLISH)**

**NAME: MOHAMMED KHAJA MOINUDDIN**  
**TITLE: MECHANICAL PROPERTIES AND DURABILITY OF  
QUATERNARY CEMENT CONCRETES**  
**MAJOR: CIVIL ENGINEERING**  
**DATE: 16<sup>th</sup> MAY 2012**

The reduction in the useful service-life of reinforced concrete construction in the coastal areas of the Arabian Gulf is well appreciated by the construction industry. Now, it is well recognized that concrete construction for the local environmental and geomorphical conditions needs to be designed for durability rather than strength alone. Several methodologies have been suggested for this purpose, among which are: (i) modifications in the concrete mixture design, (ii) incorporation of supplementary cementing materials, and (iii) protection of concrete and steel by applying coatings.

The earliest research work on the use of supplementary cementing materials has been concerned with the use of fly ash, silica fume and natural pozzolans. However, it should be pointed that both fly ash and silica fume are not available locally. As such, use of silica fume, a material that is more efficient in terms of its cost to performance ratio, has gained favor with the local construction industry. However, several problems have been

noted with the use of silica fume, namely cracking of concrete due to plastic and drying shrinkage, particularly when concrete has not been adequately cured. Due to these problems, there is a worldwide trend towards using ternary and quaternary cements in concrete. Hence, there was a need to conduct a study on quaternary cement concrete for utilization in the Arabian Gulf Environment.

The objective of this research was to develop quaternary cement concrete utilizing local natural pozzolanic materials and industrial by-products. The mechanical properties and durability of the developed quaternary cement concrete were evaluated. The mechanical properties and durability characteristics of the QCC<sup>S</sup> prepared utilizing the local pozzolans and industrial by-products were comparable to OPC and binary cement concretes. The use of developed QCC reduces cost of concrete and decreases the greenhouse gas emission.

## ملخص الرسالة (عربي)

الإسم : محمد خواجه معين الدين

عنوان البحث : الخصائص الميكانيكية والديمومة للخرسانة الاسمنتية الرباعية

التخصص : هندسة مدنية

تاريخ التخرج : ٢٥ جمادى الآخرة ١٤٣٣ هـ ( ١٦ مايو ٢٠١٢ م)

ان انخفاض عمر الخدمة المفيد لمنشآت الخرسانة المسلحة في المناطق الساحلية للخليج العربي اصبح له تقديرا كبيرا في صناعة البناء. الان، من المسلم به ان المنشآت الخرسانية في الظروف البيئية المحلية وحالات الجيومورفولوجية بحاجة ان يتم تصميمها للديمومة وليس للقوة فقط. وقد تم اقتراح منهجيات متعددة لهذا الغرض، من بينها : (1) تعديلات في تصميم خليط الخرسانة (2) ادخال مواد اسمنتية اضافية و(3) حماية الخرسانة وحديد التسليح بعمل الطلاء.

في ابحاث سابقة فقد اقتصر الامر على استخدام مواد اسمنتية اضافية وذلك باستخدام الرماد المتطاير، غبار السيليكا والبوزولان الطبيعي. على الرغم، ان كلا من الرماد المتطاير وغبار السيليكا لا تتوفر محليا. كما ان استخدام غبار السيليكا، وهي مادة فعالة جدا وفقا لنسبة كلفتها الى اداءها، قد اكسبتها حصة في صناعة الانشاءات المحلية. وبرغم ان هناك مشاكل متعددة ثم ملاحظتها عند استخدام غبار السيليكا، مثل تشققات الخرسانة بسبب الانكماش اللدن والجاف، وخصوصا عندما لا يتم معالجتها بشكل جيد. وبسبب هذه المشاكل، فان هناك اتجاه في جميع انحاء العالم نحو استخدام الاسمنت الثلاثي و الرباعي في الخرسانة. لذا فقد تم تنفيذ الدراسة على خرسانة الاسمنت الرباعي وذلك لاستخدامها في بيئة الخليج العربي.

وكان هدف هذه الدراسة هو تطوير خرسانة رباعية الاسمنت بالاستفادة من مواد البوزولان الطبيعي المحلي والنواتج الصناعية. وقد تم تقييم الخواص الميكانيكية والديمومة للخرسانة الاسمنتية الرباعية المطورة. كما تم مقارنة الخواص الميكانيكية وخصائص الديمومة ل QCC<sup>S</sup> المعده بالاستفادة من المواد البوزولانية المحلية و النواتج الصناعية بالخرسانة العادية والخرسانة الاسمنتية الثنائية. ان استخدام QCC المطورة يقلل من كلفة الخرسانة و كما يقلل من انبعاث البيت الاخضر.

درجة الماجستير في العلوم الهندسية

جامعة الملك فهد للبترول والمعادن

الظهران – ٣١٢٦١

المملكة العربية السعودية

# CHAPTER 1

## INTRODUCTION

### 1.1 Concrete Durability in the Arabian Gulf

Reinforced concrete is unique among the three most common construction materials, namely wood, steel and reinforced concrete and it has proved to be an efficient and durable construction material for construction of all kinds of structures. The low-cost, ecologically favorable profile, excellent strength and stiffness properties coupled with the ease of manufacture at site are some of the factors that have established it as the most widely used construction material in the world. It was estimated in late 1990<sup>s</sup>, that the consumption of concrete was order of 5.5 billion tons every year [1, 2] and currently it is around 10–12 billion tons next to that of water.

In spite of its good attributes, there have been many cases of failure. The poor durability of reinforced concrete structures is a major problem facing the construction

industry throughout the world. It has been estimated that annual cost is more than \$ 50 billion for the repair and rehabilitation of deteriorated concrete structures in the USA, as \$ 200 billion were estimated in the decade of 1980<sup>S</sup> [3, 4]. Similarly, it has been estimated that more than £ 20 billion are needed to repair deteriorated structures in the UK, as £ 2 billion were estimated in the decade of 1980<sup>S</sup> [5, 6]. The cost of repair and rehabilitation of the deteriorated reinforced concrete structures in the countries along the Arabian Gulf is not very well documented. However, considerable resources have to be diverted towards the repair of deteriorated concrete structures in this region.

Generally speaking all concrete structures in an environment would suffer from deterioration or distress caused by loading, exposure conditions and poor design and construction. The deterioration of concrete structures in the temperate climatic conditions, such as Europe and North America, is mainly attributed to reinforcement corrosion that is caused by the ingress of deicer salts or carbonation. Insufficient concrete cover over the reinforcing steel and/or poor quality concrete accelerates the deterioration process. The environmental and geomorphical conditions in the coastal areas of the Arabian Gulf lead to a reduction in the useful service life of concrete structures in this region. The environment, soil, and ground water, that are heavily admixed with chloride and sulfate salts, are conducive to the initiation of the deterioration processes. The daily and seasonal variations



in the temperature and the humidity accelerate the rate of concrete deterioration. The ambient temperature in the Arabian Gulf is relatively high (40 to 50 °C) compared to USA or Europe (15 to 25 °C). The direct solar radiation effect raises the temperature to as high as 70 to 80 °C on the concrete surface. This thermal effect influences the over-all mechanisms of the deterioration processes, namely reinforcement corrosion, sulfate attack, salt weathering, shrinkage and thermal cracking. Further, the rate of reinforcement corrosion increases rapidly when the ambient temperature is in the range of 20 to 40 °C.

Many researchers studied the durability problems in the Arabian Gulf in the last three decades. Condition surveys carried out at KFUPM on 42 framed reinforced concrete structures 15 to 20 years old located in the Eastern Province of Saudi Arabia indicated that the main factors for concrete deterioration are: reinforcement corrosion, sulfate attack, salt weathering and cracking due to environmental factors [7].

The accelerated deterioration of reinforced concrete structures in the Arabian Gulf, compared to those in the other parts of the world, is attributed to several factors. However, the harsh climatic conditions and the marginal quality of the local aggregates are the two main reasons for the reported deterioration [8–10]. Presently, it is very well recognized that concrete construction for the local environmental and geomorphical conditions needs to be

designed for durability rather than strength alone. Also, several methodologies have been suggested to improve the durability of concrete construction, among which are: (i) modifications in the concrete mixture design, (ii) incorporation of supplementary cementing materials, (iii) protection of steel by the application of coatings, such as fusion bonded epoxy coating, and (iv) protection of concrete itself by the application of coatings. In certain situations, more than one of the mentioned options needs to be adopted.

Whatever be the protection methodology adopted, the primary requirement is to produce quality concrete. In this direction, supplementary cementing materials, such as fly ash, silica fume, natural pozzolan and blast furnace slag, have been incorporated in concrete to improve its durability. The earliest research work on the use of supplementary cementing materials (SCMs) has been concerned with the use of fly ash and natural pozzolans. Research conducted at KFUPM [11-13] has shown that incorporation of fly ash in concrete improved its durability, particularly the corrosion- and sulfate-resistance in spite of the low early strength of concrete. Research in the 1990s was concerned with the use of silica fume in concrete. Due to its high pozzolanicity, silica fume is believed to improve the properties of concrete, both in terms of its strength and durability. As a result, silica fume is very widely used in Arabian Gulf. Silica fume, a by-product in the manufacture of ferrosilicon and also of silicon metal, is a very efficient pozzolanic material.

Silica fume concrete is an effective admixture concrete used for high strength and durability. The high reactivity of silica fume with Portland cement is primarily due to its high silica and its extreme fineness. In order to maintain the same water- (cement plus silica fume) ratio, a super plasticizer or a high range water reducer is used. Silica fume concrete is used by many major companies in the Eastern Province, like Saudi ARAMCO, SCECO, and Royal Commission for Jubail and Yanbu.

However, it should be pointed that both fly ash and silica fume are not available locally and they are imported from other countries. The cost of these materials is more than that of Portland cement. Though silica fume blended cement has been specified to combat the deterioration of reinforced concrete structures in the aggressive environment of the Arabian Gulf, several problems have been noted with its use in concrete, namely cracking of concrete due to plastic and drying shrinkage, particularly when concrete has not been adequately cured [8, 14–16].

Due to the problems noted with the use of silica fume, particularly under hot weather conditions, there is a shift towards using ternary and quaternary cement concrete. These types of concrete have two or more SCMs. An earlier study was carried at KFUPM to evaluate the properties of ternary cement concretes.

## 1.2 Need for Research

Manufacturing of cement is a source of greenhouse gas emissions. The annual production of cement in the world is about 3,300 million tons. Cement manufacture contributes greenhouse gases both directly through the production of carbon dioxide when calcium carbonate is burnt in the kilns, producing lime and carbon dioxide ( $\text{CO}_2$ ) and also indirectly through the use of energy in the kiln, particularly if the energy is sourced from fossil fuels [17]. The "greenhouse effect" is a process by which the earth is becoming warmer with time. The earth is bathed in sunlight, some of it is reflected back into space and some is absorbed. If the absorption is not matched by radiation back into space, the earth will get warmer until the intensity of that radiation matches the incoming sunlight. Some atmospheric gases absorb outward infrared radiation, warming the atmosphere. Carbon dioxide is one of these gases; so are methane, nitrous oxide, and the chlorofluorocarbons (CFCs). The concentrations of these gases are increasing, with the result that the earth is absorbing more sunlight and getting warmer [18]. The cement industry produces 5% of global man made  $\text{CO}_2$  emissions, of which 50% is from the chemical process is 40% from burning of fuel [19]. The volume of  $\text{CO}_2$  emitted by the cement industry is nearly 900 kg for every 1,000 kg of cement produced [20].

Furthermore, the cement production process is energy intensive as well as raw materials demanding. Technical improvements to lower the environmental impact of the cement production achieved by the cement industry are reaching limitations. Remaining potential to reduce environmental impacts is provided by the reduction of the clinker in cement (blended cements). Other main constituents for cement, such as granulated blastfurnace slag (GGBS), fly ash from power plants, natural and industrial pozzolanas or limestone can be used. The production of blended cements results in lower emission and lower energy consumption since less clinker from the energy intensive process is needed to produce them [21, 22]. Hence, there is a need to meet the demand for cement without a corresponding increase in the greenhouse gases. As discussed earlier, most of these materials are not available locally and they have to be imported from other countries thereby leading to an increase in the cost of concrete. Therefore, the consumption of waste materials that are generated in abundance during manufacture of building and other materials in the Kingdom of Saudi Arabia is a moral task that will certainly lead to a reduction in the greenhouse gas emissions. Blended cements developed utilizing locally available waste materials, such as bag house dust (BHD) produced during the production of steel, cement kiln dust (CKD) produced during the production of cement, clay, limestone powder (LSP) produced during the crushing of large size boulders to produce small size aggregates,

pulverized steel slag (PSS) produced during the production of steel, and natural pozzolan (NP), etc., can be utilized as part of cement. Though cement is the main source of strength in concrete, there is a need to reduce its use by the local construction industry in order to decrease the greenhouse gases and to conserve energy and mineral resources.

The above-mentioned industrial waste materials are abundantly available in the Kingdom of Saudi Arabia and they are rarely used in the construction industry. They are normally deposited in landfills. This causes environmental problems as well as contributing to large dust in the air. In addition, there is a strong desire to reduce the consumption of cement through the effective utilization of industrial waste materials, such as BHD, CKD, clay, LSP, PSS, NP, etc., in concrete in order to decrease the greenhouse effect, environmental problems and to produce a cheaper building material. A combination of these materials can be utilized to provide durable concrete.

The ternary cement consists of Portland cement, and two supplementary cementing materials, such as fly ash and silica fume while the quaternary cement consists of Portland cement, and three supplementary cementing materials, such as fly ash, blast furnace slag and silica fume. The use of other pozzolanic materials, such as natural pozzolon or metakaolin is not uncommon [23, 24]. A study was conducted at KFUPM on evaluating the ternary

cement for improving concrete durability in the Arabian Gulf [25–28]. However, limited literature is available on the performance of concrete prepared with quaternary cement. Also, research work on this aspect is yet to be conducted in the Arabian Gulf.

### **1.3 Objective**

The broad objective of this research was to develop mix design for quaternary cement concretes and assess their mechanical properties and durability characteristics. The data developed in this study will be beneficial to the local construction industry and in updating the local codes of practice. The specific objectives were the following:

1. Develop mix design for quaternary cement concretes utilizing the local materials,
2. Assess the mechanical properties and durability characteristics of the developed quaternary cement concretes, and
3. Ascertain the economic viability of utilizing the local materials to produce quaternary cement concretes.

## CHAPTER 2

# LITERATURE REVIEW

### 2.1 Multi-Component Cement

Extensive research has now established, beyond a shadow of doubt, that technically sound, economically attractive and the most direct solution to the problems of reinforced concrete durability lies in the incorporation of finely divided siliceous materials in concrete. The fact that these cement replacement materials, or supplementary cementing materials (SCMs), as they are often known and described, such as fly ash (FA), ground granulated blast-furnace slag (GGBFS), silica fume (SF), rice husk ash (RHA), natural pozzolans (NP) and volcanic ash, are all either pozzolanic or cementitious and pozzolanic materials make them ideal companions to Portland cement (PC). Indeed, Portland cement is the best chemical activator of these siliceous admixtures so that PC and FA, GGBFS and/or SF can form a life-long partnership of homogeneous interaction that can never end in divorce or unhealthy association and after-effects [23, 24]. But more importantly, the PC +



FA/slag/SF partnership will result in high quality concrete with intrinsic ability for high durability with immense social benefits in terms of resources, energy and environment – the only way forward for a sustainable development.

The incorporation of industrial byproducts, such as FA, slag and silica fume, in concrete can significantly enhance its basic properties in both the fresh and hardened state [23, 24]. Apart from enhancing the rheological properties and controlling the bleeding of fresh concrete, these materials greatly improve the durability of concrete through control of high thermal gradients, pore refinement, depletion of cement alkalis, resistance to chloride and sulfate penetration and continued microstructural development through long-term hydration and pozzolanic reactions [29–32]. Concrete can provide, through chemical binding, a safe haven for many of the toxic elements present in industrial wastes; and there are strong indications that these mineral admixtures can also reduce the severity of concrete durability problems arising from delayed ettringite and thaumasite formation.

The SCMs are either from natural sources (pozzolan, limestone, metakaolin) or industrial byproducts (fly ash, slag, silica fume, rice husk ash, etc.) [29, 32]. Binary cements, such as Portland slag cement, pozzolanic cements and limestone–Portland cements are standardized (e.g. ASTM C 595, EN197 and BS146). Further, the benefits due to the

addition of active supplementary cementing materials and fillers to Portland cement are well documented [30, 31, 33].

However, incorporating a single SCM to improve a concrete's specific durability property has some limitations with its use (depending on the SCM), such as low early age strength, extended curing period, increased admixture use, increased plastic shrinkage cracking, and freeze/thaw scaling in the presence of deicer salts [29, 32]. Using a single SCM to address one durability concern may result in failure in another. For example, the replacement level of a single SCM needed to prevent alkali silica reaction (ASR) expansion may create other problems or concerns. The incorporation of 50% slag or greater than 20% fly ash needed to ensure adequate protection against ASR may lead to poor resistance to deicer salt scaling [34–37] or low early stage strength.

Another example of materials incompatibility is the incorporation of silica fume at levels greater than 10% by mass of cement. Such replacement levels are necessary to prevent ASR expansion [38, 39], but typically lead to problems with the workability of fresh concrete as well as difficulties in adequately dispersing the silica fume [40].

Further, the binary cements are often associated with other shortcomings, such as the need for extended moist-curing, increased use of chemical admixtures, low early age

strength, increased cracking tendency due to drying shrinkage, and de-icing salt scaling problems. Thus, there is a need for research to investigate whether multi-component (ternary and quaternary) cements could be optimized with synergistic effects allowing component ingredients to compensate for any mutual shortcomings.

A viable solution is to use a high performance multi blended cement concrete that uses moderate levels (15 to 35%) of fly ash/natural pozzolan in combination with silica fume at lower than typical levels (<7% by mass) and any industrial waste materials (15 to 20%) such as BHD, CKD, Clay, LSP, PSS, etc.. The quaternary blends allow the use of one SCM to compensate for the inherent shortcomings of another. Such concretes are known to exhibit excellent fresh and mechanical properties. The suitability of blends depends on the specific performance requirements, curing conditions, exposure environment, availability of materials, and, of course, economical manufacture.

## **2.2 Early Work on Multi-Component Cements**

Producing cements incorporating high-volume replacement of ordinary Portland cement (OPC) with recycled industrial by-products is perceived as the most promising venture for the cement and concrete industry to meet its environmental obligations as well as it represents significant energy and cost savings.

The use of SCMs dates back to the ancient Greeks who incorporated volcanic ash with hydraulic lime to create a cementitious mortar. The Greeks passed this knowledge on to the Romans who would go on to construct such engineering marvels as the Roman aqueducts and Coliseum, which still stand today. Early SCMs consisted of natural, readily available materials, such as volcanic ash or diatomaceous earth.

Considerable research has been conducted on the use of SCMs as partial replacement of Portland cement in concrete since 1950. Najimi et al. [41] investigated the effect of natural pozzolan (NP) on Portland cement. Concrete mixtures with 25% replacement of cement with NP were studied. The blended and control mixtures were tested for mechanical and durability properties. Compressive strength of specimens after 180 days slightly decreased (i.e., less than 5%). The specimens with pozzolan had slightly enhanced modulus of elasticity and decreased chloride ion permeability, but did not perform well in freeze and thaw and sulphate expansion tests when compared to control specimens. Due to the lower content of amorphous silica in NP, it was also found that the hydration rate was slow. Therefore, the best properties were obtained after 90 and 180 days of curing.

de Souza et al. [42] investigated the effect of Bag House Dust (BHD) on the mechanical and chemical performance of Portland cement concrete. They found that the compressive strength of concrete specimen increased with the addition of BHD in the range of 10 to 20 wt. (%). Also, the tensile strength and setting time of specimens increased with the addition of BHD and the chloride penetration decreased. The acetic acid leaching and water solubility test results showed low movement of potentially toxic elements from BHD-based concrete.

Maslehuddin et al. [43] investigated the performance of Cement Kiln Dust (CKD) blended cement concrete specimens with 0%, 5%, 10%, and 15% CKD, replacing ASTM C 150 Type I and Type V cements. The mechanical properties and durability characteristics were assessed. Results indicated that compressive strength of concrete specimens decreased with the use of CKD and there was no significant difference in the compressive strength and drying shrinkage of 0 and 5% CKD cement concretes. The chloride permeability increased and the electrical resistivity decreased due to the incorporation of CKD. The performance of concrete with 5% CKD was almost similar to that of concrete without CKD. Therefore, it was suggested to limit the amount of CKD in concrete to 5% since the chloride permeability and electrical resistivity data indicated that the chances of reinforcement corrosion would increase with 10% and 15% CKD.

Dhir et al. [44] investigated the performance of concrete produced by blending Portland cement and limestone (LSP). They used 15, 25, 35 and 45% replacement of cement with LSP with a range of cement s from 235 to 410 kg/m<sup>3</sup>, and free water of 185 l/m<sup>3</sup>. They found that there were minor differences in the performance between Portland cement and 15% LSP blended cement concretes of the same cement and water-to-cement ratio. But, there was a decrease in the strength as the LSP increased. However, the flexural strength and modulus of elasticity decreased with an increase in the LSP. Permeation and durability properties at equal w/c ratio enhanced up to 25% LSP and poorer performance thereafter. For the latter, minor effects were generally noted up to 15–45% LSP, but there was a gradual depletion in the performance with an increase in the LSP.

The use of ternary cement prepared with Portland cement and SCMs has increased since 1990. Ternary cements have more advantages than binary cements. Ternary blended cements consisting of fly ash–silica fume or blast furnace slag–silica fume are common in practice and several studies have been published on this subject [33, 45, 46]. Studies conducted in France resulted in the commercial production of ternary cements, and in some parts of Australia, ternary cements and even quaternary cements have been available since 1966 [47].

Concrete prepared with ternary-blended cements has been used in many applications, such as dam sections, highway pavements and structural elements in high-rise buildings. Several studies indicated that ternary-blends made of Portland cement, silica fume, and fly ash offer significant advantages over binary blends and even greater enhancements over Portland cement alone [33, 45, 46]. In terms of durability, such blends are vastly superior to Portland cement concrete [45, 46, 48].

Popovic's [49] research on Portland cement-fly ash-silica fume systems in concrete indicated that the silica fume in the of 5% of the weight of the cement produces relatively greater strength increase in the presence of fly ash than without fly ash.

Dhir et al. [33] reported that the resistance to chloride ion penetration of concrete prepared with ternary cement was higher than that of concrete prepared with either Portland cement alone or a blend of Portland cement and fly ash. This was attributed mainly to the refinement of the pore structure of the concrete prepared with ternary cement.

In a study conducted by Bleszynski [50] on the performance and durability of concrete with ternary blends of silica fume and blast-furnace slag, it was reported that the

ternary blends were more effective than the binary blends in controlling deleterious expansion due to ASR.

Comparative studies between OPC, binary and ternary cementitious systems conducted by Khatri et al. [51] in Australia concluded that the most significant improvements of ternary cement concretes associated with durability aspects are related to marine environments. Furthermore, ternary mixes containing OPC, silica fume and either blast-furnace slag or fly ash yielded an optimum balance between mechanical and durability properties.

Thomas et al. [46], reported results from laboratory studies on the durability of concrete that contains ternary blends of Portland cement, silica fume, and a wide range of fly ashes. Combinations of relatively small levels of silica fume (e.g., 3 to 6%) and moderate levels of high Class C fly ash, as per ASTM C 618, (20 to 30%) were found very effective in reducing expansion due to ASR and also produced a high level of sulfate resistance. Concretes made with these proportions generally exhibited excellent fresh and hardened properties since the combination of silica fume and fly ash is somewhat synergistic. For instance, fly ash appears to compensate for some of the workability problems often associated with the use of higher levels of silica fume, whereas the silica fume appears to



compensate for the relatively low early strength of fly ash cement concrete. Diffusion testing indicated that concrete produced with ternary cementitious blends has a very high resistance to the penetration of chloride ions. Furthermore, it was indicated that the diffusivity of the concrete that contains ternary blends continued to decrease with age. The reductions were very significant and had a considerable effect on the predicted service life of reinforced concrete elements exposed to chloride environments.

Shah and Wang [52] investigated utilization of CKD and Class F fly ash (FA) in concrete in the process of developing green concrete. The effects of mechanical, chemical and thermal activation on strength and other properties of CKD-FA binders were investigated. Results indicated that, when the blend proportion and activation are properly applied, the binder made with CKD and fly ash will have satisfactory strength and performance, which provides potential applications for the new cementitious product.

Maslehuddin et al. [53] studied the mechanical properties and durability characteristics of ordinary Portland cement and blended cement (with silica fume and fly ash) concrete specimens with electric arc furnace dust (BHD). Concrete specimens were prepared with and without BHD. In the silica fume cement concrete, silica fume constituted 8% of the total cementitious material while fly ash cement concrete contained

30% fly ash. BHD was added as 2% replacement of cement in the OPC concrete and 2% replacement of the total cementitious in the blended cement concretes. Specimens were tested for compressive strength, drying shrinkage, initial and final setting time, slump retention, water absorption, chloride permeability, and reinforcement corrosion.

Results of that study [53] indicated that the setting time and slump retention tended to increase with the addition of BHD. However, there was a gain in strength with the addition of BHD. Further, the water absorption and chloride permeability were found to decrease and there was an increase in the corrosion resistance of concrete with BHD compared to OPC and blended cement concretes.

### **2.3 Effect of Multi-Component Cement on Compressive Strength**

The properties of fly ash, silica fume and cement, as well as the proportions of each in concrete influence the strength and rate of strength gain of concrete. After the rate of strength gain attributable to the Portland cement slows down, the pozzolanic activity of the fly ash and silica fume continues and contributes to increased strength gain at later ages if the concrete is kept moist [54].

A number of investigators have explored the possibility of using silica fume in combination with fly ash [54–64]. The purpose of the combined use of silica fume and fly

ash has generally been to utilize the highly reactive silica fume to compensate for the low early age strength and slow strength development in concrete by using fly ash, and to use fly ash to improve the workability of the mixes containing silica fume. Some promising results have been obtained.

In a study conducted by Ozyildirim [59], the possibility of producing concrete with adequate early and 28 day strength, and low 28 day chloride permeability for normal construction activities was reported by the combined use of silica fume and fly ash. The test results showed that adding small amounts of silica fume to fly ash concrete with w/c ratios of 0.4 to 0.5 results in concrete with satisfactory strength and very low permeability at 28 days. He also emphasized the importance of good curing procedures for concretes containing a combination of silica fume and fly ash. Increasing the early curing temperature and the duration of moist curing reduced the chloride permeability.

Studies conducted by Ghrici et al. [65] on the engineering properties of concrete containing natural pozzolan and silica fume, confirmed that the use of ternary cement contributes to the improvement of strength at an early stage. Better resistance to sulfate and acid attacks and less chloride ion penetration enhanced the durability of concrete.

Study by Bagel [66] on strength and pore structure of ternary blended cement mortars containing blast furnace slag and silica fume, indicated that ternary cement mortars with fixed workability and incorporating blast furnace slag and silica fume reached relatively satisfactory level of compressive strength and contributed to densifying the pore structure.

Lane et al. [67] investigated ternary blends, wherein small amounts of silica fume were used to augment the characteristics of concretes with lower amounts of fly ash or slag, and reported that they are generally effective in improving early strengths over high percentage binary blends.

## **2.4 Effect of Multi-Component Cements on Durability**

Several workers have demonstrated the suitability of combining silica fume and blast-furnace slag with Portland cement to increase resistance to water penetration and ingress of harmful ions, while attaining acceptable compressive strength [55, 58, 60, 64, 66–68]. Work by Thomas et al. [46] showed that mixtures of silica fume with either fly ash or slag improved the handling properties of the mixtures, and reduced the water requirement.

In China, limited work has also been conducted on Portland cement blended with both blast-furnace slag and fly ash [69]. The impetus for this work was to reduce the cost of concrete by using less Portland cement, and minimize air pollution caused by clinker processing. It was reported that a 30% slag and 20% fly ash mixture exhibited higher

compressive strength, and better control of ASR expansion than single component Portland cement mixture. However, the ternary mixtures yielded a lower resistance to drying shrinkage and carbonation.

Butler [48] reviewed the data available on the durability of multiple blends. He stated the following: “Where the necessary materials are readily available, more economical solutions, associated with improved general properties, can often be achieved with ternary and quaternary blends. Such blends typically contain less of individual components than would apply in a binary blend, the multiple blends being effectively blends of durable binary blends. Normally, any modification to a concrete mixture, which reduces the amount of water required, surplus to that required for cement hydration, or improves the pore structure (both of which reduce permeability), will enhance durability. However, ASR tends to be more destructive in high strength concretes having fewer voids available to accommodate gel expansion internally and having high modulus of elasticity, conferring low strain to failure.”

Khatri et al. [51] conducted a study on the use of ternary and quaternary binder systems used in high performance concrete in coastal and offshore structures. Mixture designs and results are summarized in Table 2.1. They stated the following: “The most

significant improvement found in concretes with SCMs was in properties which were indicative of their durability in marine environment. The triple blends of Portland cement, silica fume, and slag or fly ash gave a balance of properties as a result of the effect of each type and dosage of the SCM used. The OPC/SF/FA triple blend showed improved strengths, elastic modulus, volume stability and durability performance.

Laldji and Tagnit [70, 71] carried out an investigation to study the performance of ternary and quaternary cementitious systems incorporating glass frit. Canadian Class F fly ash, slag, as well as silica fume commonly used in Eastern Canada were also used as cementitious materials. Mixture designs and results are summarized in Table 2.2. The results described in this paper show that the presence of glass frit enhances their rheological behavior, and subsequently improves their hardened properties as well as some durability aspects such as compressive strengths, permeability, resistance to freezing-and-thawing and drying shrinkage. Despite the lower early strength of concrete made from ternary and quaternary blends, strengths developed after 91 days of hydration varied from 1.05 to 1.25 times those of the control. Permeability was also reduced and varied from 35 to 17.7% of the control.

Table 2-1 : Ternary and Quaternary Blends Used in Offshore Structures [51].

Ternary and Quaternary Blend-Mixture and Proportions.						
Cement %	60	50	80	60	83	81
Silica fume %	5	5	5	5	7	9
Slag %	25	35	0	35	0	10
Fly ash %	10	10	15	0	10	10
Binder (kg)	500	500	500	500	500	500
Water (kg)	180	180	180	180	180	180
WRA (kg)	3	3	3	3	3	3
HRWR (kg)	2.15	1.5	1.5	1.5	2.19	2..56
Compressive Strength, MPa						
1-day	10	6	14	10	17	15
3-days	31	25	37	30	42	41
7-days	45	38	50	45	54	54
28-days	67	65	68	70	75	75
Drying Shrinkage, micro strain						
3-weeks	610	610	520	560	510	.....
8-weeks	750	770	670	700	650	.....
Chloride Diffusion, *10 <sup>-12</sup> m <sup>2</sup> /s						
28-days	10	4.5	8	6.5	8.5	4
56-days	2	0.45	2	0.5	1.5	6.5
90-days	1.4	0.45	2.5	1	2	.....
Rapid Chloride Penetration, Coulombs						
28-days	970	1030	1270	1330	1110	1430
56-days	610	640	1030	870	820	.....

Table 2-2 : Ternary and Quaternary Blends [70].

<b>Concrete mixture proportions</b>				
Materials	<b>kg/m<sup>3</sup></b>			
	<b>Ter</b>	<b>QFA</b>	<b>QS</b>	<b>Control</b>
Portland cement	265.5	175	140	350
Silica fume	17.5	17.5	17.5	0
Slag	0	0	105	0
Fly ash	0	70	0	0
Glass frit	70	87.5	87.5	0
Water (w/cm = 0.45)	158.3	158.2	158.4	158.2
Sand	730	710	728	755.5
Aggregate (14 mm)	484	484	484	484
Aggregate (20 mm)	585	585	585	585
Air entraining admixture, mL/m <sup>3</sup>	385	525	385	315
Water reducer, mL/m <sup>3</sup>	770	752.5	805	735
<p>Note: <b>Ter</b> = Ternary cement made with 20% glass frit + 5% silica fume + 75% PC.</p> <p><b>QFA</b> = Quaternary cement with fly ash made of 25% glass frit +5% silica fume + 20% fly ash + 40%PC.</p> <p><b>QS</b> = Quaternary cement with slag made of 25% glass frit + 5% silica fume + 30% slag + 50% PC.</p>				
<b>Compressive Strength, MPa</b>				
3-days	19.6	10.2	8	24
7-days	29.4	19.3	21	31
28-days	44.7	37.2	38.3	36
91-days	50	42	45	40
<b>Drying Shrinkage, Microstrain</b>				
3-weeks	220	300	200	380
30-weeks	310	320	290	550
<b>Initial and final setting time</b>				
Initial setting	8h 10min	11h 30min	11h	7h 30min
Final setting	9h 40min	13h 20min	12h 40min	8h 30min
<b>Rapid Chloride Penetration, Coulombs</b>				
91-days	900	500	480	2500
<b>Resistance to freezing and thawing ASTM C 666-A</b>				
Durability factor [300 cycles]	99	97	100	104



## CHAPTER 3

# RESEARCH METHODOLOGY

### 3.1 Experimental Program

This chapter addresses the materials characterization and experimental methods utilized in this study. This research evaluates the mechanical properties and durability of quaternary cement concrete produced using locally available waste materials, such as, BHD, CKD, Clay, LSP, NP and PSS with some mineral admixtures, such as, FA and SF. To achieve these objectives, the following phases were followed. First phase was to procure the concrete ingredients and waste products. In the second phase, preparation of concrete specimens was carried out and in the third phase, following tests were conducted: accelerated pozzolanic activity index, compressive strength, drying shrinkage rapid chloride permeability, reinforcement corrosion, setting time, sulfate resistance, and water absorption. In this chapter, all these three phases are discussed thoroughly. Figure 3.1 shows the flow chart of the experimental program.

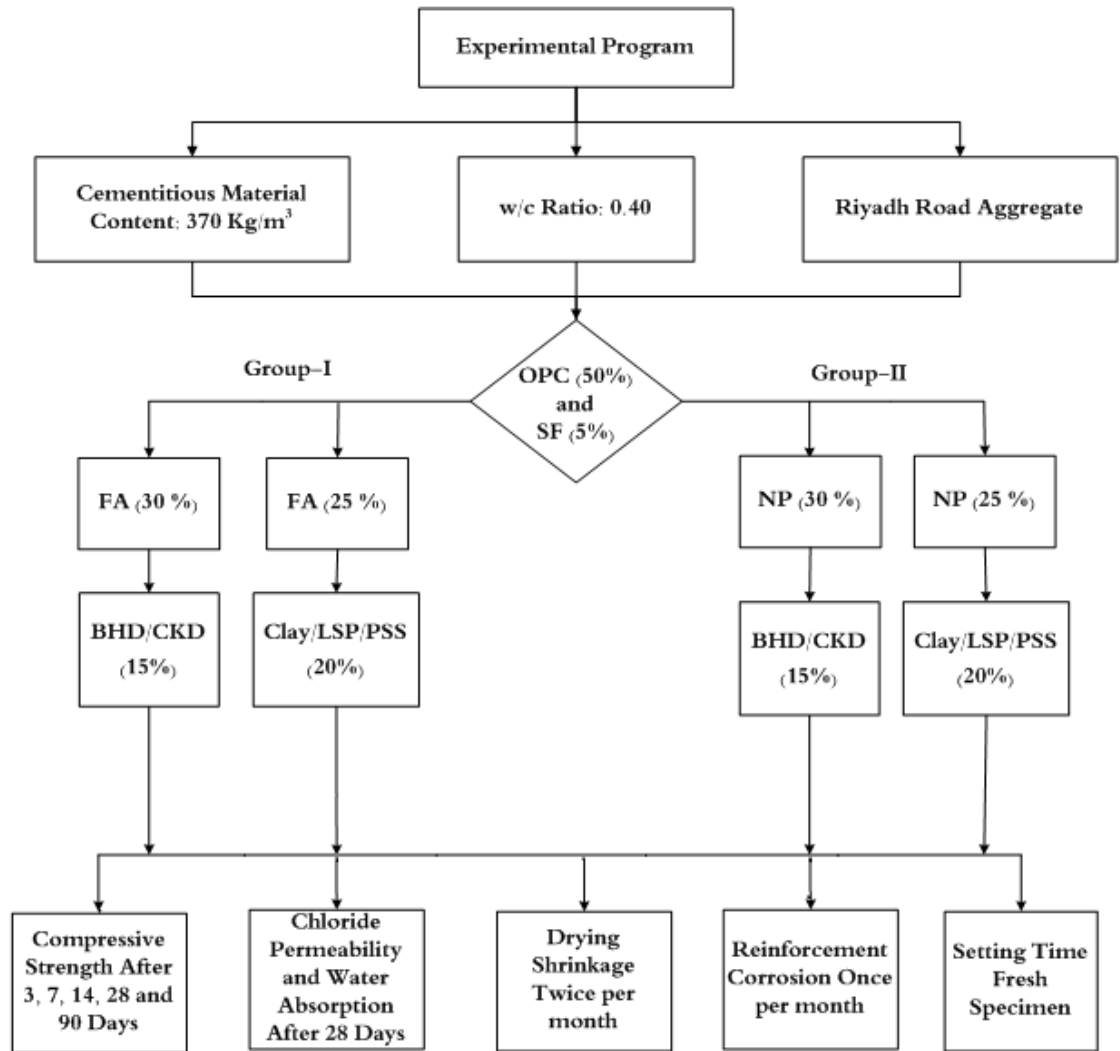


Figure 3-1: Flow Chart of the Experimental Program for QCC<sup>S</sup> only.

## 3.2 Materials

### 3.2.1 Cement

Ordinary Portland cement conforming to ASTM C 150 Type I with a specific gravity of 3.15 was used in all the concrete mixtures. Sufficient amount of cement was procured and stock piled safely to prevent its hardening. The chemical composition of the cement is shown in Table 3.1.

Table 3-1: Chemical Composition of Cement.

Constituent	Weight %
CaO	64.35
SiO <sub>2</sub>	22
Al <sub>2</sub> O <sub>3</sub>	5.64
Fe <sub>2</sub> O <sub>3</sub>	3.8
K <sub>2</sub> O	0.36
MgO	2.11
Na <sub>2</sub> O	0.19
Equivalent alkalis (Na <sub>2</sub> O + 0.658K <sub>2</sub> O)	0.33
SO <sub>3</sub>	2.1
Loss on ignition	0.7
C <sub>3</sub> S	55
C <sub>2</sub> S	19
C <sub>3</sub> A	10
C <sub>4</sub> AF	7

### 3.2.2 Coarse Aggregates

Four aggregate sizes of 12.5 mm ( $\frac{1}{2}$  inch), 9.5 mm ( $\frac{3}{8}$  inch), 4.75 mm ( $\frac{3}{16}$  inch), and 2.36 mm ( $\frac{3}{32}$  inch) crushed limestone from Riyadh Road were used in all the concrete mixtures. Absorption and specific gravity of the coarse aggregates were 1.1% and 2.6%, respectively. The grading of the coarse aggregates was selected conforming to ASTM C 33 size # 67 and is shown in Table 3.2.

Table 3-2: Grading of coarse aggregates.

Sieve opening (mm)	% Retained	Cumulative (% Retained)	% Passing	ASTM C 33 (# 67 Grading)
19	0	0	100	100
12.5	30	30	70	90-100
9.5	30	60	40	40-70
4.75	35	95	5	0-15
2.36	5	100	0	0-5

### 3.2.3 Fine Aggregates

Dune sand with water absorption of 0.6% and specific gravity of 2.56 was used as the fine aggregate.

### 3.2.4 Superplasticizer

Varying dosage of a superplasticizer (SP 430) was used to obtain a slump of  $100 \pm 25$  mm for all the mixtures.

### 3.2.5 Water

Potable water was used for casting and curing of all the concrete specimens.

### 3.3 Waste Products

#### 3.3.1 Bag House Dust (BHD)

BHD was procured from the Saudi Iron and Steel Company (HADEED). Its chemical composition is shown in Table 3.3.

Table 3-3: Chemical Composition of BHD.

Constituent	Weight %
Aluminium	0.7
Calcium	9.39
Cadmium	0.0004
Copper	0.06
Iron	33.6
Potassium	1.7
Magnesium	2.3
Manganese	1.8
Sodium	2.6
Nickel	0.01
Lead	1.31
Phosphorous	0.13
Silicon	2.38
Tin	0.03
Sulphur	0.57
Titanium	0.09
Zinc	10

### 3.3.2 Cement Kiln Dust (CKD)

CKD was obtained from the Saudi Arabian Cement Company, Jeddah, Western Saudi Arabia. Its chemical composition is shown in Table 3.4.

Table 3-4: Chemical Composition of CKD.

Constituent	Weight %
SiO <sub>2</sub>	17.1
CaO	49.3
Al <sub>2</sub> O <sub>3</sub>	4.24
Fe <sub>2</sub> O <sub>3</sub>	2.89
K <sub>2</sub> O	2.18
MgO	1.14
Na <sub>2</sub> O	3.84
P <sub>2</sub> O <sub>5</sub>	0.12
Equivalent alkalis (Na <sub>2</sub> O + 0.658K <sub>2</sub> O)	5.27
SO <sub>3</sub>	3.56
Chloride	6.9
Loss on ignition	15.8
BaO (µg/g)	78.2
Cr <sub>2</sub> O <sub>3</sub>	0.011
CuO	0.029
NiO	0.012
TiO <sub>2</sub>	0.34
V <sub>2</sub> O <sub>5</sub>	0.013
ZnO (µg/g)	65.8
ZrO <sub>2</sub>	0.011

### 3.3.3 Clay

Clay was procured from Hofuf region, Eastern Province, Saudi Arabia. The chemical composition of the clay in the study is shown in Table 3.5.

Table 3-5: Chemical Composition of Clay.

Constituent	Weight %
SiO <sub>2</sub>	43.84
Al <sub>2</sub> O <sub>3</sub>	9.19
Fe <sub>2</sub> O <sub>3</sub>	3.84
MgO	2.02
K <sub>2</sub> O	0.91
Na <sub>2</sub> O	1.26

### 3.3.4 Limestone Powder (LSP)

LSP was obtained from a quarry in Abu Hadriyah, Eastern Province, Saudi Arabia. Its chemical composition is shown in Table 3.6.

Table 3-6: Chemical Composition of LSP.

Constituent	Weight %
SiO <sub>2</sub>	11.79
CaO	45.7
Al <sub>2</sub> O <sub>3</sub>	2.17
Fe <sub>2</sub> O <sub>3</sub>	0.68
MgO	1.8
K <sub>2</sub> O	0.84
Na <sub>2</sub> O	1.72
Na <sub>2</sub> O+(0.658K <sub>2</sub> O)	2.27
Loss on Ignition	35.1
Moisture	0.2

### 3.3.5 Natural Pozzolan (NP)

NP was obtained from volcanic rocks in Western Province of Saudi Arabia. Its chemical composition is shown in Table 3.7.

Table 3-7: Chemical Composition of NP.

<b>Constituent</b>	<b>Weight %</b>
SiO <sub>2</sub>	42.13
Al <sub>2</sub> O <sub>3</sub>	15.33
Fe <sub>2</sub> O <sub>3</sub>	12.21
MgO	8.5
K <sub>2</sub> O	0.84
Na <sub>2</sub> O	2.99

### 3.3.6 Pulverized Steel Slag (PSS)

PSS was procured from the Saudi Iron and Steel Company (HADEED). Its chemical composition is shown in Table 3.8.

Table 3-8: Chemical Composition of PSS.

<b>Constituent</b>	<b>Weight %</b>
SiO <sub>2</sub>	16.47
Al <sub>2</sub> O <sub>3</sub>	6.67
Fe <sub>2</sub> O <sub>3</sub>	26.58
MgO	6.14
K <sub>2</sub> O	0.099
Na <sub>2</sub> O	0.26
Na <sub>2</sub> O+(0.658K <sub>2</sub> O)	0.26
Loss on Ignition	3.8
Moisture	0.2



### 3.4 Supplementary Cementitious Materials (SCMs) or Mineral Admixtures

Mineral admixtures are finely divided siliceous materials which are added to concrete in relatively large amounts, generally in the range 20 to 70 percent by mass of the total cementitious material.

#### 3.4.1 Fly Ash (FA)

FA is a byproduct of burning pulverized coal in electric power generation plants.

The chemical composition of FA used is shown in Table 3.9.

Table 3-9: Chemical Composition of FA.

Constituent	Weight %
SiO <sub>2</sub>	45.3
Al <sub>2</sub> O <sub>3</sub>	34.4
Fe <sub>2</sub> O <sub>3</sub>	2.37
CaO	8.38
MgO	1.86
SO <sub>3</sub>	0.46
K <sub>2</sub> O	0.57
Na <sub>2</sub> O	0.4
L.O.I	3.5

### 3.4.2 Silica Fume (SF)

SF is by-product of the induction arc furnaces in the silicon metal and ferrosilicon alloy industries. The chemical composition of SF used is shown in Table 3.10.

Table 3-10: Chemical Composition of SF.

Constituent	Weight %
SiO <sub>2</sub>	92.5
Al <sub>2</sub> O <sub>3</sub>	0.72
Fe <sub>2</sub> O <sub>3</sub>	0.96
CaO	0.48
MgO	1.78
SO <sub>3</sub>	-
K <sub>2</sub> O	0.84
Na <sub>2</sub> O	0.5
L.O.I	1.55

### 3.5 Concrete Mixture Design

Concrete mixtures were designed according to absolute volume method, and the proportioning of materials was carried out on weight basis. All the concrete mixtures were prepared with cementitious materials of 370 kg/m<sup>3</sup>, effective water to cementitious materials ratio of 0.4, and coarse to total aggregate ratio of 0.6. All the afore-mentioned parameters were kept constant in all the concrete mixtures. A superplasticizer was added to the concrete mixtures to obtain a slump of 100±25 mm. Table 3.11 shows the details of the

quaternary cements investigated while Table 3.12 shows the weights of the materials and Table 3.13 shows the weights of the aggregates used in all the 16 concrete mixtures prepared in this study.

Table 3-11: Details of control and quaternary cement Concrete mixtures.

<b>Mix</b>	<b>OPC, %</b>	<b>SF, %</b>	<b>FA, %</b>	<b>NP, %</b>	<b>BHD, %</b>	<b>CKD, %</b>	<b>Clay, %</b>	<b>LSP, %</b>	<b>PSS, %</b>
M 1	100	0	0						
M 2	95	5	0						
M 3	75	0	25						
M 4	70	0	30						
M 5	75	0	0	25					
M 6	70	0	0	30					
M 7	50	5	30		15				
M 8	50	5	30			15			
M 9	50	5	25				20		
M 10	50	5	25					20	
M 11	50	5	25						20
M 12	50	5	0	30	15				
M 13	50	5	0	30		15			
M 14	50	5	0	25			20		
M 15	70	5	0	25				20	
M 16	75	5	0	25					20

Table 3-12: Weights of materials in the mixtures investigated.

<b>Mix</b>	<b>W/CM</b>	<b>Cement</b> kg/m <sup>3</sup>	<b>S F</b> kg/m <sup>3</sup>	<b>F A</b> kg/m <sup>3</sup>	<b>N P</b> kg/m <sup>3</sup>	<b>BHD</b> kg/m <sup>3</sup>	<b>CKD</b> kg/m <sup>3</sup>	<b>Clay</b> kg/m <sup>3</sup>	<b>LSP</b> kg/m <sup>3</sup>	<b>PSS</b> kg/m <sup>3</sup>
M 1	0.4	370	--	--	--	--	--	--	--	--
M 2	0.4	351.5	18.5	--	--	--	--	--	--	--
M 3	0.4	277.5	--	92.5	--	--	--	--	--	--
M 4	0.4	259	--	111	--	--	--	--	--	--
M 5	0.4	277.5	--	--	92.5	--	--	--	--	--
M 6	0.4	259	--	--	111	--	--	--	--	--
M 7	0.4	185	18.5	111	--	55.5	--	--	--	--
M 8	0.4	185	18.5	111	--	--	55.5	--	--	--
M 9	0.4	185	18.5	92.5	--	--	--	74	--	--
M 10	0.4	185	18.5	92.5	--	--	--	--	74	--
M 11	0.4	185	18.5	92.5	--	--	--	--	--	74
M 12	0.4	185	18.5	--	111	55.5	--	--	--	--
M 13	0.4	185	18.5	--	111	--	55.5	--	--	--
M 14	0.4	185	18.5	--	92.5	--	--	74	--	--
M 15	0.4	185	18.5	--	92.5	--	--	--	74	--
M 16	0.4	185	18.5	--	92.5	--	--	--	--	74

Table 3-13: Weights of aggregates in each mix used in this investigation.

Mix	Coarse Aggregate (Kg/m <sup>3</sup> )					Fine Aggregate (kg/m <sup>3</sup> )
	1/2 "	3/8 "	# 4	# 8	Total	
M 1	341.63	341.63	398.57	56.94	1138.77	759.18
M 2	340.54	340.54	397.29	56.76	1135.13	756.75
M 3	336.17	336.17	392.19	56.03	1120.56	747.04
M 4	335.07	335.07	390.92	55.85	1116.91	744.61
M 5	340.95	340.95	397.77	56.82	1136.49	757.66
M 6	340.81	340.81	397.61	56.8	1136.03	757.36
M 7	329.77	329.77	384.73	54.96	1099.23	732.81
M 8	332.92	332.92	388.41	55.49	1109.74	739.83
M 9	328.79	328.79	383.59	54.8	1095.97	732.65
M 10	324.49	324.49	378.57	54.08	1081.63	721.09
M 11	336.82	336.82	392.96	56.14	1122.74	748.49
M 12	335.5	335.5	391.42	55.92	1118.34	745.56
M 13	338.66	338.66	395.1	56.44	1128.86	752.58
M 14	333.57	333.57	389.17	55.6	1111.91	741.27
M 15	329.27	329.27	384.15	54.88	1097.57	731.71
M 16	341.6	341.6	398.54	56.93	1138.67	759.12

### 3.6 Preparation and Curing of Concrete Specimens

Concrete specimens were prepared and cured to carry out various tests planned in this investigation. Batching of each mix was proportioned by weight. Aggregates were

initially sieved to obtain the required sizes. The concrete constituents were thoroughly mixed in a concrete mixer of 1.7 m<sup>3</sup> capacity till a uniform consistency was obtained. After mixing, the slump was measured then concrete was poured in the moulds. The moulds were then vibrated till complete consolidation was achieved, as indicated a thin film of mortar appeared on the concrete surface. After casting, the specimens were covered with plastic sheet for 24 hours in the laboratory environment ( $22 \pm 3$  °C) to minimize loss of mix water. After 24 hours, the specimens were demoulded and placed in a curing tank till the time of test. Table 3.14 shows the type and number of specimens prepared and tested. Figure 3.2 shows a set of concrete specimens prepared from each mixture.



Figure 3-2: Set of concrete specimens from each concrete mixture.

Table 3-14: Details of concrete specimens and tests.

<b>Property</b>	<b>Specimen size &amp; shape</b>	<b>Test period, days</b>	<b>Test method</b>	<b>Specimens Tested</b>
<b>Compressive Strength</b>	100 mm cubes	3, 7, 28, & 90	ASTM C 39	240
<b>Chloride Permeability</b>	100 x 200 mm cylinders	28	ASTM C 1202	16
<b>Drying Shrinkage</b>	40 x 40 x 160 mm prisms	3, 7, 28, 90 & 180	ASTM C 157	48
<b>Reinforcement Corrosion</b>	75 x 150 mm cylinders	Every 30 days after 28 days of curing	ASTM C 876 & linear polarization resistance method	48
<b>Setting Time</b>	Paste specimens	Fresh paste	ASTM C 191	10
<b>Water Absorption</b>	75 x 150 mm cylinders	28	ASTM C 642	48

## 3.7 Testing of Concrete Specimens

### 3.7.1 Compressive Strength

The compressive strength of a material is that value of the uniaxial compressive stress at which the material fails completely. Strength test results of cubes can be used for quality control purposes. The compressive strength was calculated from the failure load divided by the cross-sectional area resisting the load and reported in mega pascals (MPa). Compressive strength was determined on 100 mm cube specimens according to ASTM C 39 [72] using a digital compression testing machine (MATEST) after 3, 7, 14, 28 and 90 days of water curing. Three specimens were tested at each age and the average values are reported. Figure 3.3 shows the compression testing machine used for compression testing.



Figure 3-3: Compression Testing Machine.



### 3.7.2 Drying Shrinkage

Shrinkage is the reduction in the volume of concrete caused by the loss of water mainly due to evaporation from a freshly hardened concrete exposed to air. Shrinkage may result in the cracking of restrained concrete members. Concrete specimens, 40 x 40 x 160 mm were used for determining the drying shrinkage according to ASTM C 157 [73]. Three specimens were tested and the average values are reported. A set of shrinkage specimens with demec gauge and the measuring device are shown in Figure 3.4.



Figure 3-4: Drying Shrinkage Specimens and dial gauge.

### **3.7.3 Rapid Chloride Permeability**

The rate of reinforcement corrosion is influenced by the electrical resistivity of concrete. The rapid chloride penetration test (RCPT) has been developed as a quick test to measure the electrical resistance of concrete. Chloride permeability was determined on a 50 mm thick disk which was sliced from the center of the 100 x 200 mm cylindrical specimen according to ASTM C1202. The curved surface of the disk was coated with an epoxy coating to avoid evaporation of moisture during testing. The disk specimens were saturated with water under vacuum and kept saturated for about 24 hours. The saturated disk specimen was clamped between two cells and a potential difference of 60 V DC was maintained across them. The upstream cell was filled with 3% sodium chloride (NaCl) solution and the downstream cell was filled with 0.3 M sodium hydroxide (NaOH) solution. The current flowing in the electric circuit was monitored through a resistor at every 30 min for a period of six hours. The value of current for each cell was calculated and the total charge passed through the specimen was determined. The whole test was performed at room temperature of 20 to 25 °C. Three specimens were tested and the average values are reported. The quality of material is quantitatively assessed based on the total charge passed during the test, which is considered to be a measure of the chloride permeability of concrete. Typical chloride permeability specimens, cells and setup are

shown in Figures 3.5 and 3.6, respectively. Table 3.15 shows the concrete classification based on the chloride permeability values according to ASTM C1202.



Figure 3-5: Specimens and cells utilized for determining the Rapid Chloride Permeability.

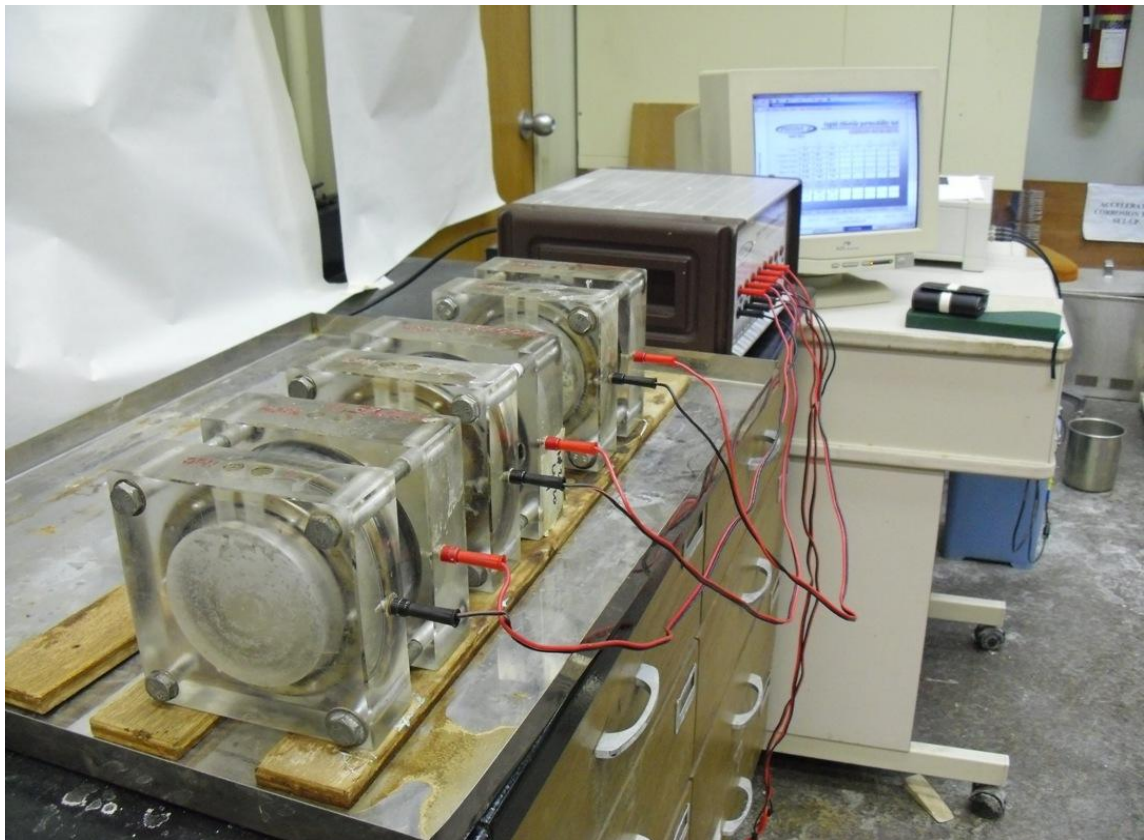


Figure 3-6: Rapid Chloride Permeability Test Setup.

Table 3-15: Chloride Permeability and its Classification.

Charge passed, Coulombs	Concrete Classification
<1000	Very Low
1000–2000	Low
2000–4000	Moderate
>4000	High
>4000	High

### 3.7.4 Reinforcement Corrosion

Reinforcement corrosion was evaluated by measuring corrosion potentials and corrosion current density. The concrete specimens were partially (4 cm from the bottom) exposed to 5% NaCl and potentials were measured after every two weeks while the corrosion current density was measured every month.

#### ***Corrosion Potentials***

Corrosion potentials were measured to evaluate the probability of reinforcement corrosion. The corrosion status is related to the measured corrosion potential value. For this purpose, reinforcement corrosion was monitored by exposing reinforced concrete specimens, 75 mm in diameter and 150 mm high with a centrally placed 12 mm diameter steel bar, as shown in Figure 3.7, to 5% sodium chloride solution after 28 days of curing and corrosion potentials were measured according to ASTM C 876 [74]. Saturated calomel electrode (SCE) was used as the reference electrode. If the potential reaches a threshold value  $-270$  mV, then there is a 90% probability for initiation of reinforcement corrosion.

Three specimens were tested and the average values are reported. The potential measurement setup is depicted in Figure 3.8 while Figure 3.9 shows a set of reinforced concrete specimens. Table 3.16 indicates the possibility of reinforcement corrosion as reported in ASTM C 876 [74].

Table 3-16: Probability of Occurrence of Reinforcement Corrosion.

Open circuit potential (OCP) values		Corrosion condition
(mV vs. SCE)	(mV vs. CSE)	
< -426	< -500	Severe corrosion
< -276	< -350	High (<90% risk of corrosion)
> -125 but < -276	> -200 but < -350	Intermediate corrosion risk
> -125	< -200	Low(10% risk of corrosion)

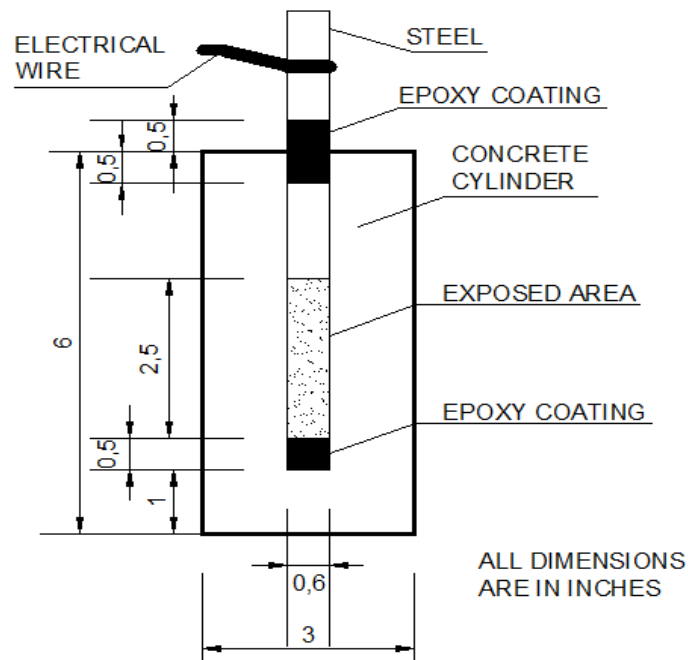


Figure 3-7: Reinforcement Corrosion Specimen.





Figure 3-8: Corrosion Potential Measurement Setup.



Figure 3-9: Specimens utilized for corrosion potentials and corrosion rate measurements.

### ***Corrosion Current Density***

The corrosion current density measurements provide an indication of the rate at which the reinforcement corrosion is progressing. This information is of great importance in knowing the extent of corrosion damage and in predicting the remaining service life, which is useful in taking decisions regarding the repair and rehabilitation works. The

corrosion current density was measured according to the linear polarization resistance method (LPRM) [75].

In the LPRM experiments, a stainless steel plate was used as a counter electrode. The steel bar and stainless steel plate was connected to a Potentiostat/Galvanostat. The polarization resistance ( $R_p$ ) was determined by conducting a linear polarization scan in the range of  $\pm 10$  mV of the corrosion potential. A scan rate of 0.1 mV/s was used. The corrosion current density ( $I_{corr}$ ) was determined using the Stern and Geary formula shown below [75]. A schematic representation of the experimental set-up utilized to measure  $I_{corr}$  on steel in the concrete specimens is shown in Figure 3.10 and the experimental set-up is in Figure 3.11 and 3.12. Three specimens were tested and the average  $I_{corr}$  values are reported.

$$I_{corr} = B/R_p$$

Where  $I_{corr}$  = Corrosion current density,  $\mu\text{A}/\text{cm}^2$ ,

$R_p$  = Polarization resistance  $\Omega \text{ cm}^2$ ,

$$B = \frac{(\beta_a * \beta_c)}{2.3(\beta_a + \beta_c)}$$

$\beta_a$  and  $\beta_c$  are the anodic and cathodic Tafel constants, mV/decade respectively.

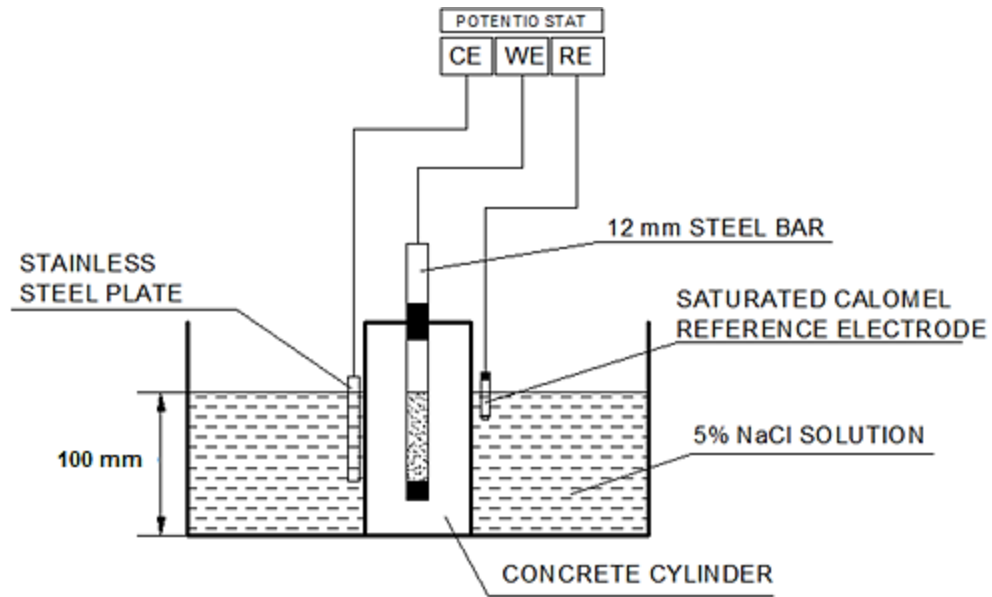


Figure 3-10: Schematic Representation of the Corrosion Current Density Measurements.

The Tafel constants are normally obtained by polarizing the steel to 250 mV of the corrosion potential (Tafel plot). However, in the absence of sufficient data on  $\beta_a$  and  $\beta_c$ , a value of B equal to 26 mV for steel in active condition and 52 mV for steel in passive condition is often used. Lambert et al. [17] and Al-Amoudi et al. [18] reported a good correlation between corrosion rates determined using these values and the gravimetric weight loss method.





Figure 3-11: Corrosion Current Density Measurement Setup.



Figure 3-12: A close-up view of the concrete specimen with counter and reference electrodes.

### 3.7.5 Setting Time

The term setting is used to describe the stiffening of the cement paste. The initial set indicates that the paste is beginning to stiffen considerably and can no longer be moulded. Final set indicates that the cement has hardened to the point at which it can sustain marginal load. The setting time was determined using the Vicat apparatus according to ASTM C 191[76]. The initial setting time is the time from the instant at which water is added to the cement to the instant at which the Vicat needle penetrates 25 mm into the cement paste. The final setting time corresponds to the time at which the needle does not sink visibly into the cement paste. The setup used to determine the initial and final setting time is shown in Figure 3.13.



Figure 3-13: Vicat Apparatus.

### 3.7.6 Water Absorption

Some voids will be left behind after the hydration of cement. These voids affect the strength and durability of concrete. With the presence of air voids in concrete, it is vulnerable to penetration and attack by aggressive ions, such as sulfates, chlorides, CO<sub>2</sub> etc. A good quality concrete is characterized by having minimal voids left by excess water and, therefore, water absorption test is adopted for assessing the quality of concrete in terms of density, durability and imperviousness.

The water absorption was determined using 75 mm diameter and 150 mm high cylindrical concrete specimens according to ASTM C 642 [77] after 28 days of water curing. First, the specimens were dried in oven for 24 hours at a temperature of 110 °C and then their weights were recorded. They were then soaked in water for 48 hours and their saturated surface dry weights were taken. Water absorption was calculated utilizing the following formula.

$$\text{Water Absorption} = \frac{A - B}{B} \times 100\%$$

A = Weight of saturated surface dried specimen, and

B = Weight of oven dried specimen.

Three specimens were tested and the average values are reported. Equipment used for determining the water absorption is shown in Figure 3.14.



(a) Cylindrical Specimens      (b) Specimens dried in oven      (c) Specimens immersed in water

Figure 3-14: Equipment Used to Determine Water Absorption. .

## CHAPTER 4

### RESULTS AND DISCUSSION

The experimental program was discussed in Chapter 3. In this chapter, the results of the experimental work conducted in this study to produce Quaternary Cement Concrete (QCC) by replacing 50% cement by 30–35% supplementary cementing materials (FA or NP with SF) and 15–20% of the selected local materials (BHD, CKD, Clay, LSP or PSS) are presented.

#### 4.1 Compressive Strength

The average compressive strength of concrete specimens, tested after 3, 7, 14, 28, and 90 days of water curing is presented in Tables 4.1 through 4.3. The results have been grouped into two categories: (i) QCC specimens produced by replacing 50% cement with 5% silica fume, 25–30% fly ash and 15–20% by a local material (BHD, CKD, Clay, LSP or PSS), i.e. Mix 7, 8, 9, 10 and 11; (ii) QCC specimens produced by replacing 50% cement with 5% silica fume, 25–30% natural pozzolan and 15–20% by a locally available material (BHD, CKD, Clay, LSP or PSS), i.e. Mix 12, 13, 14, 15 and 16.

Table 4-1: Average Compressive Strength of Plain and five Control mixes.

<b>Age, days</b>	<b>100% OPC</b>	<b>95%C + 5%SF</b>	<b>75%C + 25%FA</b>	<b>70%C + 30%FA</b>	<b>75%C + 25%NP</b>	<b>70%C + 30%NP</b>
3	38.16	40.85	30.49	28.95	28.91	28.68
7	43.75	46.53	35.77	36.36	36.08	31.67
14	47.84	50.26	38.30	40.00	39.88	35.77
28	53.22	56.20	46.32	48.65	42.03	40.06
90	61.64	64.52	55.59	56.62	50.80	48.91

Table 4-2: Average Compressive Strength of Group-I QCC mixes.

<b>Age, Days</b>	<b>50%C + 5%SF + 30%FA + 15%BHD</b>	<b>50%C + 5%SF + 30%FA + 15%CKD</b>	<b>50%C + 5%SF + 25%FA + 20%Clay</b>	<b>50%C + 5%SF + 25%FA + 20%LSP</b>	<b>50%C + 5%SF + 25%FA + 20%PSS</b>
3	16.60	22.22	20.90	20.11	22.91
7	19.36	26.27	26.74	29.79	27.98
14	25.46	33.82	32.76	36.54	34.57
28	33.34	44.77	42.00	42.55	38.03
90	37.47	53.35	51.37	52.51	47.38

Table 4-3: Average Compressive Strength of Group-II QCC mixes.

<b>Age, Days</b>	<b>50%C + 5%SF + 30%NP + 15%BHD</b>	<b>50%C + 5%SF + 30%NP + 15%CKD</b>	<b>50%C + 5%SF + 25%NP + 20%Clay</b>	<b>50%C + 5%SF + 25%NP + 20%LSP</b>	<b>50%C + 5%SF + 25%NP + 20%PSS</b>
3	21.95	27.69	22.54	19.94	17.55
7	28.25	31.56	28.57	22.76	21.54
14	32.99	38.14	34.63	30.07	26.88
28	36.62	40.89	38.78	36.69	36.69
90	42.87	48.66	44.86	43.30	43.30

The compressive strength development in quaternary cement concrete specimens replacing 50% cement with 5% silica fume (SF), 30% fly ash (FA) and 15% bag house dust (BHD) and the three control mixes is plotted in Figure 4.1. The compressive strength increased with age in all the mixes. Incorporation of silica fume (SF) in plain cement concrete increased the compressive strength while in the other mixes, the compressive strength decreased with the cement replacement. The compressive strength of the QCC specimens was the least though it doubled after 90 days from its 3 day strength. After 90 days of curing, the compressive strength of plain, 95% OPC with 5% SF, 70% OPC with 30% FA and 50% OPC with 5% SF + 30% FA + 15% BHD was 61.64, 64.52, 56.62 and 37.47 MPa, respectively.

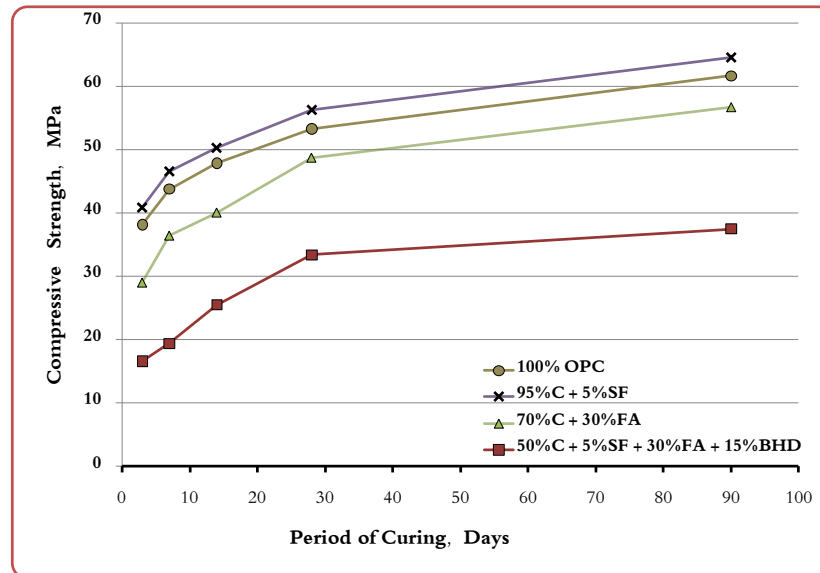


Figure 4-1: Compressive Strength Development of QCC Specimens Prepared with 15% BHD.

The compressive strength development in quaternary cement concrete specimens replacing 50% cement with 5% silica fume (SF), 30% fly ash (FA) and 15% cement kiln dust (CKD) and the three control mixes is plotted in Figure 4.2. The compressive strength increased with age in all the mixes. Incorporation of silica fume (SF) in plain cement concrete increased the compressive strength while in the other mixes, the compressive strength decreased with the cement replacement; though the strength differential was not that significant. The compressive strength of the QCC specimens was the least though it doubled after 90 days from its 3 day strength. After 90 days of curing, the compressive strength of plain, 95% OPC with 5% SF, 70% OPC with 30% FA and 50% OPC with 5%SF + 30%FA + 15% CKD was 61.64, 64.52, 56.62 and 53.35 MPa, respectively.

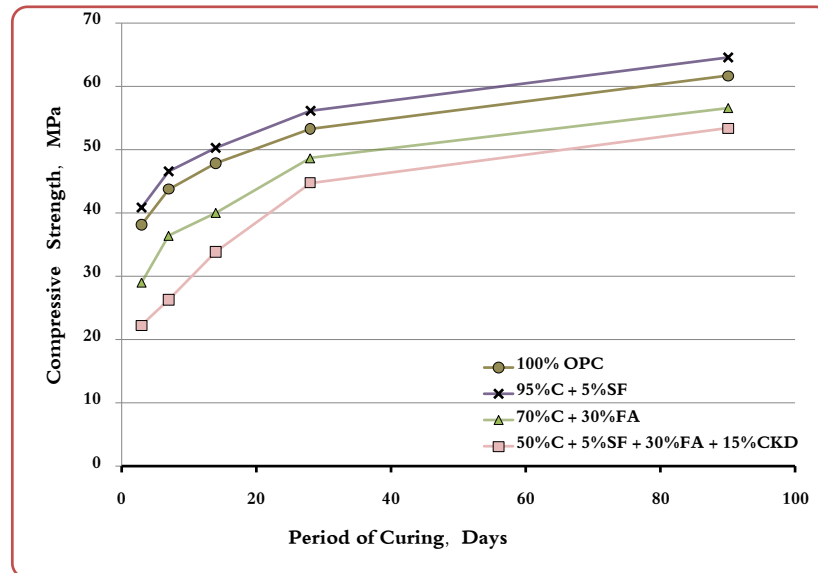


Figure 4-2: Compressive Strength Development of QCC Specimens Prepared with 15% CKD.



The compressive strength development in quaternary cement concrete specimens replacing 50% cement with 5% silica fume (SF), 25% fly ash (FA) and 20% clay (Clay) and the three control mixes is plotted in Figure 4.3. The compressive strength increased with age in all the mixes. Incorporation of silica fume (SF) in plain cement concrete increased the compressive strength while in the other mixes, the compressive strength decreased with the cement replacement; though the strength differential was not that significant. The compressive strength of the QCC specimens was the least though it doubled after 90 days from its 3 day strength. After 90 days of curing, the compressive strength of plain, 95% OPC with 5% SF, 75% OPC with 25% FA and 50% OPC with 5% SF + 25%FA + 20% Clay was 61.64, 64.52, 55.59 and 51.37 MPa, respectively.

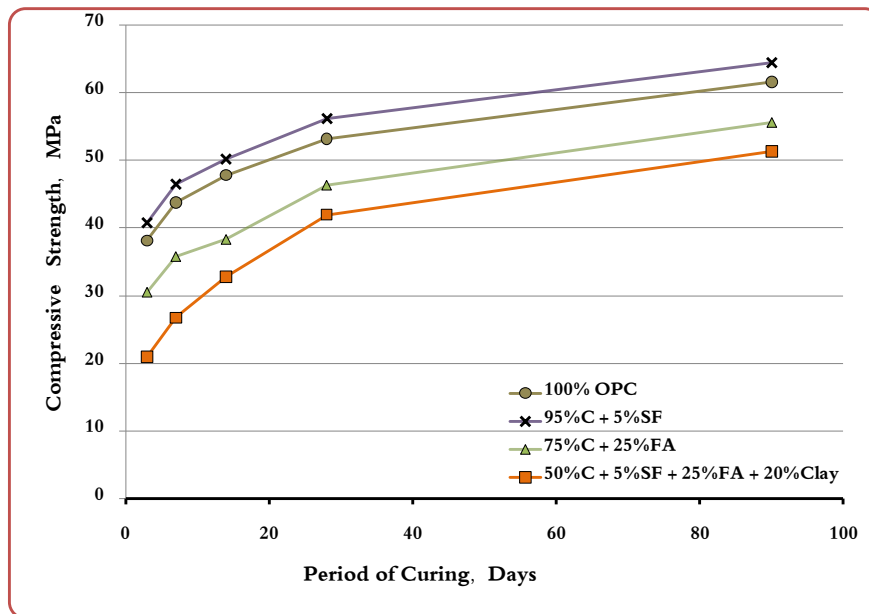


Figure 4-3: Compressive Strength Development of QCC Specimens Prepared with 20% Clay.

The compressive strength development in quaternary cement concrete specimens replacing 50% cement with 5% silica fume (SF), 25% fly ash (FA) and 20% lime stone powder (LSP) and the three control mixes is plotted in Figure 4.4. The compressive strength increased with age in all the mixes. Incorporation of silica fume (SF) in plain cement concrete increased the compressive strength while in the other mixes, the compressive strength decreased with the cement replacement; though the strength differential was not that significant. The compressive strength of the QCC specimens was the least though it doubled after 90 days from its 3 day strength. After 90 days of curing, the compressive strength of plain, 95% OPC with 5% SF, 75% OPC with 25% FA and 50% OPC with 5% SF + 25% FA + 20% LSP was 61.64, 64.52, 55.59 and 52.51 MPa, respectively.

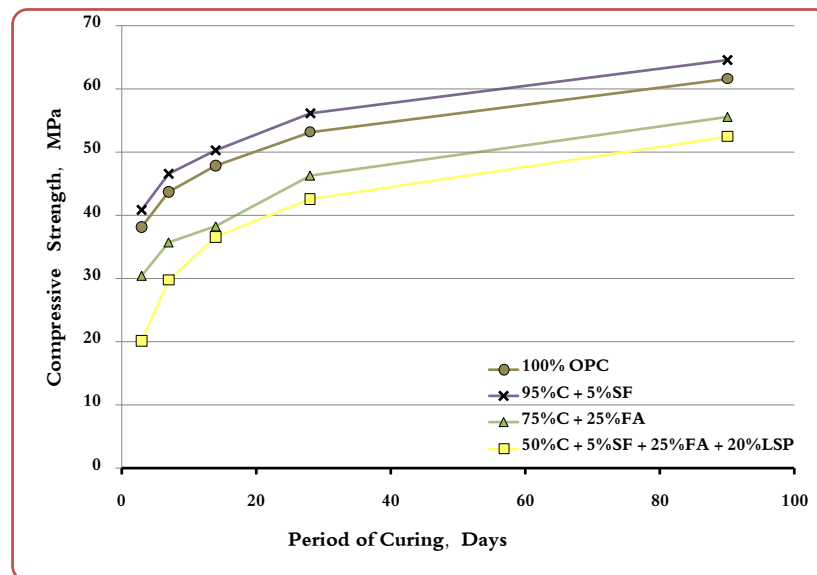


Figure 4-4: Compressive Strength Development of QCC Specimens Prepared with 20% LSP.

The compressive strength development in quaternary cement concrete specimens replacing 50% cement with 5% silica fume (SF), 25% fly ash (FA) and 20% pulverized steel slag (PSS) and the three control mixes is plotted in Figure 4.5. The compressive strength increased with age in all the mixes. Incorporation of silica fume (SF) in plain cement concrete increased the compressive strength while in the other mixes, the compressive strength decreased with the cement replacement. The compressive strength of the QCC specimens was the least though it doubled after 90 days from its 3 day strength. After 90 days of curing, the compressive strength of plain, 95% OPC with 5% SF, 75% OPC with 25% FA and 50% OPC with 5% SF + 25% FA + 20% PSS was 61.64, 64.52, 55.59 and 52.51 MPa, respectively.

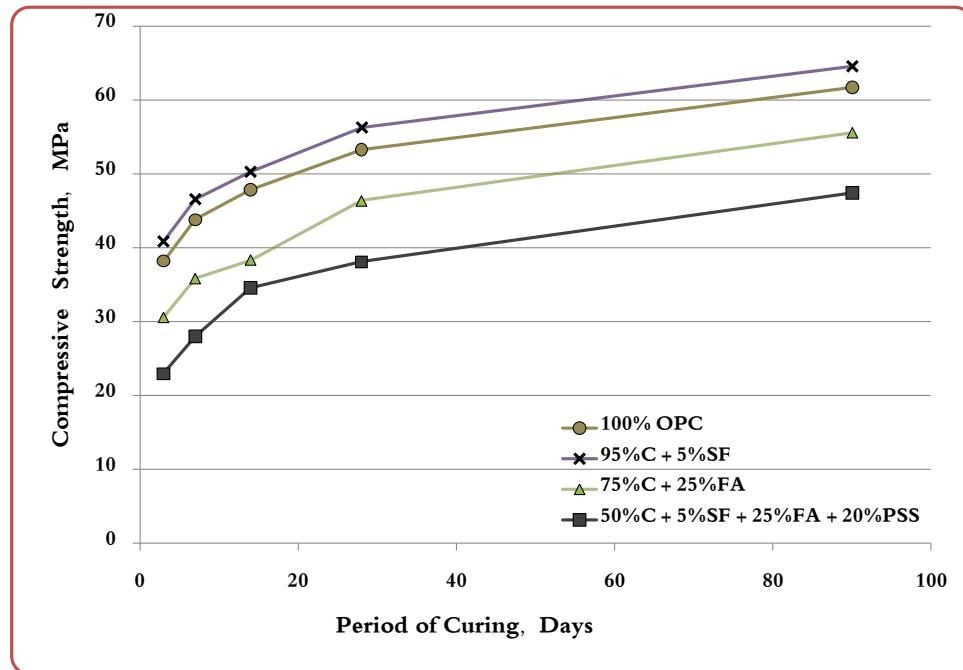


Figure 4-5: Compressive Strength Development of QCC Specimens Prepared with 20% PSS.

The compressive strength development in quaternary cement concrete specimens replacing 50% cement with 5% silica fume (SF), 30% natural pozzolan (NP) and 15% bag house dust (BHD) and the three control mixes is plotted in Figure 4.6. The compressive strength increased with age in all the mixes. Incorporation of silica fume (SF) in plain cement concrete increased the compressive strength while in the other mixes, the compressive strength decreased with the cement replacement. The compressive strength of the QCC specimens was the least though it doubled after 90 days from its 3 day strength. After 90 days of curing, the compressive strength of plain, 95% OPC with 5% SF, 70% OPC with 30% NP and 50% OPC with 5% SF + 30% NP + 15% BHD was 61.64, 64.52, 48.91 and 42.87 MPa, respectively.

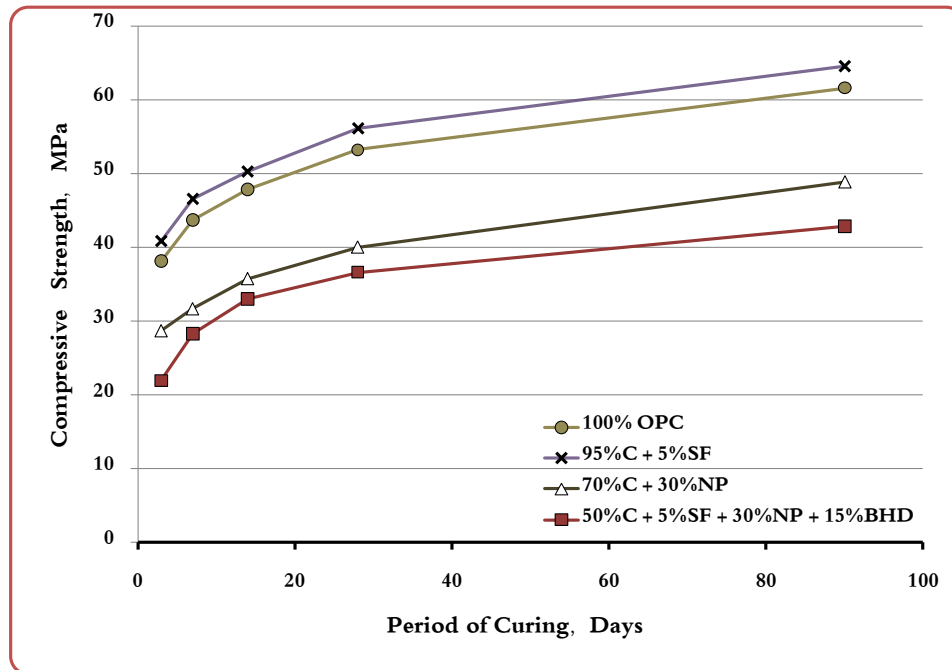


Figure 4-6: Compressive Strength Development of QCC Specimens Prepared with 15% BHD.

The compressive strength development in quaternary cement concrete specimens replacing 50% cement with 5% silica fume (SF), 30% natural pozzolan (NP) and 15% cement kiln dust (CKD) and the three control mixes is plotted in Figure 4.7. The compressive strength increased with age in all the mixes. Incorporation of silica fume (SF) in plain cement concrete increased the compressive strength while in the other mixes, the compressive strength decreased with the cement replacement; though the strength differential was not that significant. The compressive strength of the QCC specimens was the least though it doubled after 90 days from its 3 day strength. After 90 days of curing, the compressive strength of plain, 95% OPC with 5% SF, 70% OPC with 30% NP and 50% OPC with 5%SF + 30%NP + 15% CKD was 61.64, 64.52, 48.91 and 48.66 MPa, respectively.

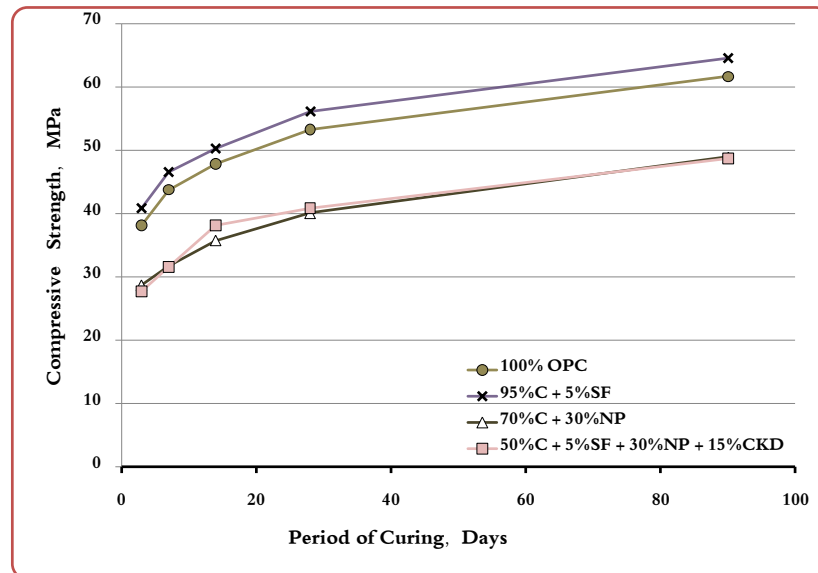


Figure 4-7: Compressive Strength Development of QCC Specimens Prepared with 15% CKD.

The compressive strength development in quaternary cement concrete specimens replacing 50% cement by 5% silica fume (SF), 25% natural pozzolan (NP) and 20% clay (Clay) and the three control mixes is plotted in Figure 4.8. The compressive strength increased with age in all the mixes. Incorporation of silica fume (SF) in plain cement concrete increased the compressive strength while in the other mixes, the compressive strength decreased with the cement replacement; though the strength differential was not that significant. The compressive strength of the QCC specimens was the least though it doubled after 90 days from its 3 day strength. After 90 days of curing, the compressive strength of plain, 95% OPC with 5% SF, 75% OPC with 25% NP and 50% OPC with 5%SF + 25% NP + 20% Clay was 61.64, 64.52, 50.80 and 44.86 MPa, respectively.

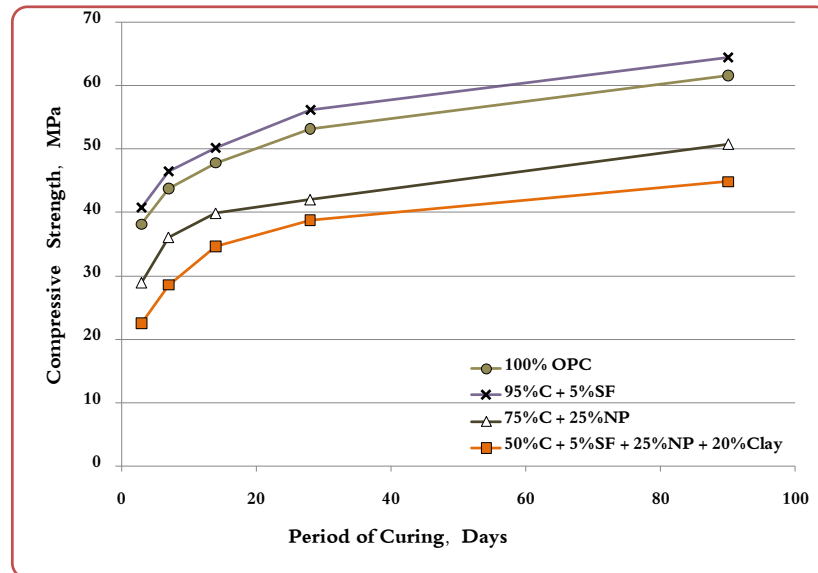


Figure 4-8: Compressive Strength Development of QCC Specimens Prepared with 20% Clay.

The compressive strength development in quaternary cement concrete specimens replacing 50% cement with 5% silica fume (SF), 25% natural pozzolan (NP) and 20% lime stone powder (LSP) and the three control mixes is plotted in Figure 4.9. The compressive strength increased with age in all the mixes. Incorporation of silica fume (SF) in plain cement concrete increased the compressive strength while in the other mixes, the compressive strength decreased with the cement replacement; though the strength differential was not that significant. The compressive strength of the QCC specimens was the least though it doubled after 90 days from its 3 day strength. After 90 days of curing, the compressive strength of plain, 95% OPC with 5% SF, 75% OPC with 25% NP and 50% OPC with 5% SF + 25% NP + 20% C was 61.64, 64.52, 50.80 and 43.30 MPa, respectively.

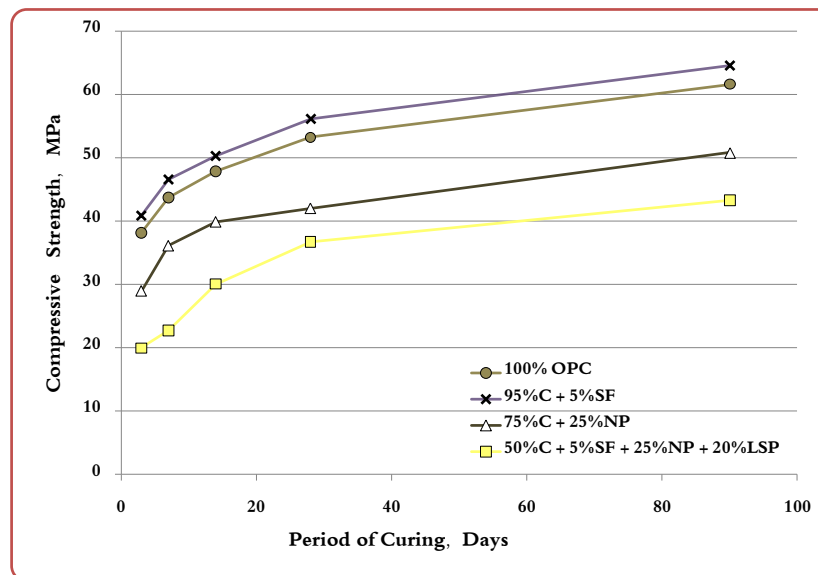


Figure 4-9: Compressive Strength Development of QCC Specimens Prepared with 20% LSP.

The compressive strength development in quaternary cement concrete specimens replacing 50% cement with 5% silica fume (SF), 25% natural pozzolan (NP) and 20% pulverized steel slag (PSS) and the three control mixes is plotted in Figure 4.10. The compressive strength increased with age in all the mixes. Incorporation of silica fume (SF) in plain cement concrete increased the compressive strength while in the other mixes, the compressive strength decreased with the cement replacement. The compressive strength of QCC specimens was the least though it doubled after 90 days from its 3 day strength. After 90 days of curing, the compressive strength of plain, 95% OPC with 5% SF, 75% OPC with 25% NP and 50% OPC with 5% SF + 25% NP + 20% C was 61.64, 64.52, 50.80 and 43.30 MPa, respectively.

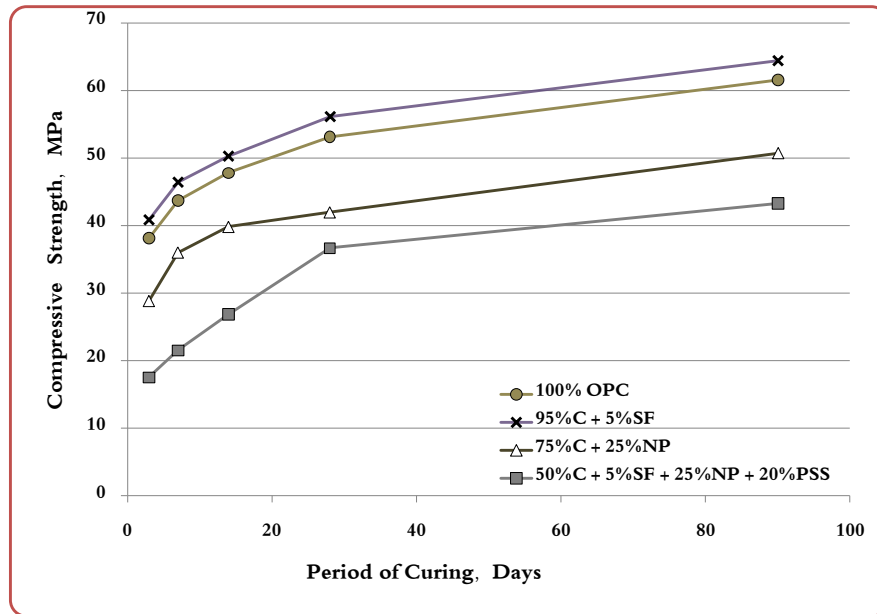


Figure 4–10: Compressive Strength Development of QCC Specimens Prepared with 20% PSS.



## 4.2 Chloride Permeability

The average chloride permeability of concrete specimens, tested after 28 days of water curing is presented in Tables 4.4 through 4.6. The results have been grouped into two categories: (i) QCC specimens produced by replacing 50% cement with 5% silica fume, 25–30% fly ash and 15–20% by a local material (BHD, CKD, Clay, LSP or PSS), i.e. Mix 7, 8, 9, 10 and 11; (ii) QCC specimens produced by replacing 50% cement with 5% silica fume, 25–30% natural pozzolan and 15–20% by a locally available material (BHD, CKD, Clay, LSP or PSS), i.e. Mix 12, 13, 14, 15 and 16.

Table 4-4: Average Chloride Permeability of Plain and five Control mixes.

Period of Curing, Days	Chloride Permeability, Coulombs					
	100% OPC	95%C + 5%SF	75%C + 25%FA	70%C + 30%FA	75%C + 25%NP	70%C + 30%NP
28	2540	1613	1486	1366	1504	1681

Table 4-5: Average Chloride Permeability of Group-I QCC mixes.

Period of Curing, Days	Chloride Permeability, Coulombs				
	50%C + 5%SF + 30%FA + 15%BHD	50%C + 5%SF + 30%FA + 15%CKD	50%C + 5%SF + 25%FA + 20%Clay	50%C + 5%SF + 25%FA + 20%LSP	50%C + 5%SF + 25%FA + 20%PSS
28	1181	1240	805	2211	1532

Table 4-6: Average Chloride Permeability of Group-II QCC mixes.

Period of Curing, Days	Chloride Permeability, Coulombs				
	50%C + 5%SF + 30%NP + 15%BHD	50%C + 5%SF + 30%NP + 15%CKD	50%C + 5%SF + 25%NP + 20%Clay	50%C + 5%SF + 25%NP + 20%LSP	50%C + 5%SF + 25%NP + 20%PSS
28	3178	2373	2048	3074	2553

The chloride permeability in quaternary cement concrete specimens replacing 50% cement with 5% silica fume (SF), 30% fly ash (FA) and 15% bag house dust (BHD) and the three control mixes is plotted in Figure 4.11. The chloride permeability of all these concrete specimens decreased with the level of cement replacement. The chloride permeability of plain cement concrete specimens was the highest whereas incorporation of fly ash (FA) or silica fume (SF) in plain cement concrete decreased the chloride permeability significantly. The chloride permeability of the QCC specimens was the least. After 28 days of curing, the chloride permeability of plain, 95% OPC with 5% SF, 70% OPC with 30% FA and 50% OPC with 5% SF + 30% FA + 15% BHD was 2540, 1613, 1366 and 1181 Coulombs, respectively.

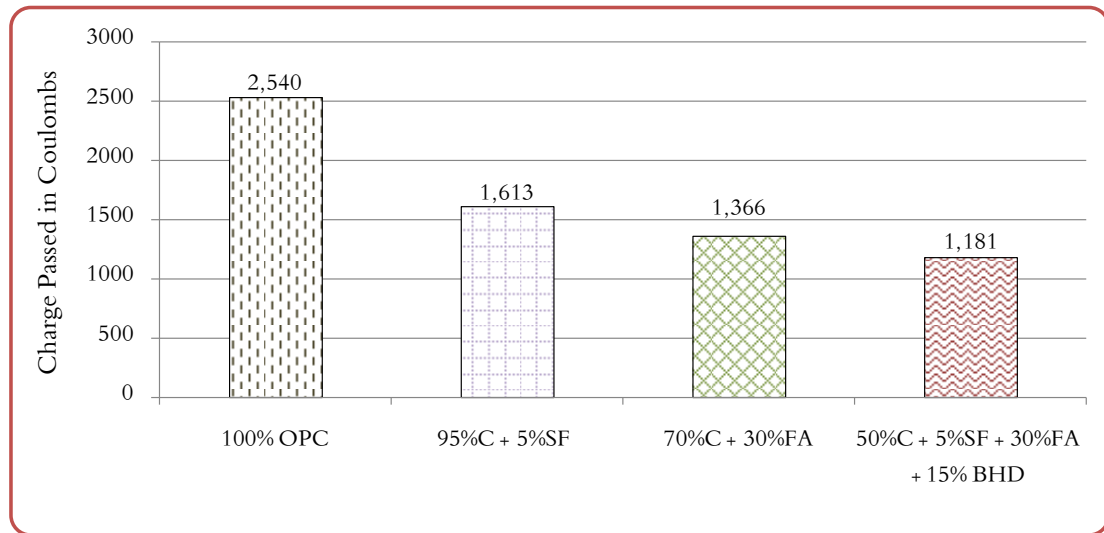


Figure 4-11: Chloride permeability of QCC specimens with 15% BHD after 28 days of curing.

The chloride permeability in quaternary cement concrete specimens replacing the 50% cement with 5% silica fume (SF), 30% fly ash (FA) and 15% cement kiln dust (CKD) and the three control mixes is plotted in Figure 4.12. The chloride permeability of all these concrete specimens decreased with the level of cement replacement. The chloride permeability of plain cement concrete specimens was the highest whereas incorporation of fly ash (FA) or silica fume (SF) in plain cement concrete decreased the chloride permeability significantly. The chloride permeability of the QCC specimens was the least. After 28 days of curing, the chloride permeability of plain, 95% OPC with 5% SF, 70% OPC with 30% FA and 50% OPC with 5% SF + 30% FA + 15% CKD was 2540, 1613, 1366 and 1240 Coulombs, respectively.

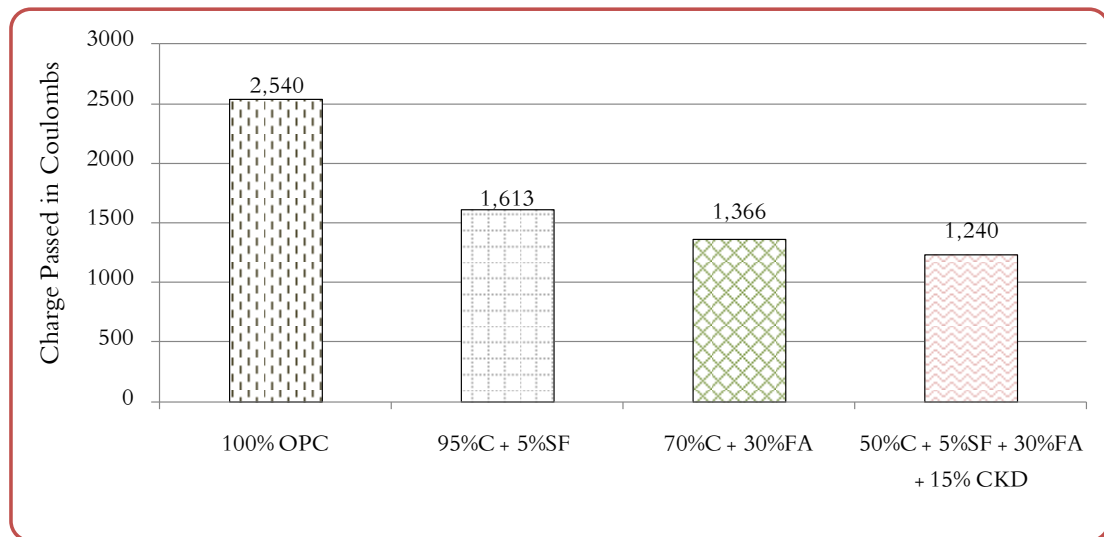


Figure 4-12: Chloride permeability of QCC specimens with 15% CKD after 28 days of curing.

The chloride permeability in quaternary cement concrete specimens replacing 50% cement with 5% silica fume (SF), 25% fly ash (FA) and 20% clay (Clay) and the three control mixes is plotted in Figure 4.13. The chloride permeability of all these concrete specimens decreased with the level of cement replacement. The chloride permeability of plain cement concrete specimens was the highest whereas incorporation of fly ash (FA) or silica fume (SF) in plain cement concrete decreased the chloride permeability significantly. The chloride permeability of the QCC specimens was the least. After 28 days of curing, the chloride permeability of plain, 95% OPC with 5% SF, 75% OPC with 25% FA and 50% OPC with 5% SF + 25% FA + 20% Clay was 2540, 1613, 1486 and 805 Coulombs, respectively.

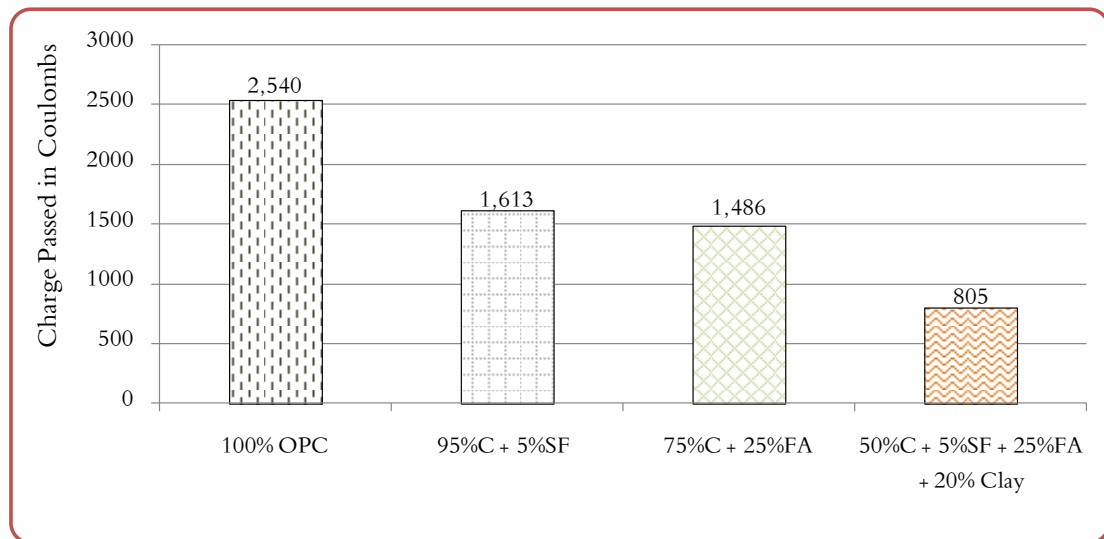


Figure 4-13: Chloride permeability of QCC specimens with 20% Clay after 28 days of curing.

The chloride permeability in quaternary cement concrete specimens replacing 50% cement with 5% silica fume (SF), 25% fly ash (FA) and 20% lime stone powder (LSP) is plotted against three control mixes in Figure 4.14. The chloride permeability of all these concrete specimens decreased with the level of cement replacement. The chloride permeability of plain cement concrete specimens was the highest whereas incorporation of fly ash (FA) or silica fume (SF) in plain cement concrete decreased the chloride permeability significantly. The chloride permeability of the QCC specimens was the least. After 28 days of curing, the chloride permeability of plain, 95% OPC with 5% SF, 75% OPC with 25% FA and 50% OPC with 5% SF + 25% FA + 15% LSP was 2540, 1613, 1486 and 2211 Coulombs, respectively.

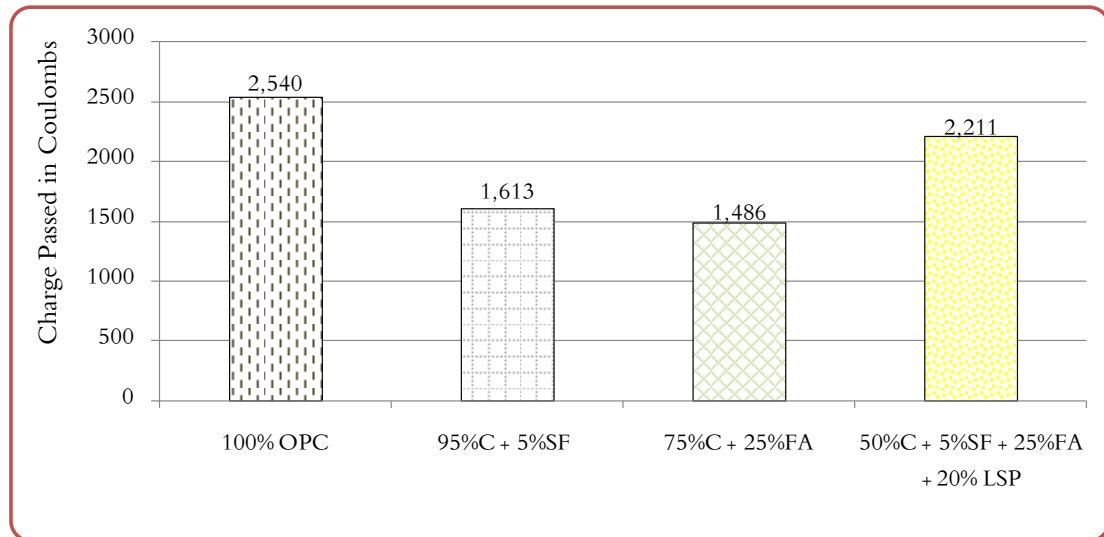


Figure 4-14: Chloride permeability of QCC specimens with 20% LSP after 28 days of curing.

The chloride permeability in quaternary cement concrete specimens replacing 50% cement with 5% silica fume (SF), 25% fly ash (FA) and 20% pulverized steel slag (PSS) is plotted against three control mixes in Figure 4.15. The chloride permeability of all these concrete specimens decreased with the level of cement replacement. The chloride permeability of plain cement concrete specimens was the highest whereas incorporation of fly ash (FA) or silica fume (SF) in plain cement concrete decreased the chloride permeability significantly. The chloride permeability of the QCC specimens was the least. After 28 days of curing, the chloride permeability of plain, 95% OPC with 5% SF, 75% OPC with 25% FA and 50% OPC with 5% SF + 25% FA + 15% PSS was 2540, 1613, 1486 and 1532 Coulombs, respectively.

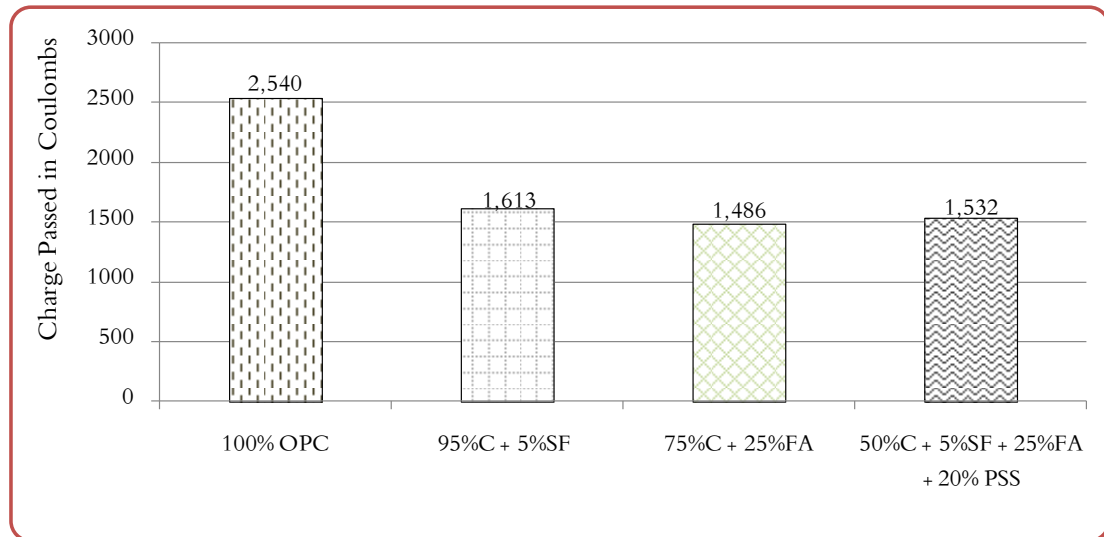


Figure 4-15: Chloride permeability of QCC specimens with 20% PSS after 28 days of curing.

The chloride permeability in quaternary cement concrete specimens replacing 50% cement with 5% silica fume (SF), 30% natural pozzolan (NP) and 15% bag house dust (BHD) and three control mixes is plotted against in Figure 4.16. The chloride permeability of all the concrete specimens decreased with the level of cement replacement. The chloride permeability of plain cement concrete specimens was the highest whereas incorporation of natural pozzolan (NP) or silica fume (SF) in plain cement concrete decreased the chloride permeability significantly. The chloride permeability of the QCC specimens was the least. After 28 days of curing, the chloride permeability of plain, 95% OPC with 5% SF, 70% OPC with 30% NP and 50% OPC with 5% SF + 30% NP + 15% BHD was 2540, 1613, 1681 and 3178 Coulombs, respectively.

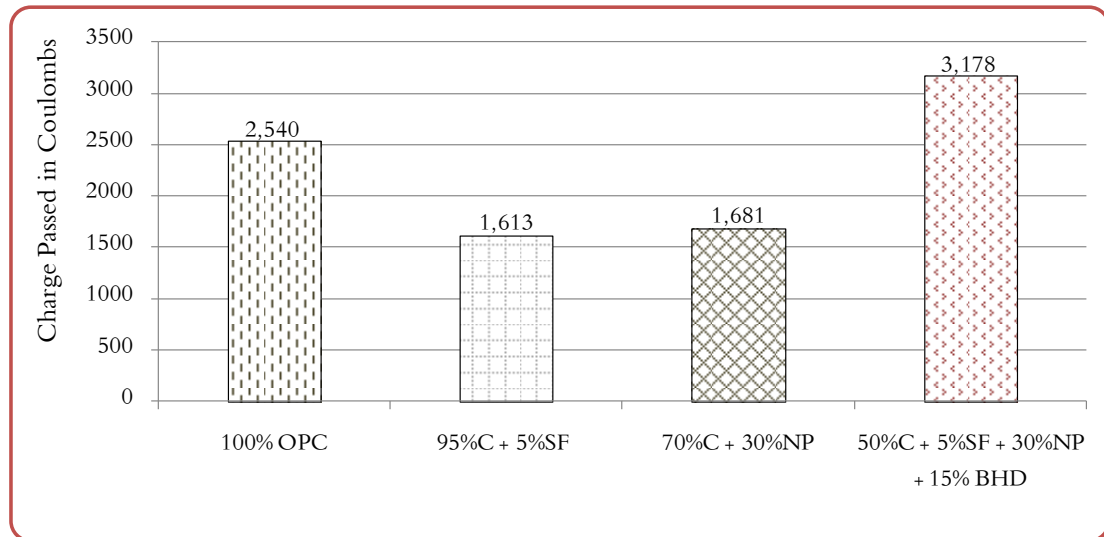


Figure 4-16: Chloride permeability of QCC specimens with 15% BHD after 28 days of curing.

The chloride permeability in quaternary cement concrete specimens replacing 50% cement with 5% silica fume (SF), 30% natural pozzolan (NP) and 15% cement kiln dust (CKD) and the three control mixes is plotted in Figure 4.17. The chloride permeability of all these concrete specimens decreased with the level of cement replacement. The chloride permeability of plain cement concrete specimens was the highest whereas incorporation of natural pozzolan (NP) or silica fume (SF) in plain cement concrete decreased the chloride permeability significantly. The chloride permeability of the QCC specimens was the least. After 28 days of curing, the chloride permeability of plain, 95% OPC with 5% SF, 70% OPC with 30% NP and 50% OPC with 5% SF + 30% NP + 15% CKD was 2540, 1613, 1681 and 2373 Coulombs, respectively.

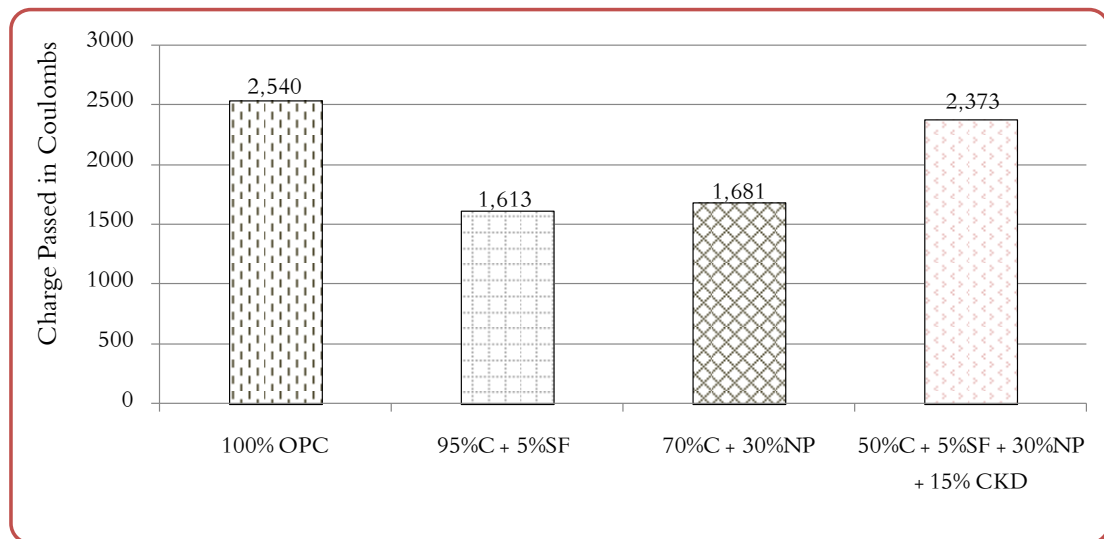


Figure 4-17: Chloride permeability of QCC specimens with 15% CKD after 28 days of curing.



The chloride permeability in quaternary cement concrete specimens replacing 50% cement with 5% silica fume (SF), 25% natural pozzolan (NP) and 20% clay (Clay) and the three control mixes is plotted in Figure 4.18. The chloride permeability of all these concrete specimens decreased with the level of cement replacement. The chloride permeability of plain cement concrete specimens was the highest whereas incorporation of natural pozzolan (NP) or silica fume (SF) in plain cement concrete decreased the chloride permeability significantly. The chloride permeability of the QCC specimens was the least. After 28 days of curing, the chloride permeability of plain, 95% OPC with 5% SF, 75% OPC with 25% NP and 50% OPC with 5% SF + 25% NP + 20% Clay was 2540, 1613, 1504 and 2048 Coulombs, respectively.

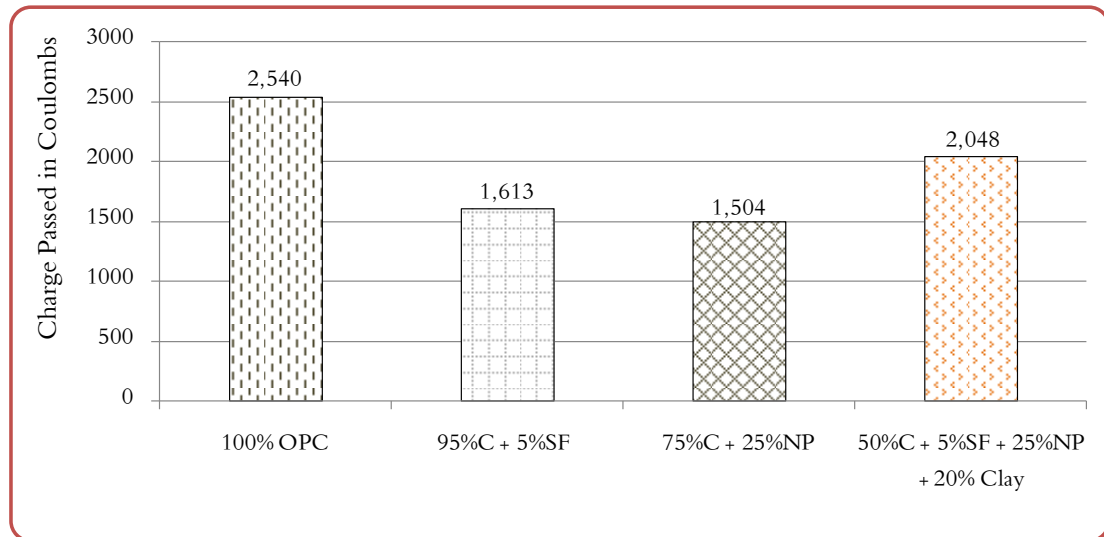


Figure 4-18: Chloride permeability of QCC specimens with 20% Clay after 28 days of curing.

The chloride permeability in quaternary cement concrete specimens replacing 50% cement with 5% silica fume (SF), 25% natural pozzolan (NP) and 20% lime stone powder (LSP) and the three control mixes is plotted in Figure 4.19. The chloride permeability of all these concrete specimens decreased with the level of cement replacement. The chloride permeability of plain cement concrete specimens was the highest whereas incorporation of natural pozzolan (NP) or silica fume (SF) in plain cement concrete decreased the chloride permeability significantly. The chloride permeability of the QCC specimens was the least. After 28 days of curing, the chloride permeability of plain, 95% OPC with 5% SF, 75% OPC with 25% NP and 50% OPC with 5% SF + 25% NP + 15% LSP was 2540, 1613, 1504 and 3074 Coulombs, respectively.

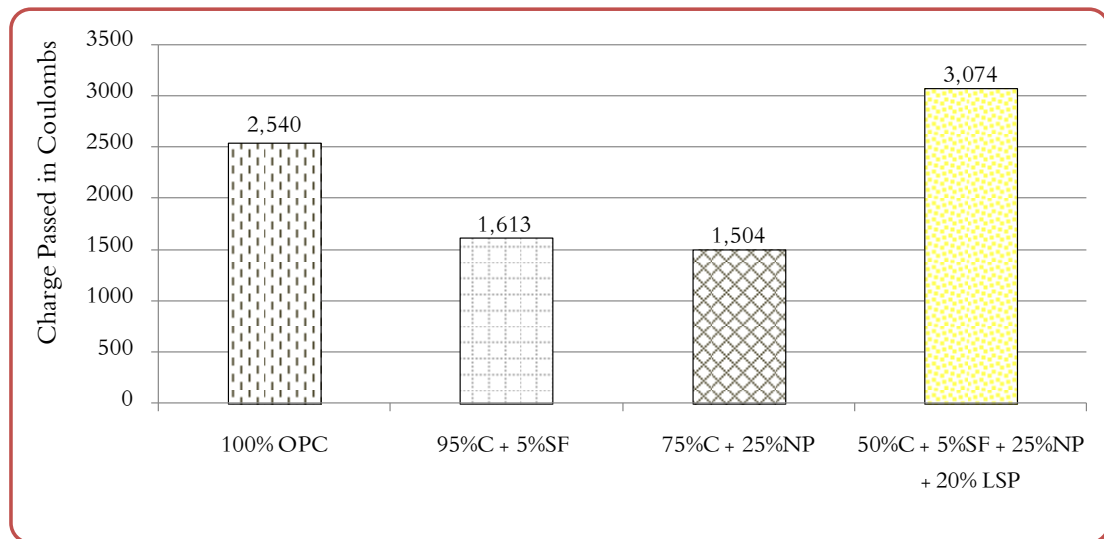


Figure 4-19: Chloride permeability of QCC specimens with 20% LSP after 28 days of curing.

The chloride permeability in quaternary cement concrete specimens replacing 50% cement with 5% silica fume (SF), 25% natural pozzolan (NP) and 20% pulverized steel slag (PSS) and the three control mixes is plotted in Figure 4.20. The chloride permeability of all the concrete specimens decreased with the level of cement replacement. The chloride permeability of plain cement concrete specimens was the highest whereas incorporation of natural pozzolan (NP) or silica fume (SF) in plain cement concrete decreased the chloride permeability significantly. The chloride permeability of the QCC specimens was the least. After 28 days of curing, the chloride permeability of plain, 95% OPC with 5% SF, 75% OPC with 25% NP and 50% OPC with 5% SF + 25% NP + 15% PSS was 2540, 1613, 1504 and 2553 Coulombs, respectively.

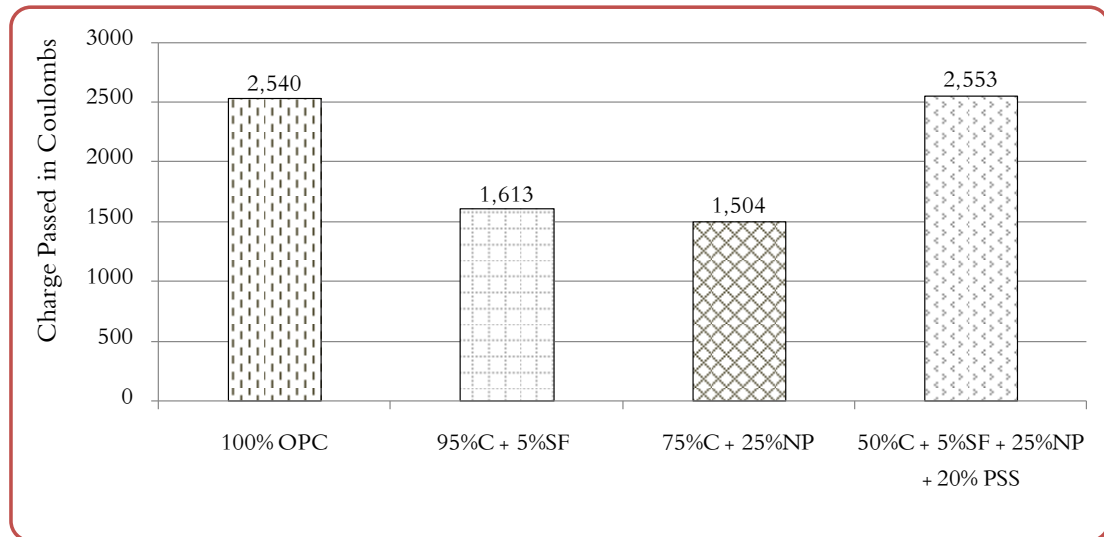


Figure 4-20: Chloride permeability of QCC specimens with 20% PSS after 28 days of curing.

### **4.3 Corrosion Potentials**

The corrosion potentials of concrete specimens were recorded twice a month. The results have been grouped into two categories: (i) QCC specimens produced by replacing 50% cement with 5% silica fume, 25–30% fly ash and 15–20% by a selected local material (BHD, CKD, Clay, LSP or PSS), i.e. Mix 7, 8, 9, 10 and 11; (ii) QCC specimens produced by replacing 50% cement with 5% silica fume, 25–30% natural pozzolan and 15–20% by a locally available material (BHD, CKD, Clay, LSP or PSS), i.e. Mix 12, 13, 14, 15 and 16.

The corrosion potentials on steel in quaternary cement concrete specimens replacing 50% cement with 5% silica fume (SF), 25–30% fly ash (FA) natural pozzolan (NP) and 15–20% locally available material and three control mixes are plotted and discussed in their respective figures. The potentials decreased (became more negative) with time of exposure to the chloride solution in all the reinforced concrete specimens. The corrosion potentials of QCC specimens were less negative than those in the plain cement concrete during 300 days of exposure. A similar trend was observed in fly ash, natural pozzolan and silica fume cement concrete specimens.

The corrosion potentials on steel in quaternary cement concrete specimens replacing 50% cement with 5% silica fume (SF), 30% fly ash (FA) and 15% bag house dust (BHD) and three control mixes are plotted in Figure 4.21. The potentials decreased (became more negative) with time of exposure to the chloride solution in all the reinforced concrete specimens. The corrosion potentials of QCC specimens were less negative than those in the plain cement concrete during 300 days of exposure. A similar trend was observed in fly ash and silica fume cement concrete specimens. The time to initiation of corrosion (i.e., to cross the -270 mV line) of plain, 95% OPC with 5% SF, 70% OPC with 30% FA and 50% OPC with 5% SF + 30% FA + 15% BHD was about 202, 186, 251 days, respectively. However, corrosion initiation was not noted in the QCC specimens.

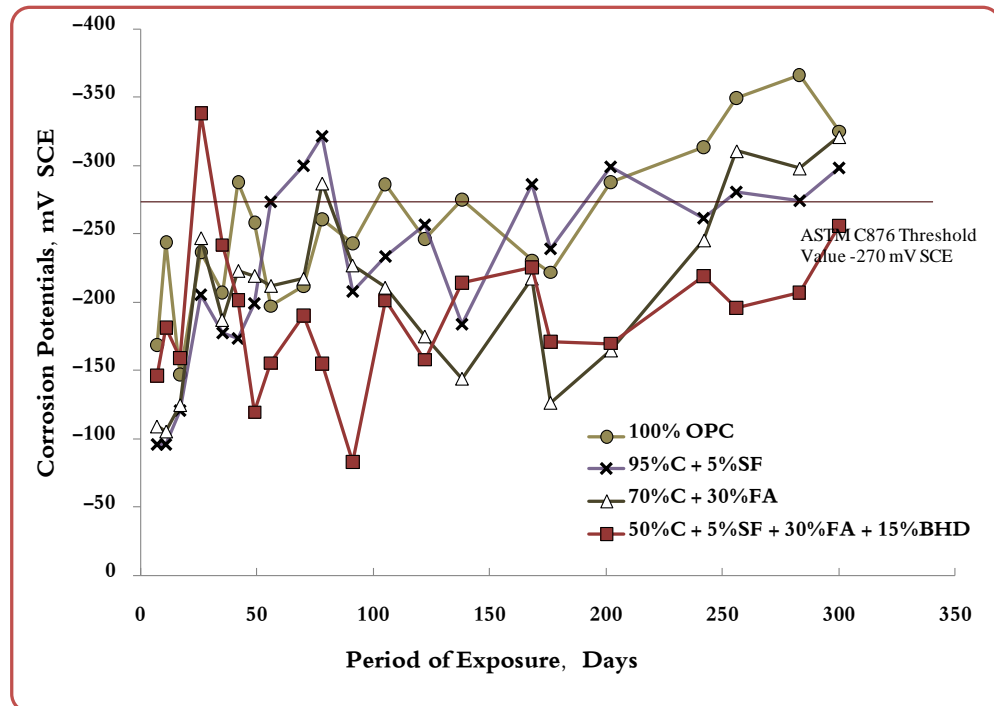


Figure 4-21: Corrosion Potentials on Steel in the QCC Specimens Prepared with 15% BHD.

The corrosion potentials on steel in quaternary cement concrete specimens replacing 50% cement with 5% silica fume (SF), 30% fly ash (FA) and 15% cement kiln dust (CKD) and three control mixes are plotted in Figure 4.22. The corrosion potentials of QCC specimens were more negative than the ASTM C 876 threshold value of -270 mV SCE since the time of immersion in the chloride solution. The corrosion potentials on steel in the concrete specimens with fly ash or silica fume were less negative than that of plain cement concrete. The time to initiation of corrosion (i.e., to cross the -270 mV line) of plain, 95% OPC with 5% SF and 70% OPC with 30% FA was about 202, 186 and 251 days, respectively.

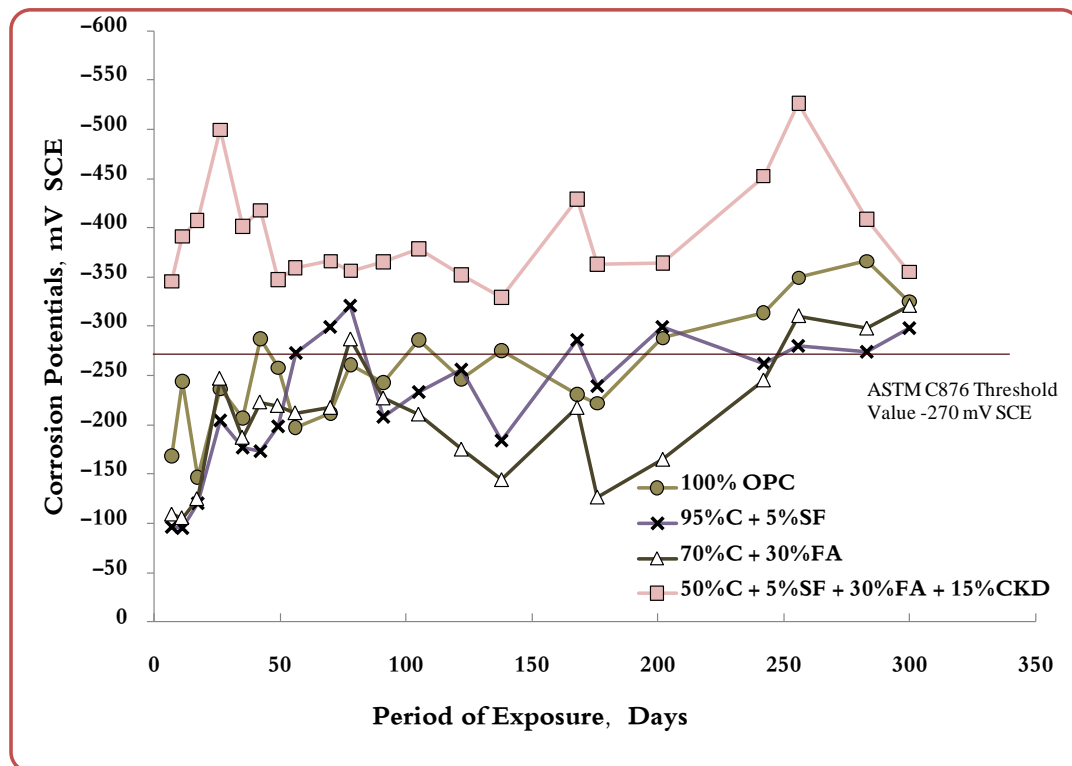


Figure 4-22: Corrosion Potentials on Steel in the QCC Specimens Prepared with 15% CKD.

The corrosion potentials on steel in quaternary cement concrete specimens replacing 50% cement with 5% silica fume (SF), 25% fly ash (FA) and 20% Clay and three control mixes are plotted in Figure 4.23. The corrosion potentials of the QCC specimens were less negative than those in the plain cement concrete specimens. A similar trend was observed in the fly ash and silica fume cement concrete specimens. The time to initiation of corrosion (i.e., to cross the -270 mV potential) of plain, 95% OPC with 5% SF, 50% OPC with 5% SF + 25% FA + 20% Clay was about 202, 186 days, respectively. However, corrosion initiation was noted in the QCC and fly ash cement concrete specimens.

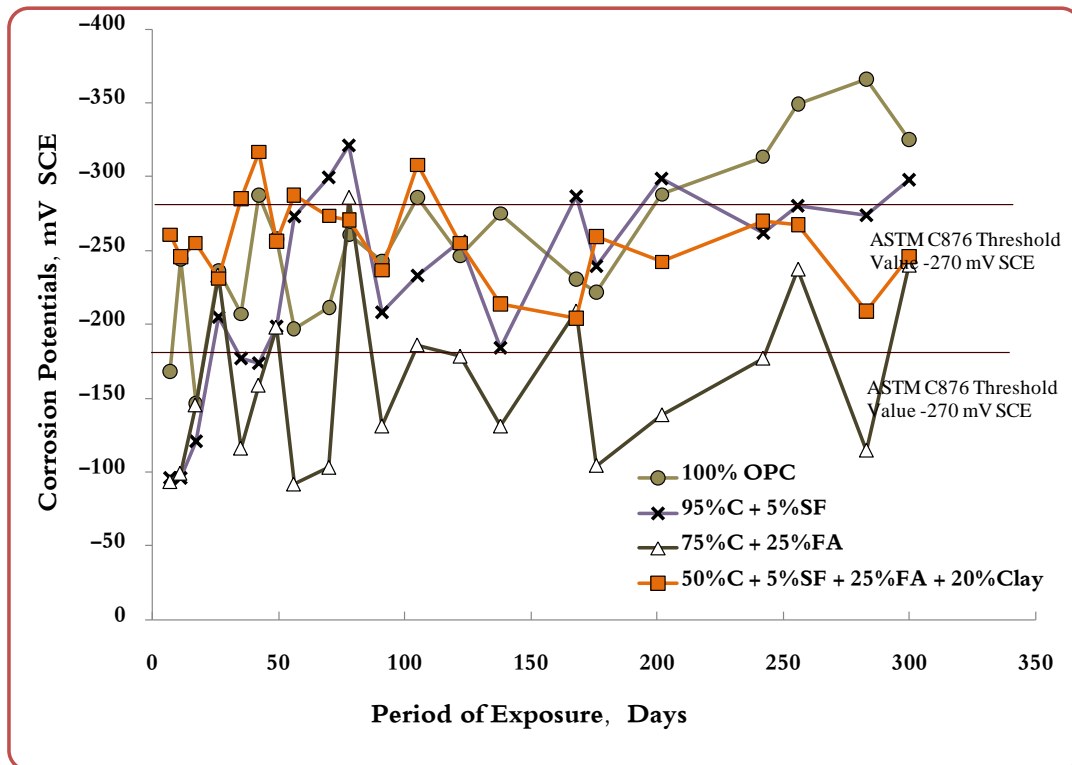


Figure 4-23: Corrosion Potentials on Steel in the QCC Specimens Prepared with 20% Clay.

The corrosion potentials on steel in quaternary cement concrete specimens replacing 50% cement with 5% silica fume (SF), 25% fly ash (FA) and 20% lime stone powder (LSP) and three control mixes are plotted in Figure 4.24. The corrosion potentials of the QCC specimens were more than those in the plain cement concrete specimens during 300 days of exposure. The corrosion potentials on steel in the concrete specimens with fly ash or silica fume were less than that of plain cement concrete. The time to initiation of corrosion (i.e., to cross the -270 mV potential) of plain, 95% OPC with 5% SF, 50% OPC with 5% SF + 25% FA + 20% LSP was about 202, 186 and 175 days, respectively.

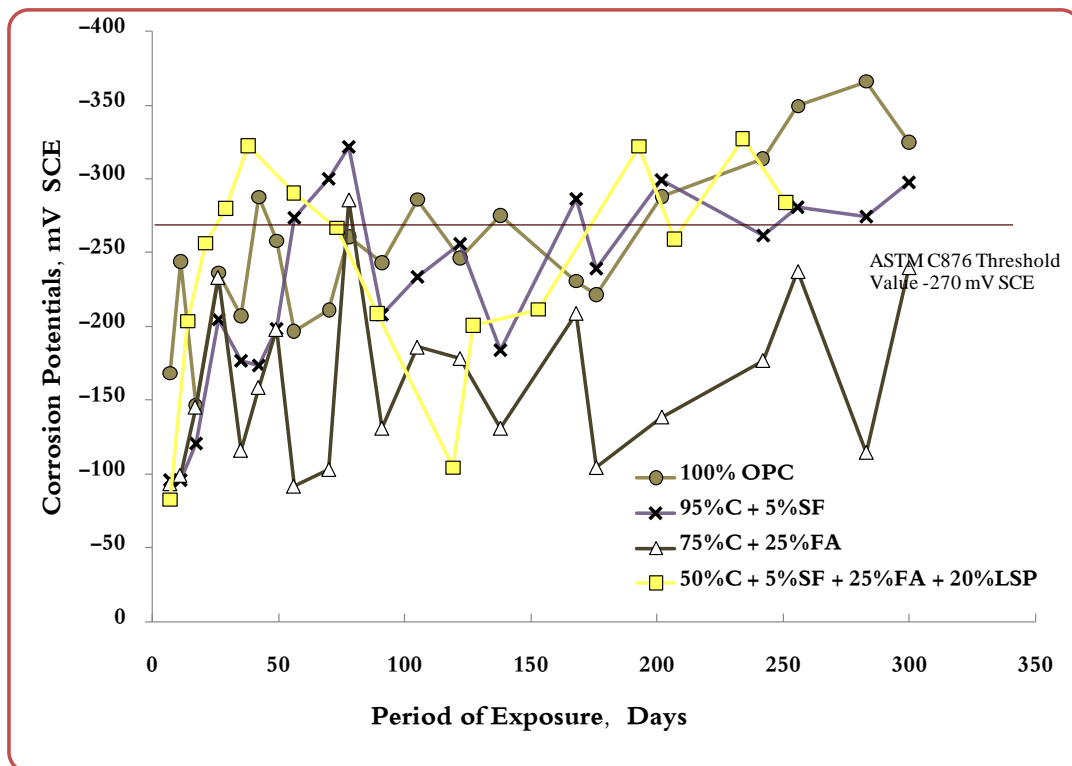


Figure 4-24: Corrosion Potentials on Steel in the QCC Specimens Prepared with 20% LSP.



The corrosion potentials on steel in quaternary cement concrete specimens replacing 50% cement with 5% silica fume (SF), 25% fly ash (FA) and 20% pulverized steel slag (PSS) and three control mixes are plotted in Figure 4.25. The corrosion potentials on the QCC specimens were almost similar to those in the plain cement concrete specimens. The corrosion potentials on steel in the concrete specimens with fly ash or silica fume were less than that of plain cement concrete. The time to initiation of corrosion (i.e., to cross the -270 mV potential) of plain, 95% OPC with 5% SF, 50% OPC with 5% SF + 25% FA + 20% PSS was about 202, 186 and 145 days, respectively.

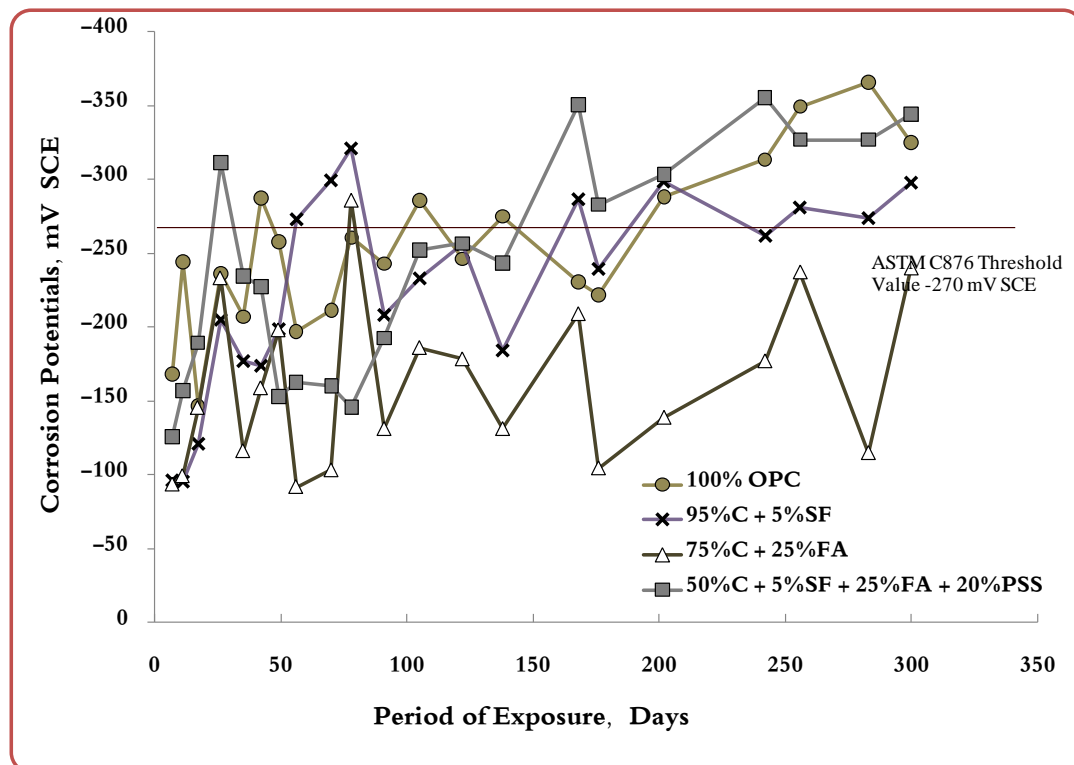


Figure 4-25: Corrosion Potentials on Steel in the QCC Specimens Prepared with 20% PSS.

The corrosion potentials on steel in quaternary cement concrete specimens replacing 50% cement with 5% silica fume (SF), 30% natural pozzolan (NP) and 15% bag house dust (BHD) and the three control mixes are plotted in Figure 4.26. The potentials decreased (became more negative) with time of exposure to the chloride solution. The corrosion potentials on steel in the concrete specimens with natural pozzolan or silica fume were less than that of plain cement concrete. The time to initiation of corrosion (i.e., to cross the -270 mV potential line) of plain, 95% OPC with 5% SF, 70% OPC with 30% NP and 50% OPC with 5% SF + 30% NP + 15% BHD was about 202, 186, 150 and 192 days, respectively.

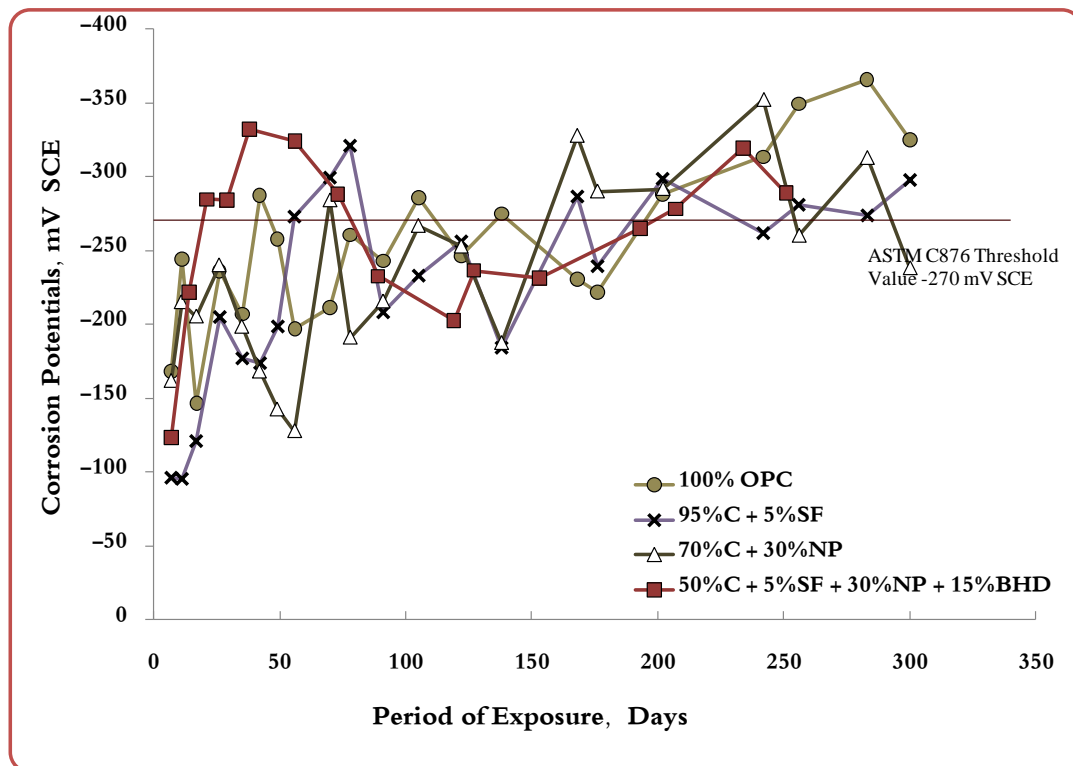


Figure 4-26: Corrosion Potentials on Steel in the QCC Specimens Prepared with 15% BHD.

The corrosion potentials on steel in quaternary cement concrete specimens replacing 50% cement with 5% silica fume (SF), 30% natural pozzolan (NP) and 15% cement kiln dust (CKD) and the three control mixes are plotted in Figure 4.27. The corrosion potentials of the QCC specimens were more negative than the ASTM C 876 threshold value of -270 mV CSE after 20 days to the chloride solution. The corrosion potentials on steel in the other concrete specimens were almost similar. The time to initiation of corrosion (i.e., to cross the -270 mV potential) of plain, 95% OPC with 5% SF, 70% OPC with 30% NP and 50% OPC with 5% SF + 30% NP + 15% CKD was about 202, 186, 150 and 18 days, respectively.

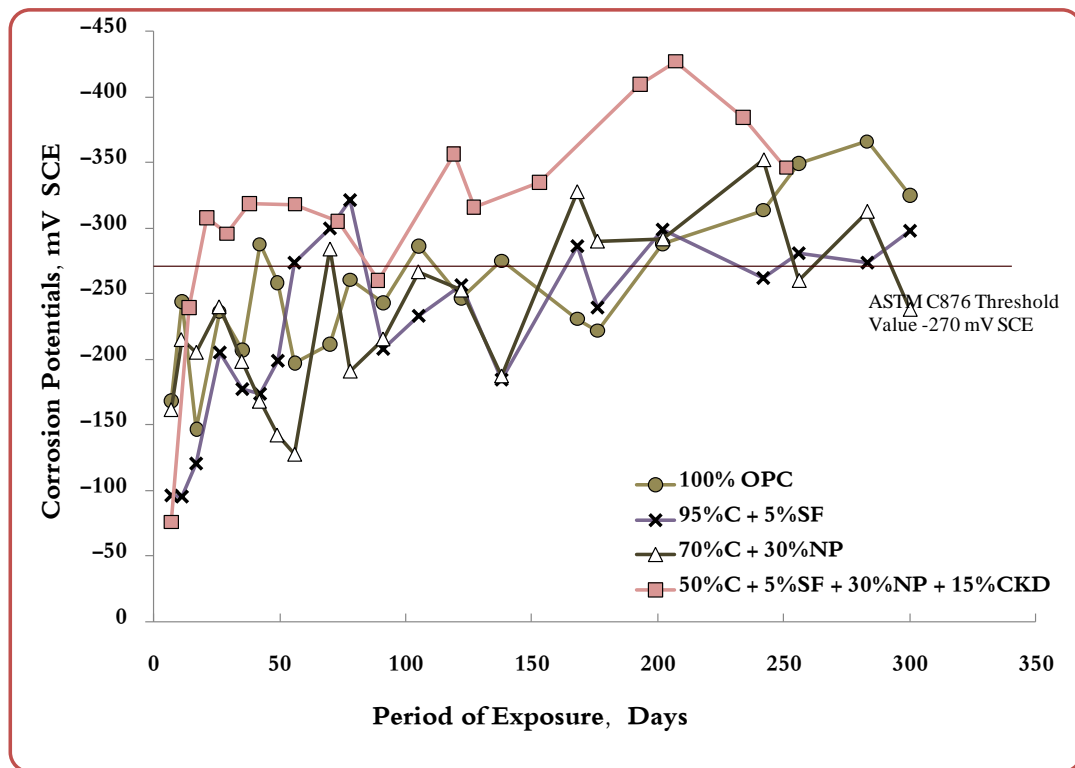


Figure 4-27: Corrosion Potentials on Steel in the QCC Specimens Prepared with 15% CKD.

The corrosion potentials on steel in quaternary cement concrete specimens replacing 50% cement with 5% silica fume (SF), 25% natural pozzolan (NP) and 20% Clay and the three control mixes are plotted in Figure 4.28. The potentials decreased (became more negative) with time of exposure to the chloride solution in all the reinforced concrete specimens. The corrosion potentials on steel in the concrete specimens with natural pozzolan or silica fume were less than that of plain cement concrete. The time to initiation of corrosion (i.e., to cross the  $-270$  mV potential) of plain, 95% OPC with 5% SF, 75% OPC with 25% NP and 50% OPC with 5% SF + 25% NP + 20% Clay was about 202, 186, 262, and 238 days, respectively.

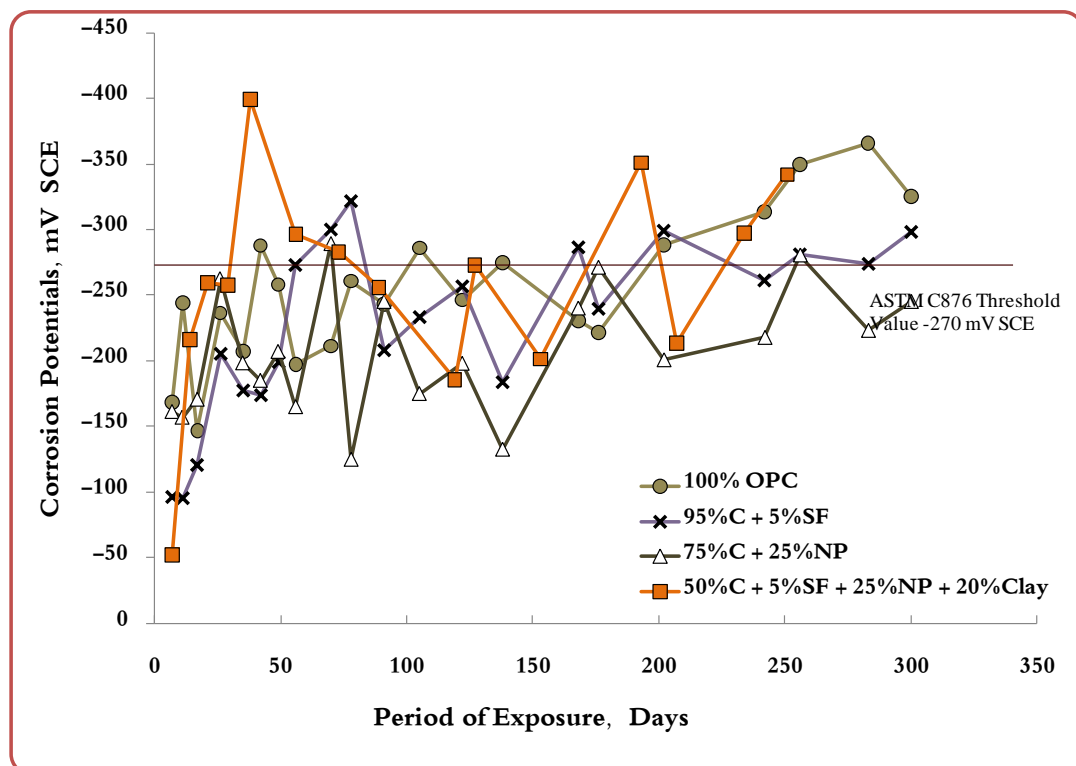


Figure 4-28: Corrosion Potentials on Steel in the QCC Specimens Prepared with 20% Clay.

The corrosion potentials on steel in quaternary cement concrete specimens replacing 50% cement with 5% silica fume (SF), 25% natural pozzolan (NP) and 20% limestone powder (LSP) and the three control mixes are plotted in Figure 4.29. The potentials decreased (became more negative) with time of exposure to the chloride solution in all the reinforced concrete specimens. The corrosion potentials on steel in the concrete specimens with natural pozzolan or silica fume were less than that of plain cement concrete. The time to initiation of corrosion (i.e., to cross the -270 mV potential) of plain, 95% OPC with 5% SF, 75% OPC with 25% NP and 50% OPC with 5% SF + 25% NP + 20% LSP was about 202, 186, 262 and 170 days, respectively.

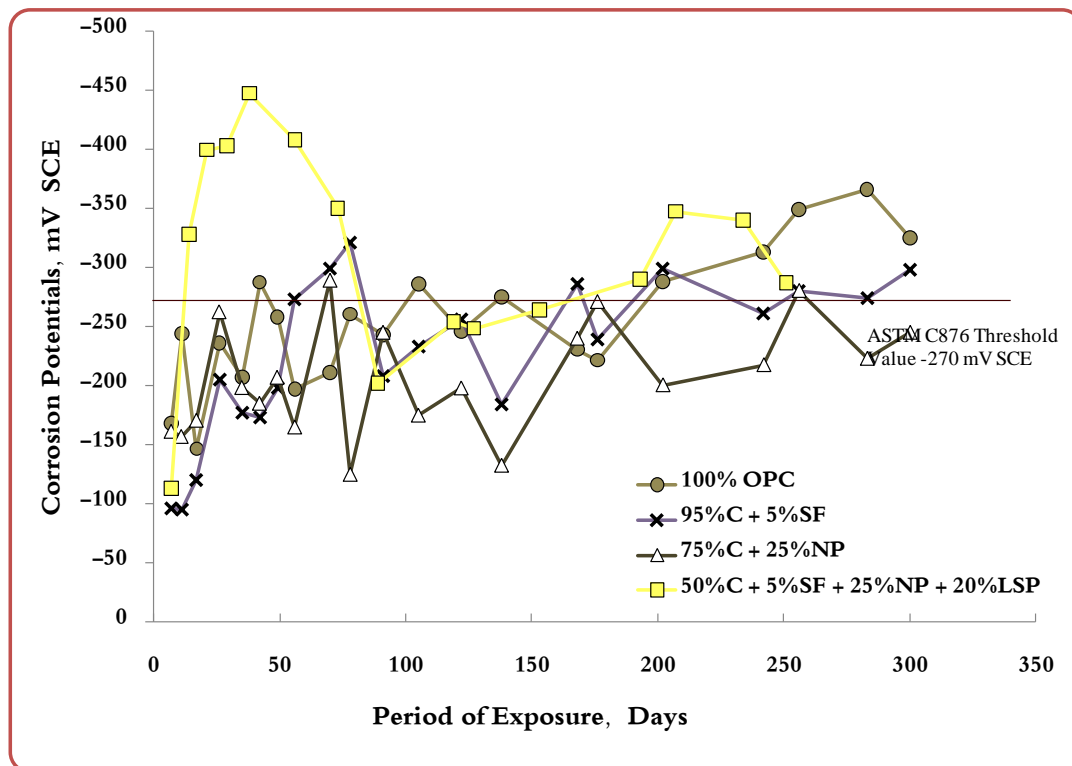


Figure 4-29: Corrosion Potentials on Steel in the QCC Specimens Prepared with 20% LSP.

The corrosion potentials on steel in quaternary cement concrete specimens replacing 50% cement with 5% silica fume (SF), 25% natural pozzolan (NP) and 20% pulverized steel slag (PSS) and three control mixes are plotted in Figure 4.30. The potentials decreased (became more negative) with time of exposure to the chloride solution. The corrosion potentials of the QCC specimens were more negative than those on the plain cement concrete. A similar trend was noted in the natural pozzolan and silica fume concrete specimens. The time to initiation of corrosion (i.e., to cross the -270 mV potential) of plain, 95% OPC with 5% SF, 75% OPC with 25% NP and 50% OPC with 5% SF + 25% NP + 20% PSS was about 202, 186, 262, and 128 days, respectively.

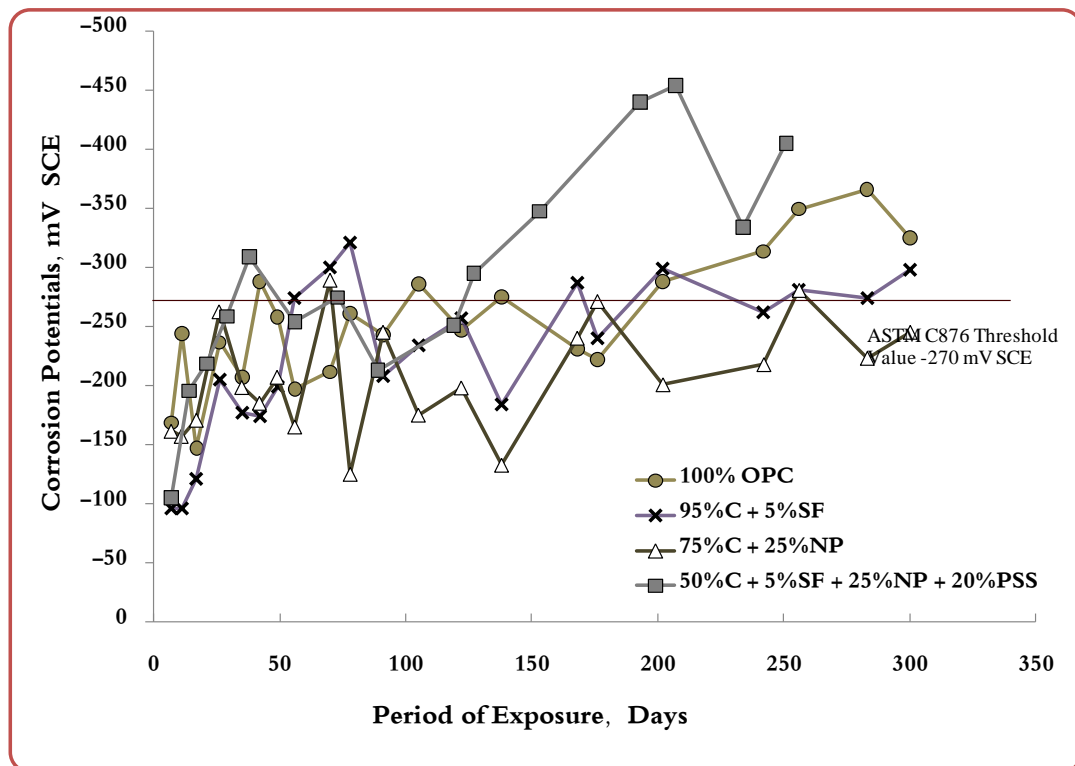


Figure 4–30: Corrosion Potentials on Steel in the QCC Specimens Prepared with 20% PSS.

#### 4.4 Corrosion Current Density

The average corrosion current density ( $I_{\text{corr}}$ ) on steel in the concrete specimens, recorded every month, is presented in Tables 4.7 through 4.9. The results have been grouped into two categories: (i) QCC specimens produced by replacing 50% cement with 5% silica fume, 25–30% fly ash and 15–20% by a locally available material (BHD, CKD, Clay, LSP or PSS), i.e. Mix 7, 8, 9, 10 and 11; (ii) QCC specimens produced by replacing 50% cement with 5% silica fume, 25–30% natural pozzolan and 15–20% by a selected local material (BHD, CKD, Clay, LSP or PSS), i.e. Mix 12, 13, 14, 15 and 16.

Table 4-7: Average Corrosion Current Density ( $I_{\text{corr}}$ ) of Plain and five Control mixes.

Exposure Period, Days	Corrosion Current Density ( $I_{\text{corr}}$ ), $\mu\text{A}/\text{cm}^2$					
	100% OPC	95%C + 5%SF	75%C + 25%FA	70%C + 30%FA	75%C + 25%NP	70%C + 30%NP
40	0.190	0.108	0.018	0.031	0.012	0.010
70	0.203	0.123	0.026	0.043	0.014	0.044
101	0.216	0.137	0.027	0.049	0.024	0.145
131	0.240	0.150	0.042	0.052	0.049	0.182
176	0.260	0.157	0.050	0.065	0.107	0.190
202	0.280	0.180	0.067	0.068	0.120	0.210
242	0.310	0.185	0.078	0.081	0.140	0.225
282	0.330	0.192	0.095	0.099	0.190	0.230
313	0.353	0.205	0.110	0.120	0.207	0.249

Table 4-8: Average Corrosion Current Density ( $I_{corr}$ ) of Group-I QCC mixes.

Exposure Period, Days	Corrosion Current Density ( $I_{corr}$ ) , $\mu A/cm^2$			
	50%C + 5%SF + 30%FA + 15%BHD	50%C + 5%SF + 30%FA + 15%CKD	50%C + 5%SF + 25%FA + 20%Clay	50%C + 5%SF + 25%FA + 20%PSS
40	0.018	0.040	0.058	
70	0.027	0.060		0.049
101	0.031	0.080		0.086
131	0.040	0.160		
176	0.049	0.190	0.067	0.124
202	0.061	0.240	0.069	0.139
242	0.068	0.260	0.071	0.147
282	0.155	0.280	0.085	0.160
313	0.172	0.298	0.096	0.189

Table 4-9: Average Corrosion Current Density ( $I_{corr}$ ) of Group-II QCC mixes.

Exposure Period, Days	Corrosion Current Density ( $I_{corr}$ ) , $\mu A/cm^2$					
	50%C + 5%SF + 30%NP + 15%BHD	50%C + 5%SF + 30%NP + 15%CKD	50%C + 5%SF + 25%NP + 20%Clay	50%C + 5%SF + 25%NP + 20%LSP	50%C + 5%SF + 25%NP + 20%PSS	50%C + 5%SF + 25%FA + 20%LSP
45	0.052	0.040	0.032	0.041	0.051	0.012
127	0.063	0.100	0.034	0.049	0.086	0.029
153	0.077	0.180	0.038	0.119	0.220	0.078
193	0.128	0.200	0.100	0.240	0.280	0.096
233	0.211	0.260	0.160	0.304	0.290	0.230
264	0.229	0.277	0.196	0.322	0.313	0.243



The corrosion current density ( $I_{\text{corr}}$ ) on steel in quaternary cement concrete specimens replacing 50% cement with 5% silica fume (SF), 30% fly ash (FA) and 15% bag house dust (BHD) is plotted against three control mixes in Figure 4.31. The  $I_{\text{corr}}$  increased with the period of exposure to the chloride solution in all the specimens. Incorporation of Fly Ash (FA) in plain cement concrete reduced the  $I_{\text{corr}}$  significantly while QCC specimens also performed better than plain and SF cement concrete specimens. After 10 months of exposure, the  $I_{\text{corr}}$  values on the steel in plain, 95% OPC with 5% SF, 70% OPC with 30% FA and 50% OPC with 5% SF + 30% FA + 15% BHD were 0.353, 0.205, 0.12 and 0.172  $\mu\text{A}/\text{cm}^2$ , respectively.

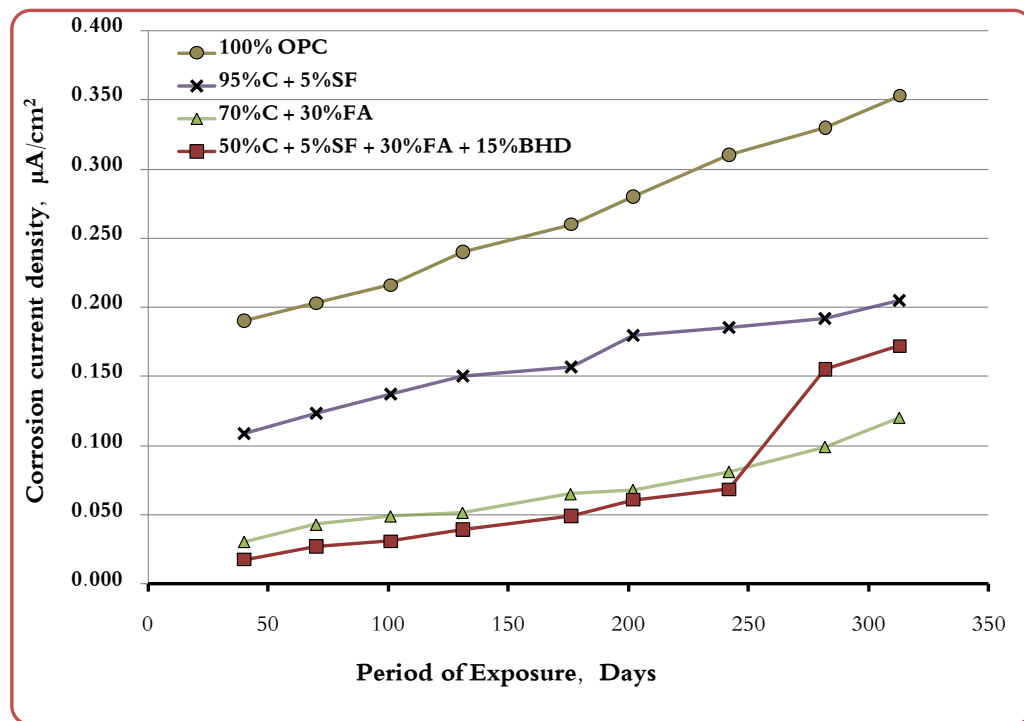


Figure 4-31: Corrosion Current Density on Steel in QCC specimens prepared with 15% BHD.

The corrosion current density ( $I_{\text{corr}}$ ) on steel in quaternary cement concrete specimens replacing 50% cement with 5% silica fume (SF), 30% fly ash (FA) and 15% cement kiln dust (CKD) and the three control mixes is plotted in Figure 4.32. The  $I_{\text{corr}}$  increased with the period of exposure to the chloride solution in all the concrete specimens. Incorporation of Fly Ash (FA) in plain cement concrete reduced the  $I_{\text{corr}}$  significantly while the QCC specimens also performed better than plain control mix. After 10 months of exposure, the  $I_{\text{corr}}$  values on steel in the plain, 95% OPC with 5% SF, 70% OPC with 30% FA and 50% OPC with 5% SF + 30% FA + 15% CKD were 0.353, 0.205, 0.12 and 0.298  $\mu\text{A}/\text{cm}^2$ , respectively.

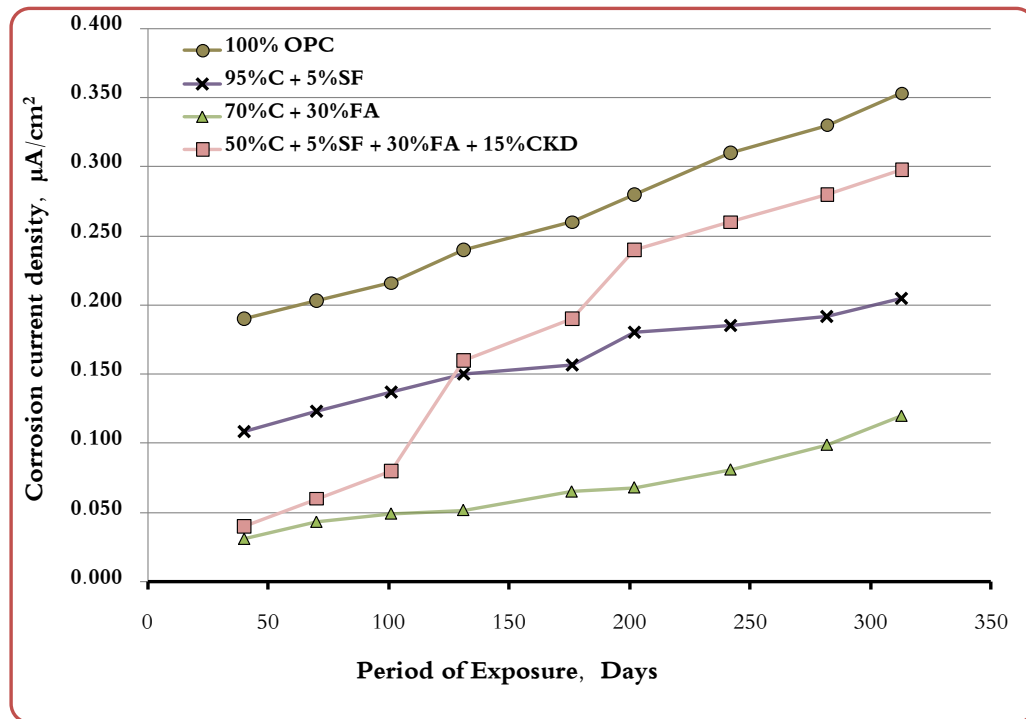


Figure 4-32: Corrosion Current Density on Steel in QCC specimens prepared with 15% CKD.

The corrosion current density ( $I_{\text{corr}}$ ) on steel in the quaternary cement concrete specimens replacing 50% cement with 5% silica fume (SF), 25% fly ash (FA) and 20% clay and the three control mixes is plotted in Figure 4.33. The  $I_{\text{corr}}$  increased with the period of exposure to the chloride solution in all the concrete specimens. Incorporation of Fly Ash (FA) in plain cement concrete reduced the  $I_{\text{corr}}$  significantly while the QCC specimens also performed better than control and SF mixes. After 10 months of exposure, the  $I_{\text{corr}}$  on the steel in plain, 95% OPC with 5% SF, 75% OPC with 25% FA and 50% OPC with 5% SF + 75% FA + 20% Clay are 0.353, 0.205, 0.11 and 0.096  $\mu\text{A}/\text{cm}^2$ , respectively.

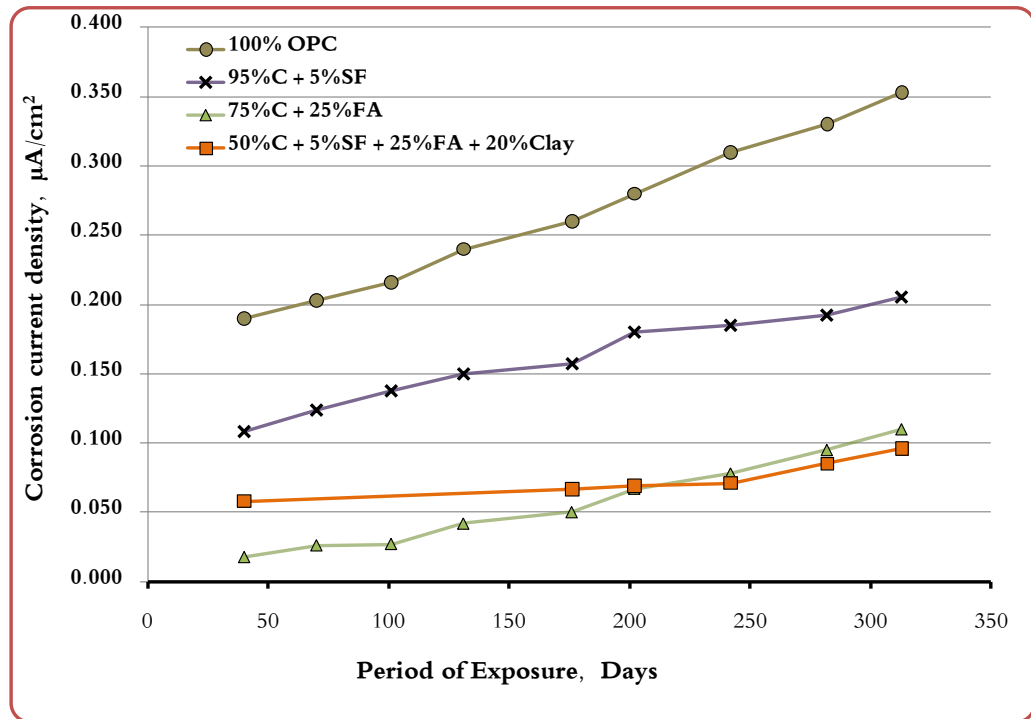


Figure 4-33: Corrosion Current Density on Steel in QCC specimens prepared with 20% Clay.

The corrosion current density ( $I_{\text{corr}}$ ) on steel in quaternary cement concrete specimens replacing 50% cement with 5% silica fume (SF), 25% fly ash (FA) and 20% lime stone powder (LSP) and the three control mixes is plotted in Figure 4.34. The  $I_{\text{corr}}$  increased with the period of exposure to the chloride solution in all the concrete specimens. Incorporation of Fly Ash (FA) in plain cement concrete reduced the  $I_{\text{corr}}$  significantly while QCC specimens also performed better than plain control mix. After 10 months of exposure, the  $I_{\text{corr}}$  on the steel in plain, 95% OPC with 5% SF, 75% OPC with 25% FA and 50% OPC with 5% SF + 75% FA + 20% LSP was 0.353, 0.205, 0.11 and 0.243  $\mu\text{A}/\text{cm}^2$ , respectively.

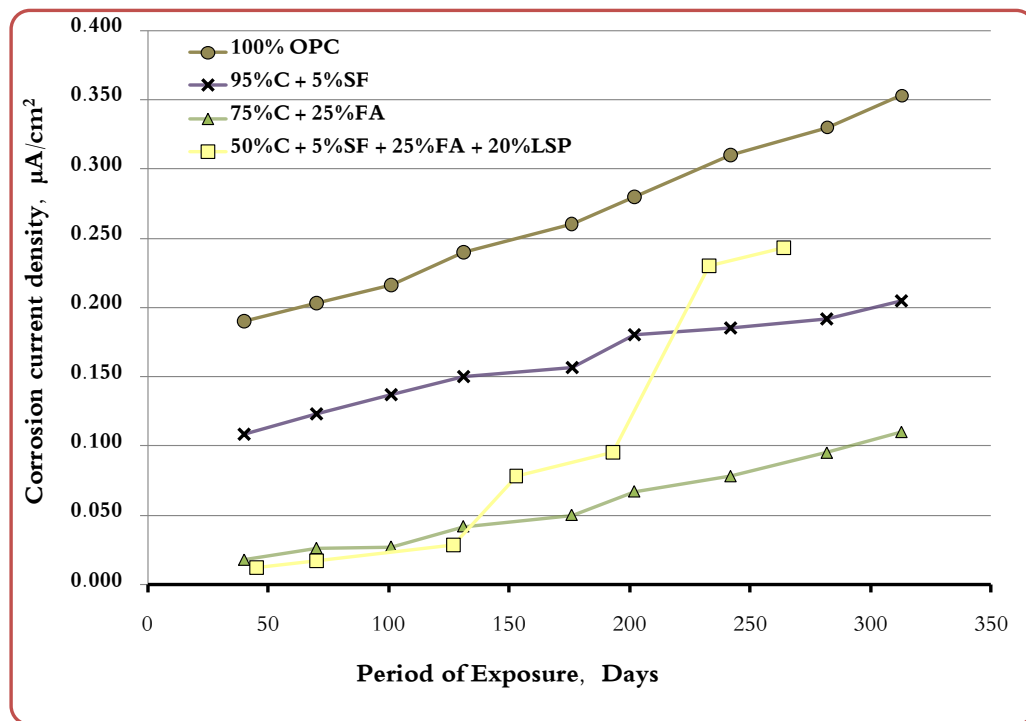


Figure 4–34: Corrosion Current Density on Steel in QCC specimens prepared with 20% LSP.

The corrosion current density ( $I_{\text{corr}}$ ) on steel in quaternary cement concrete specimens replacing 50% cement with 5% silica fume (SF), 25% fly ash (FA) and 20% pulverized steel slag (PSS) and three control mixes is plotted in Figure 4.35. The  $I_{\text{corr}}$  increased with the period of exposure to the chloride solution in all the concrete specimens. Incorporation of Fly Ash (FA) in plain cement concrete reduced the  $I_{\text{corr}}$  significantly while QCC specimens also performed better than two control mixes. After 10 months of exposure, the  $I_{\text{corr}}$  on the steel in plain, 95% OPC with 5% SF, 75% OPC with 25% FA and 50% OPC with 5% SF + 25% FA + 20% PSS was 0.353, 0.205, 0.11 and 0.189  $\mu\text{A}/\text{cm}^2$ , respectively.

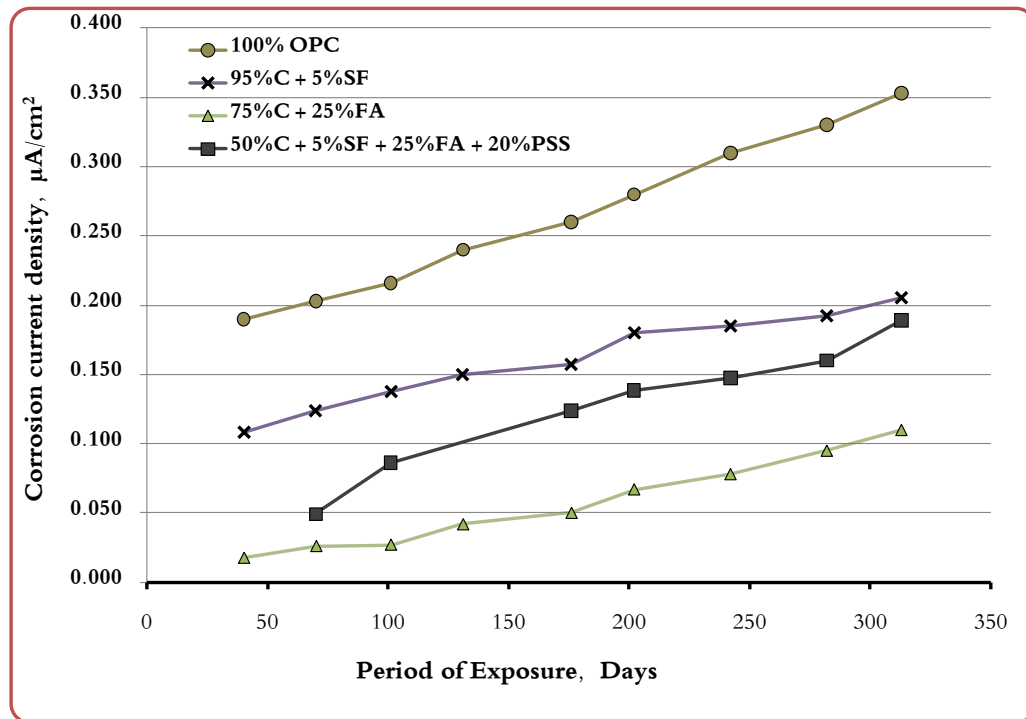


Figure 4-35: Corrosion Current Density on Steel in QCC specimens prepared with 20% PSS.

The corrosion current density ( $I_{\text{corr}}$ ) on steel in quaternary cement concrete specimens replacing 50% cement with 5% silica fume (SF), 30% natural pozzolan (NP) and 15% bag house dust (BHD) and the three control mixes is plotted in Figure 4.36. The  $I_{\text{corr}}$  increased with the period of exposure to the chloride solution in all the concrete specimens. Incorporation of natural pozzolan (NP) in plain cement concrete reduced the  $I_{\text{corr}}$  significantly while the QCC specimens also performed better than OPC. After 10 months of exposure, the  $I_{\text{corr}}$  values on the steel of plain, 95% OPC with 5% SF, 70% OPC with 30% NP and 50% OPC with 5% SF + 30% NP + 15% BHD are 0.353, 0.205, 0.249 and 0.229  $\mu\text{A}/\text{cm}^2$ , respectively.

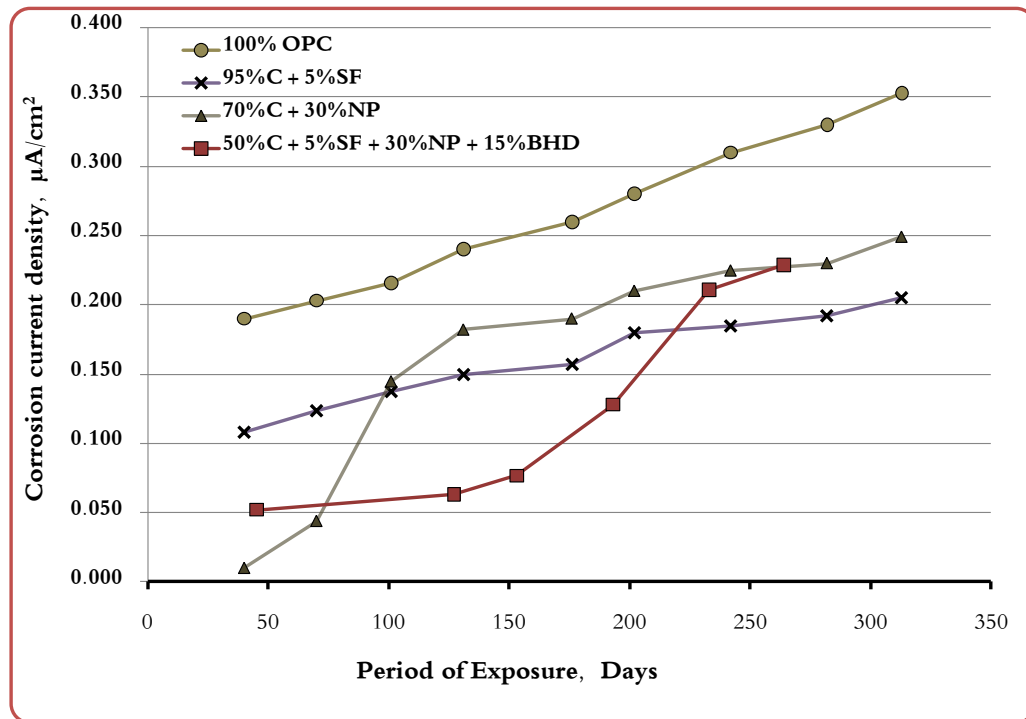


Figure 4-36: Corrosion Current Density on Steel in QCC specimens prepared with 15% BHD.

The corrosion current density ( $I_{\text{corr}}$ ) on steel in quaternary cement concrete specimens replacing 50% cement with 5% silica fume (SF), 30% natural pozzolan (NP) and 15% cement kiln dust (CKD) and the three control mixes is plotted in Figure 4.37. The  $I_{\text{corr}}$  increased with the period of exposure to the chloride solution in all the specimens. Incorporation of natural pozzolan (NP) in plain cement concrete reduced the  $I_{\text{corr}}$  significantly. The QCC specimens also performed better than plain cement concrete mix. After 10 months of exposure, the  $I_{\text{corr}}$  values on the steel in plain, 95% OPC with 5% SF, 70% OPC with 30% NP and 50% OPC with 5% SF + 30% NP + 15% CKD were 0.353, 0.205, 0.249 and 0.277  $\mu\text{A}/\text{cm}^2$ , respectively.

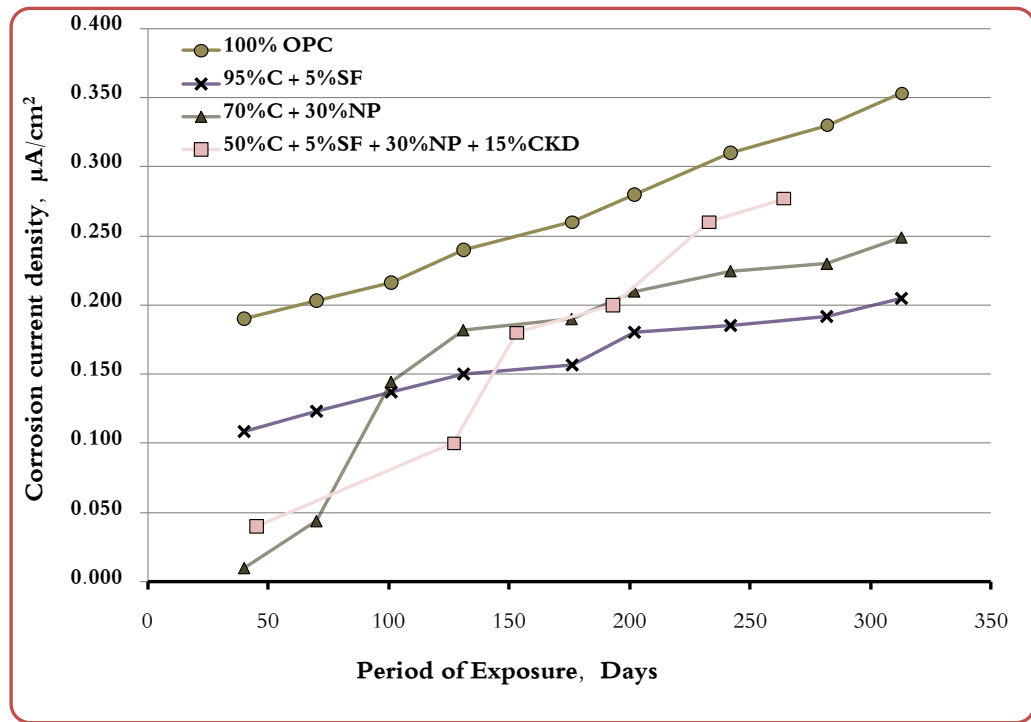


Figure 4-37: Corrosion Current Density on Steel in QCC specimens prepared with 15% CKD.

The corrosion current density ( $I_{\text{corr}}$ ) on steel in quaternary cement concrete specimens replacing 50% cement with 5% silica fume (SF), 25% natural pozzolan (NP) and 20% clay (Clay) and the three control mixes is plotted in Figure 4.38. The  $I_{\text{corr}}$  increased with the period of exposure to the chloride solution in all the concrete specimens. The incorporation of natural pozzolan (NP) in plain cement concrete reduced the  $I_{\text{corr}}$  significantly while QCC specimens also performed better than all control mixes. After 10 months of exposure, the  $I_{\text{corr}}$  values on the steel of plain, 95% OPC with 5% SF, 75% OPC with 30% NP and 50% OPC with 5% SF + 25% NP + 20% Clay were 0.353, 0.205, 0.207 and 0.196  $\mu\text{A}/\text{cm}^2$ , respectively.

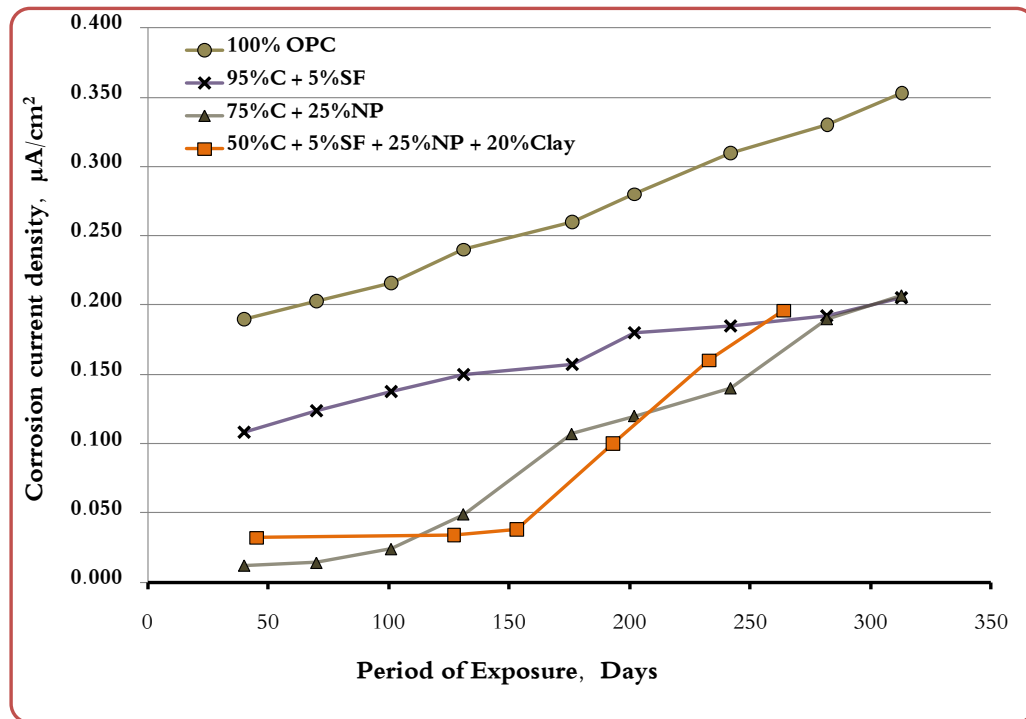


Figure 4–38: Corrosion Current Density on Steel in QCC specimens prepared with 20% Clay.



The corrosion current density ( $I_{\text{corr}}$ ) on steel in quaternary cement concrete specimens replacing 50% cement with 5% silica fume (SF), 25% natural pozzolan (NP) and 20% lime stone powder (LSP) and the three control mixes is plotted in Figure 4.39. The  $I_{\text{corr}}$  increased with the period of exposure to the chloride solution in all the specimens. Incorporation of natural pozzolan (NP) in plain cement concrete reduced the  $I_{\text{corr}}$  significantly and QCC specimens also performed better than plain concrete specimens. After 10 months of exposure, the  $I_{\text{corr}}$  values on the steel of plain, 95% OPC with 5% SF, 75% OPC with 25% NP and 50% OPC with 5% SF + 25% NP + 20% LSP are 0.353, 0.205, 0.207 and 0.322  $\mu\text{A}/\text{cm}^2$ , respectively.

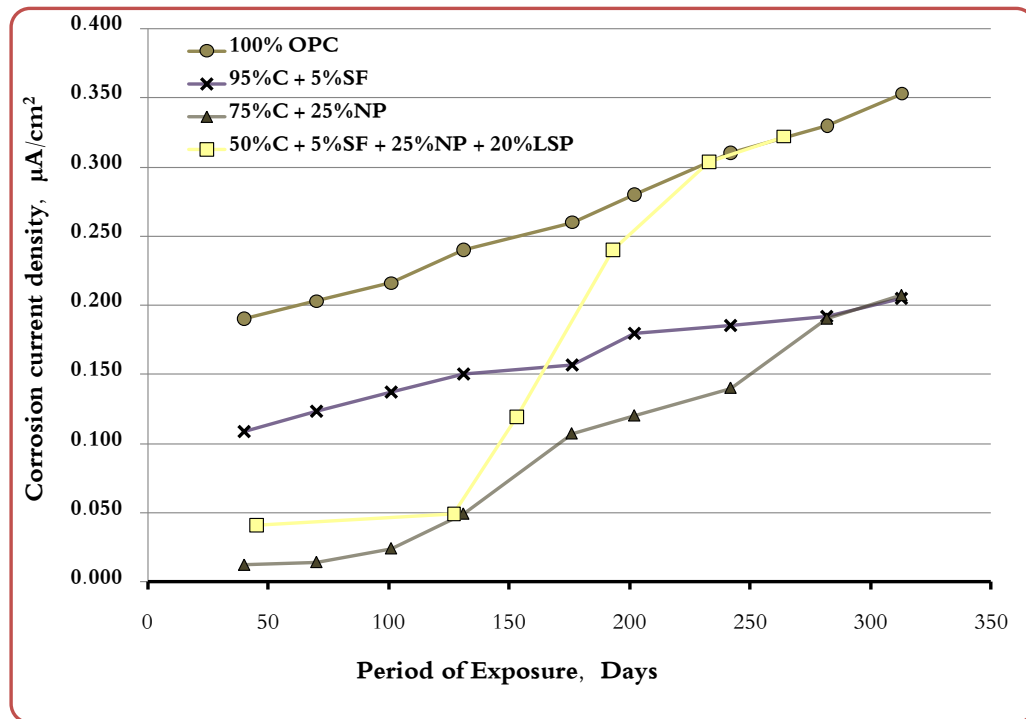


Figure 4–39: Corrosion Current Density on Steel in QCC specimens prepared with 20% LSP.

The corrosion current density ( $I_{\text{corr}}$ ) on steel in quaternary cement concrete specimens replacing 50% cement with 5% silica fume (SF), 25% natural pozzolan (NP) and 20% pulverized steel slag (PSS) and the three control mixes is plotted in Figure 4.40. The  $I_{\text{corr}}$  increased with the period of exposure to the chloride solution in all the specimens. Incorporation of Natural Pozzolan (NP) in plain cement concrete reduced the  $I_{\text{corr}}$  significantly and the QCC specimens also performed better than plain control mixes. After 10 months of exposure, the  $I_{\text{corr}}$  values on the steel in the plain, 95% OPC with 5% SF, 75% OPC with 25% NP and 50% OPC with 5% SF + 25% NP + 20% PSS are 0.353, 0.205, 0.207 and 0.313  $\mu\text{A}/\text{cm}^2$ , respectively.

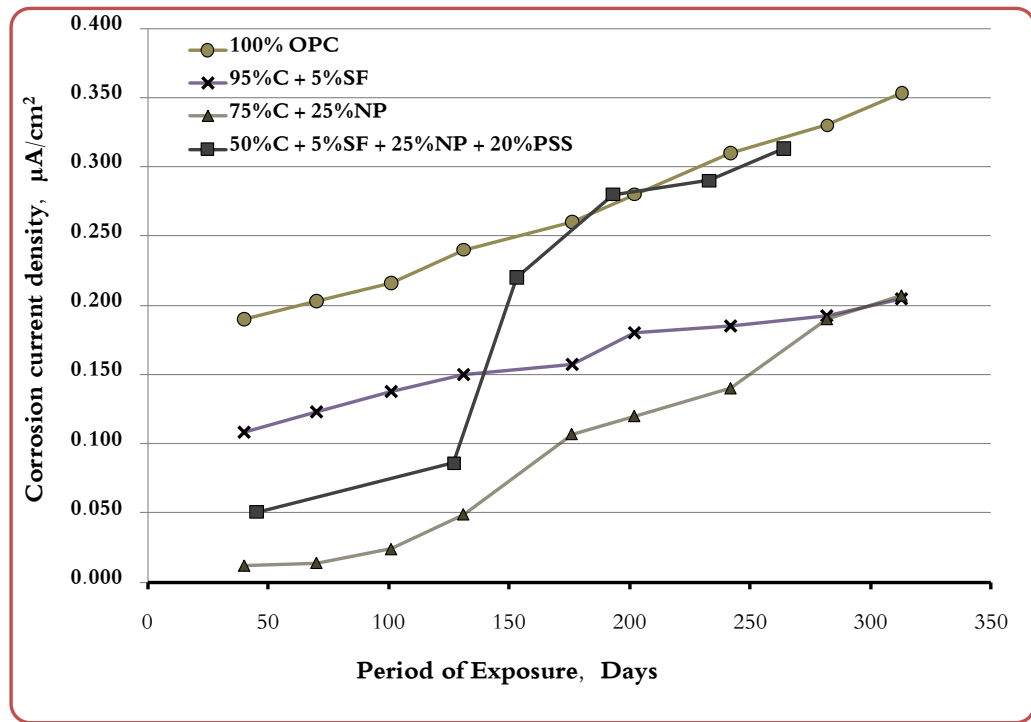


Figure 4-40: Corrosion Current Density on Steel in QCC specimens prepared with 20% PSS.

## 4.5 Drying Shrinkage

The average drying shrinkage of concrete specimens, recorded twice a month is presented in Tables 4.10 through 4.12. The results have been grouped into two categories:

- (i) QCC specimens produced by replacing 50% cement with 5% silica fume, 25–30% fly ash and 15–20% by a local waste material (BHD, CKD, Clay, LSP or PSS), i.e. Mix 7, 8, 9, 10 and 11; (ii) QCC specimens produced by replacing 50% cement with 5% silica fume, 25–30% natural pozzolan and 15–20% by a local waste material (BHD, CKD, Clay, LSP or PSS), i.e. Mix 12, 13, 14, 15 and 16.

Table 4-10: Average Drying Shrinkage of Plain and Five Control mixes.

Exposure Period, Days	Drying Shrinkage, Microns					
	100% OPC	95%C + 5%SF	75%C + 25%FA	70%C + 30%FA	75%C + 25%NP	70%C + 30%NP
2	90	99	56	69	56	47
4	137	163	103	142	112	107
8	176	210	155	198	163	163
12	228	253	206	236	202	210
18	296	305	262	288	245	253
28	343	365	326	356	283	296
36	391	416	387	408	309	339
46	442	468	438	464	339	382
56	477	511	494	511	365	421
67	507	558	550	558	395	442
87	545	601	606	605	429	460
103	575	631	636	627	451	477
124	588	653	640	640	451	485
152	588	653	648	644	455	485
181	597	665	653	657	460	490

Table 4-11: Average Drying Shrinkage of Group-I QCC mixes.

<b>Exposure Period, Days</b>	<b>Drying Shrinkage, Microns</b>				
	<b>50%C + 5%SF + 30%FA + 15%BHD</b>	<b>50%C + 5%SF + 30%FA + 15%CKD</b>	<b>50%C + 5%SF + 25%FA + 20%Clay</b>	<b>50%C + 5%SF + 25%FA + 20%LSP</b>	<b>50%C + 5%SF + 25%FA + 20%PSS</b>
2	107	142	129	129	133
4	172	262	163	197	197
8	236	352	202	249	270
12	335	429	258	300	348
18	386	459	309	373	442
28	451	537	361	450	494
36	511	575	416	506	532
46	562	627	464	566	571
56	631	687	511	609	623
67	687	734	550	652	670
87	725	777	605	686	696
103	747	799	635	712	713
124	764	812	648	729	717
152	764	812	653	729	717
181	768	816	661	734	721

Table 4-12: Average Drying Shrinkage of Group-II QCC mixes.

Exposure Period, Days	Drying Shrinkage, Microns				
	50%C + 5%SF + 30%NP + 15%BHD	50%C + 5%SF + 30%NP + 15%CKD	50%C + 5%SF + 25%NP + 20%Clay	50%C + 5%SF + 25%NP + 20%LSP	50%C + 5%SF + 25%NP + 20%PSS
2	90	94	56	77	90
4	146	159	99	133	167
8	228	202	142	185	257
11	309	266	189	258	326
18	361	318	236	305	399
28	416	408	296	339	463
35	464	459	352	369	498
50	507	493	386	399	541
56	541	515	416	429	562
71	562	536	442	455	584
87	597	562	472	489	609
99	622	575	494	515	627
128	631	579	502	520	635
156	631	579	502	520	635
181	635	584	506	524	639

The drying shrinkage strain in quaternary cement concrete specimens replacing 50% cement with 5% silica fume (SF), 30% fly ash (FA) and 15% bag house dust (BHD) and the three control mixes is plotted in Figure 4.41. The drying shrinkage increased with age in all the mixes. The increase was more rapid initially, stabilizing with time and remaining almost unchanged thereafter. The drying shrinkage of plain cement concrete specimens was the least. Incorporation of silica fume (SF) or fly ash (FA) in plain cement concrete increased the drying shrinkage. The drying shrinkage of the QCC specimens was the highest; however, it didn't cross the threshold limit of 500 microns within first seven days. After 180 days of curing, the drying shrinkage of plain, 95% OPC with 5% SF, 70% OPC with 30% FA and 50% OPC with 5% SF + 30% FA + 15% BHD was and 597, 665, 657 and 768 microns, respectively.

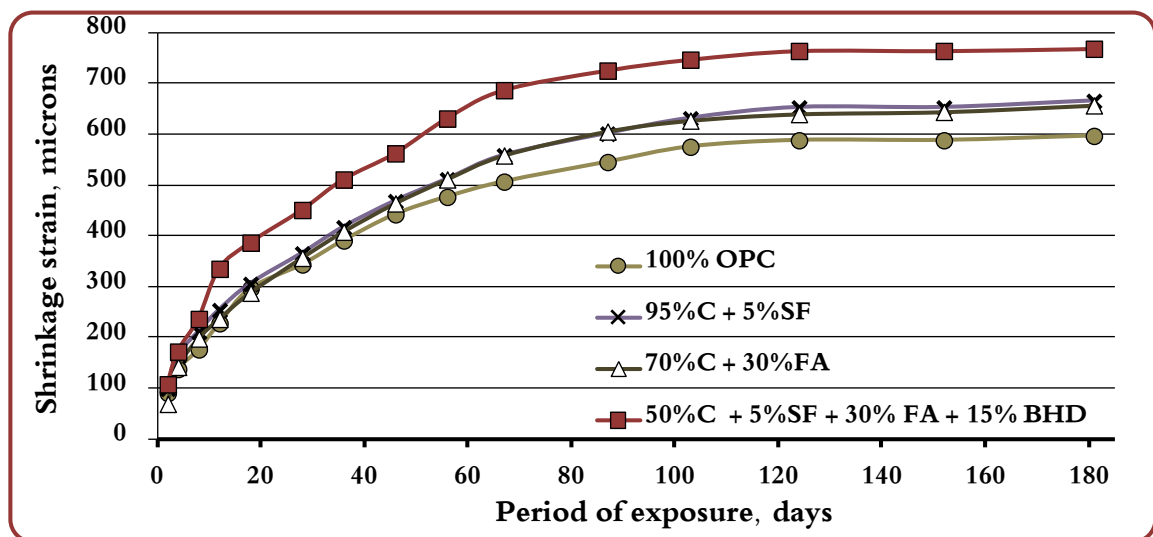


Figure 4-41: Drying Shrinkage Strain in QCC Specimens Prepared with 15% BHD.

The drying shrinkage strain in quaternary cement concrete specimens replacing 50% cement with 5% silica fume (SF), 30% fly ash (FA) and 15% cement kiln dust (CKD) and the three control mixes is plotted in Figure 4.42. The drying shrinkage increased with age in all the mixes. The increase was more rapid initially, stabilizing with time and remaining almost unchanged thereafter. The drying shrinkage of plain cement concrete specimens was the least. Incorporation of silica fume (SF) or fly ash (FA) in plain cement concrete increased the drying shrinkage. The drying shrinkage of the QCC specimens was the highest however it didn't cross the threshold limit of 500 microns within first seven days. After 180 days of curing, the drying shrinkage of plain, 95% OPC with 5% SF, 70% OPC with 30% FA and 50% OPC with 5% SF + 30% FA + 15% CKD was and 597, 665, 657 and 816 microns, respectively.

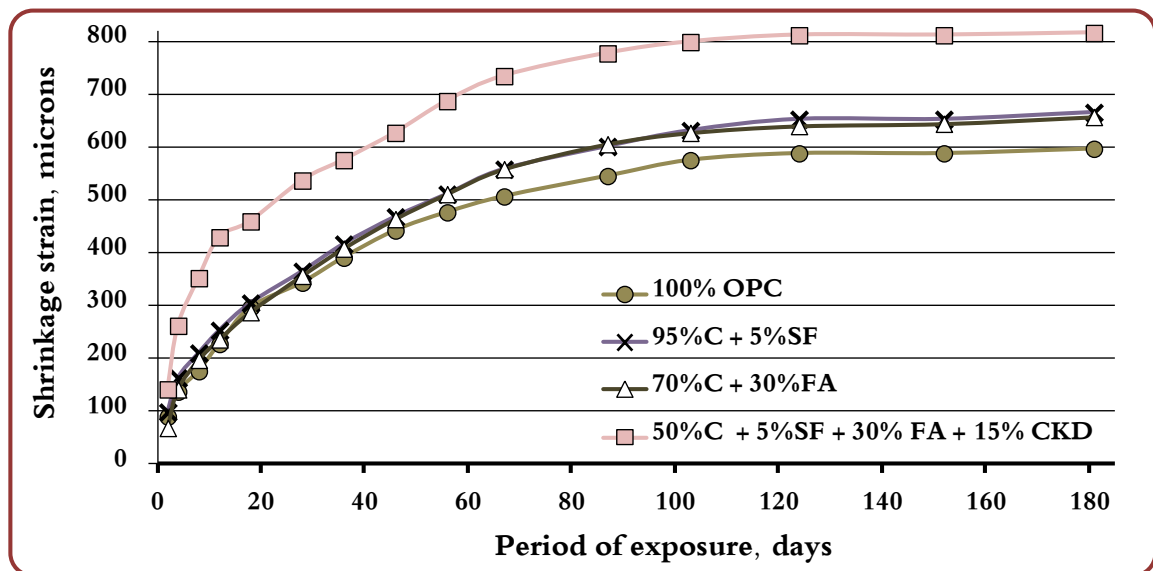


Figure 4-42: Drying Shrinkage Strain in QCC Specimens Prepared with 15% CKD.

The drying shrinkage strain in quaternary cement concrete specimens replacing 50% cement with 5% silica fume (SF), 30% fly ash (FA) and 20% clay (Clay) and the three control mixes is plotted in Figure 4.43. The drying shrinkage increased with age in all the mixes. The increase was more rapid initially, stabilizing with time and remaining almost unchanged thereafter. The drying shrinkage of plain cement concrete specimens was the least. Incorporation of silica fume (SF) or fly ash (FA) in plain cement concrete increased the drying shrinkage while with the natural pozzolan the drying shrinkage kept low. The drying shrinkage of QCC specimens was the highest however it didn't cross the threshold limit of 500 microns within first seven days. After 180 days of curing, the drying shrinkage of plain, 95% OPC with 5% SF, 75% OPC with 25% FA and 50% OPC with 5% SF + 25% FA + 15% Clay was and 597, 665, 653 and 661 microns, respectively.

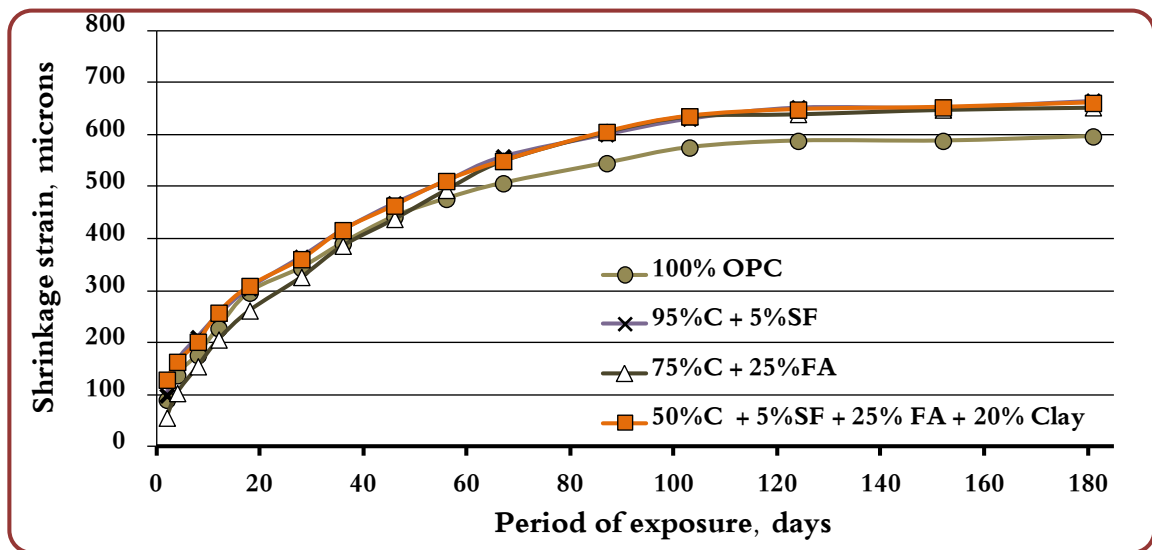


Figure 4-43: Drying Shrinkage Strain in QCC Specimens Prepared with 20% Clay.



The drying shrinkage strain in quaternary cement concrete specimens replacing 50% cement with 5% silica fume (SF), 30% fly ash (FA) and 20% lime stone powder (LSP) is plotted against three control mixes in Figure 4.44. The drying shrinkage increased with age in all the mixes. The increase was more rapid initially, stabilizing with time and remaining almost unchanged thereafter. The drying shrinkage of plain cement concrete specimens was the least. Incorporation of silica fume (SF) or fly ash (FA) in plain cement concrete increased the drying. The drying shrinkage of QCC specimens was the highest however it didn't cross the threshold limit of 500 microns within first seven days. After 180 days of curing, the drying shrinkage of plain, 95% OPC with 5% SF, 75% OPC with 25% FA and 50% OPC with 5% SF + 25% FA + 15% LSP was and 597, 665, 653 and 734 microns, respectively.

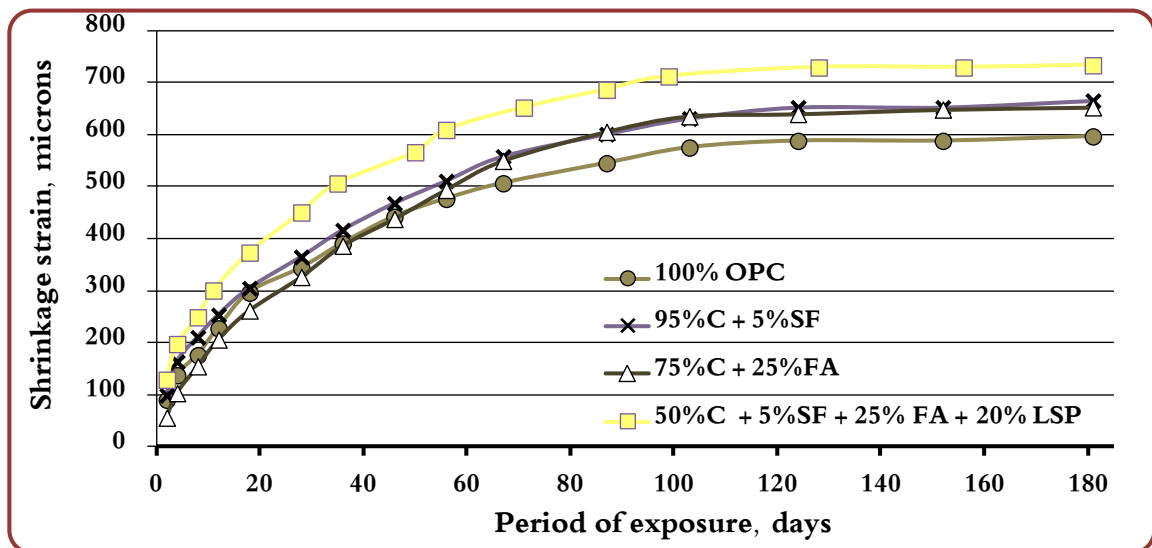


Figure 4-44: Drying Shrinkage Strain in QCC Specimens Prepared with 20% LSP.

The drying shrinkage strain in quaternary cement concrete specimens replacing 50% cement with 5% silica fume (SF), 30% fly ash (FA) and 20% pulverized steel slag (PSS) and the three control mixes is plotted in Figure 4.45. The drying shrinkage increased with age in all the mixes. The increase was more rapid initially, stabilizing with time and remaining almost unchanged thereafter. The drying shrinkage of plain cement concrete specimens was the least. Incorporation of silica fume (SF) or fly ash (FA) in plain cement concrete increased the drying shrinkage. The drying shrinkage of QCC specimens was the highest however it didn't cross the threshold limit of 500 microns within first seven days. After 180 days of curing, the drying shrinkage of plain, 95% OPC with 5% SF, 75% OPC with 25% FA and 50% OPC with 5% SF + 25% FA + 15% PSS was and 597, 665, 653 and 721 microns, respectively.

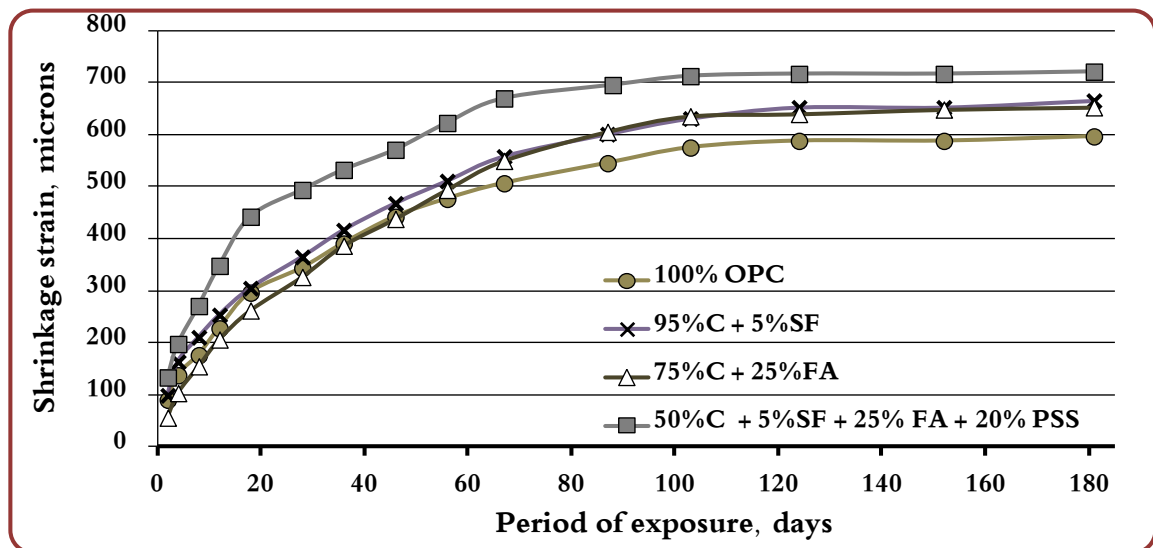


Figure 4-45: Drying Shrinkage Strain in QCC Specimens Prepared with 20% PSS.

The drying shrinkage strain in quaternary cement concrete specimens replacing 50% cement with 5% silica fume (SF), 30% natural pozzolan (NP) and 15% bag house dust (BHD) and the three control mixes is plotted in Figure 4.46. The drying shrinkage increased with age in all the mixes. The increase was more rapid initially, stabilizing with time and remaining almost unchanged thereafter. The drying shrinkage of plain cement concrete specimens was the least. Incorporation of silica fume (SF) or fly ash (FA) in plain cement concrete increased the drying shrinkage while with the natural pozzolan the drying shrinkage kept low. The drying shrinkage of QCC specimens was comparable however it didn't cross the threshold limit of 500 microns within first seven days. After 180 days of curing, the drying shrinkage of plain, 95% OPC with 5% SF, 70% OPC with 30% NP and 50% OPC with 5% SF + 30% NP + 15% BHD was and 597, 665, 490 and 635 microns.

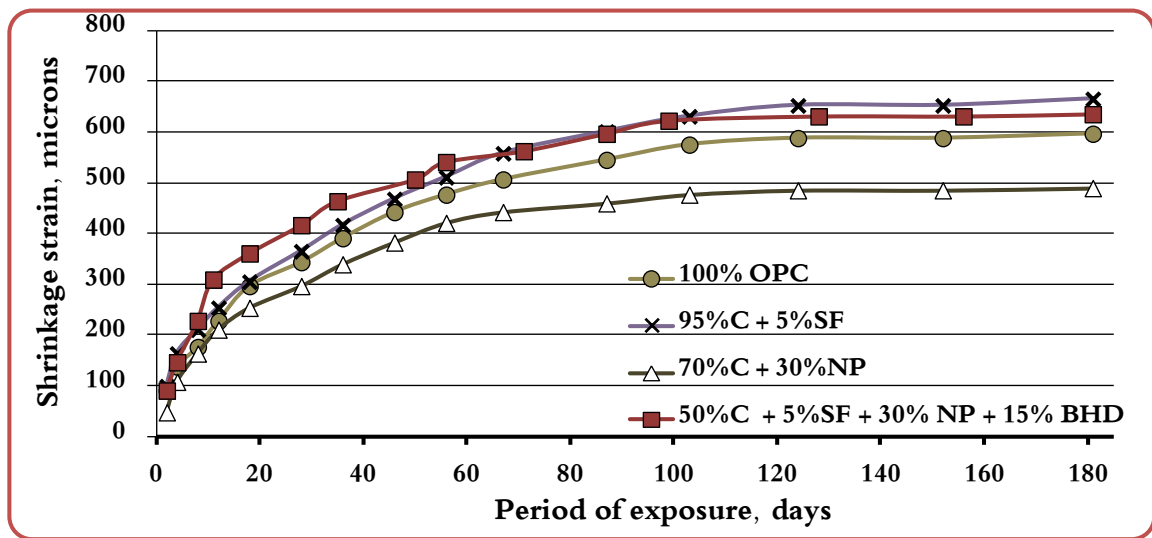


Figure 4-46: Drying Shrinkage Strain in QCC Specimens Prepared with 15% BHD.

The drying shrinkage strain in quaternary cement concrete specimens replacing 50% cement with 5% silica fume (SF), 30% natural pozzolan (NP) and 15% cement kiln dust (CKD) and the three control mixes is plotted in Figure 4.47. The drying shrinkage increased with age in all the mixes. The increase was more rapid initially, stabilizing with time and remaining almost unchanged thereafter. The drying shrinkage of plain cement concrete specimens was the least. Incorporation of silica fume (SF) or fly ash (FA) in plain cement concrete increased the drying shrinkage while with the natural pozzolan the drying shrinkage kept low. The drying shrinkage of QCC specimens was very comparable and it didn't cross the threshold limit of 500 microns within first seven days. After 180 days of curing, the drying shrinkage of plain, 95% OPC with 5% SF, 70% OPC with 30% NP and 50% OPC with 5% SF + 30% NP + 15% CKD was and 597, 665, 490 and 584 microns.

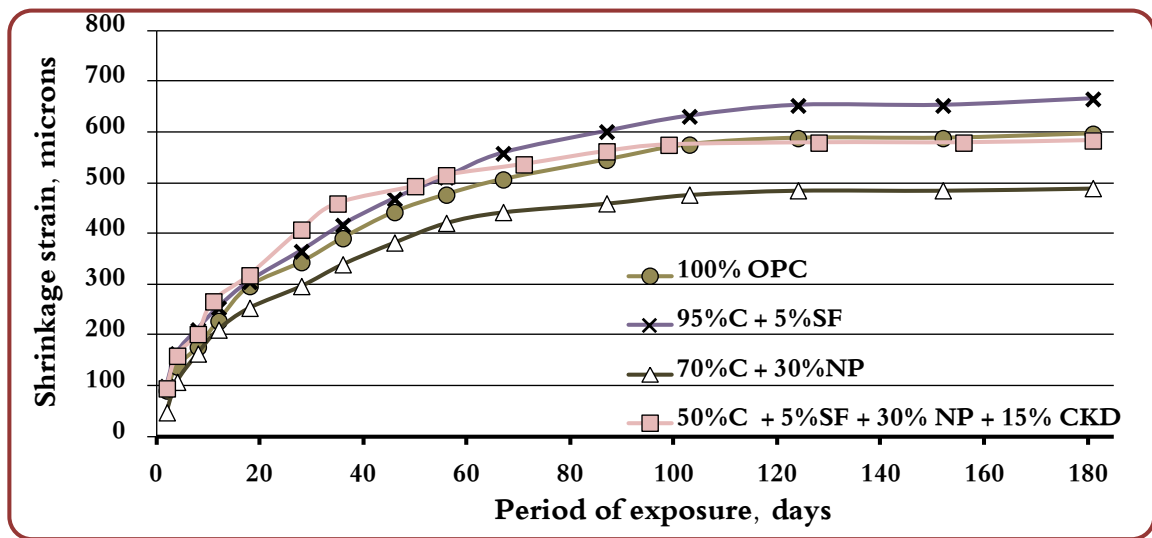


Figure 4-47: Drying Shrinkage Strain in QCC Specimens Prepared with 15% CKD.

The drying shrinkage strain in quaternary cement concrete specimens replacing 50% cement with 5% silica fume (SF), 30% natural pozzolan (NP) and 20% clay (Clay) and the three control mixes is plotted in Figure 4.48. The drying shrinkage increased with age in all the mixes. The increase was more rapid initially, stabilizing with time and remaining almost unchanged thereafter. The drying shrinkage of plain cement concrete specimens was the least. Incorporation of silica fume (SF) or fly ash (FA) in plain cement concrete increased the drying shrinkage while with the natural pozzolan the drying shrinkage kept low. The drying shrinkage of the QCC specimens was lower than OPC and it didn't cross the threshold limit of 500 microns within first seven days. After 180 days of curing, the drying shrinkage of plain, 95% OPC with 5% SF, 75% OPC with 25% NP and 50% OPC with 5% SF + 25% NP + 15% Clay was and 597, 665, 460 and 506 microns, respectively.

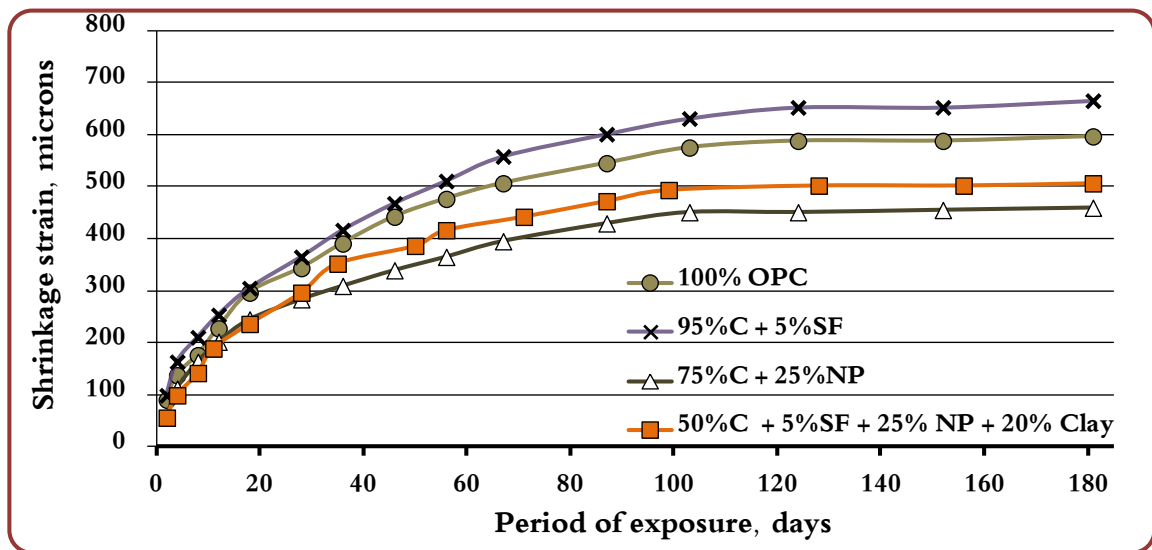


Figure 4-48: Drying Shrinkage Strain in QCC Specimens Prepared with 20% Clay.

The drying shrinkage strain in quaternary cement concrete specimens replacing 50% cement with 5% silica fume (SF), 30% natural pozzolan (NP) and 20% lime stone powder (LSP) and the three control mixes is plotted in Figure 4.49. The drying shrinkage increased with age in all the mixes. The increase was more rapid initially, stabilizing with time and remaining almost unchanged thereafter. The drying shrinkage of plain cement concrete specimens was the least. Incorporation of silica fume (SF) or fly ash (FA) in plain cement concrete increased the drying shrinkage while with the natural pozzolan the drying shrinkage kept low. The drying shrinkage of QCC specimens was lower than OPC and it didn't cross the threshold limit of 500 microns within first seven days. After 180 days of curing, the drying shrinkage of plain, 95% OPC with 5% SF, 75% OPC with 25% NP and 50% OPC with 5% SF + 25% NP + 15% LSP was and 597, 665, 460 and 524 microns.

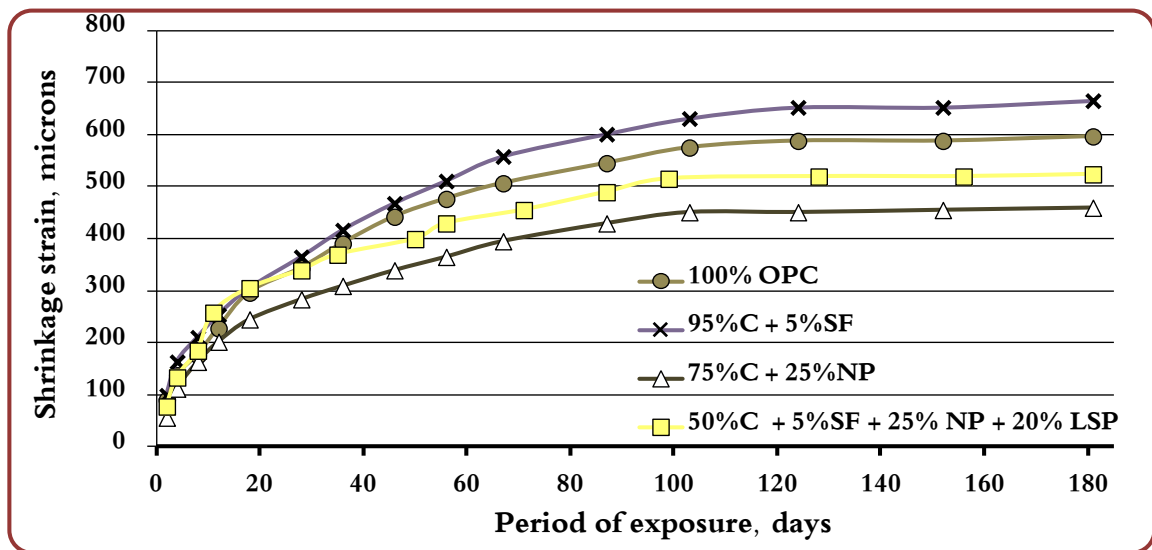


Figure 4-49: Drying Shrinkage Strain in QCC Specimens Prepared with 20% LSP.

The drying shrinkage strain in quaternary cement concrete specimens replacing 50% cement with 5% silica fume (SF), 30% natural pozzolan (NP) and 20% pulverized steel slag (PSS) and the three control mixes is plotted in Figure 4.50. The drying shrinkage increased with age in all the mixes. The increase was more rapid initially, stabilizing with time and remaining almost unchanged thereafter. The drying shrinkage of plain cement concrete specimens was the least. Incorporation of silica fume (SF) or fly ash (FA) in plain cement concrete increased the drying shrinkage while with the natural pozzolan the drying shrinkage kept low. The drying shrinkage of QCC specimens was comparable however it didn't cross the threshold limit of 500 microns within first seven days. After 180 days of curing, the drying shrinkage of plain, 95% OPC with 5% SF, 75% OPC with 25% NP and 50% OPC with 5% SF + 25% NP + 15% PSS was and 597, 665, 460 and 639 microns.

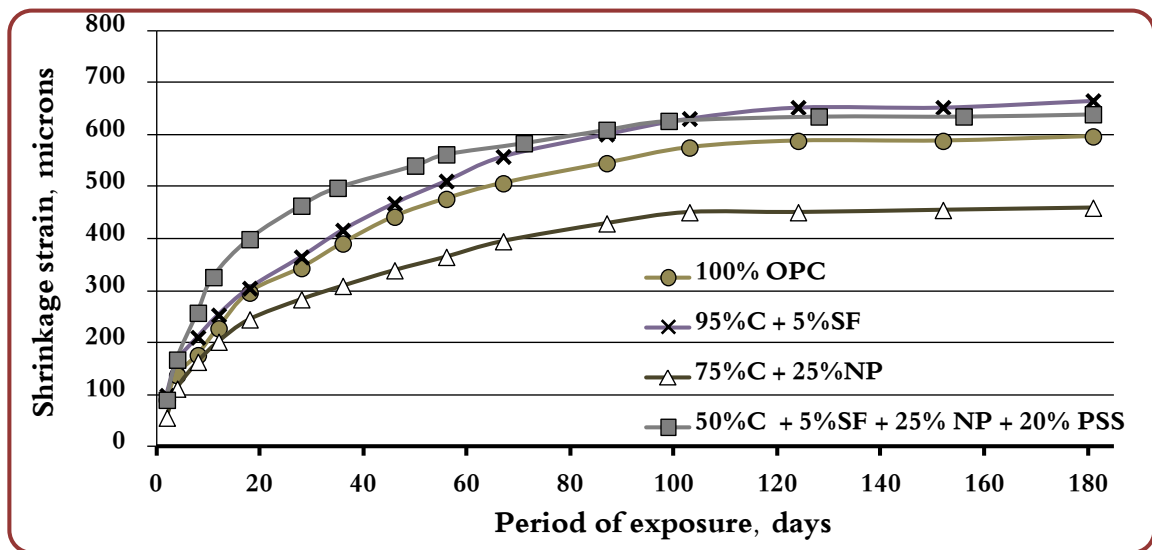


Figure 4-50: Drying Shrinkage Strain in QCC Specimens Prepared with 20% PSS.

## 4.6 Water Absorption

The average water absorption of concrete specimens, tested after 28 days of water curing is presented in Tables 4.13 through 4.15. The results have been grouped into two categories: (i) QCC specimens produced by replacing 50% cement with 5% silica fume, 25–30% fly ash and 15–20% by a selected local material (BHD, CKD, Clay, LSP or PSS), i.e. Mix 7, 8, 9, 10 and 11; (ii) QCC specimens produced by replacing 50% cement with 5% silica fume, 25–30% natural pozzolan and 15–20% by a locally available material (BHD, CKD, Clay, LSP or PSS), i.e. Mix 12, 13, 14, 15 and 16.

Table 4-13: Average Water Absorption of Plain and Five Control mixes.

Period of Curing, Days	Water Absorption					
	100% OPC	95%C + 5%SF	75%C + 25%FA	70%C + 30%FA	75%C + 25%NP	70%C + 30%NP
28	4.61	4.33	4.52	4.48	4.54	4.57

Table 4-14: Average Water Absorption of Group-I QCC mixes.

Period of Curing, Days	Water Absorption				
	50%C + 5%SF + 30%FA + 15%BHD	50%C + 5%SF + 30%FA + 15%CKD	50%C + 5%SF + 25%FA + 20%Clay	50%C + 5%SF + 25%FA + 20%LSP	50%C + 5%SF + 25%FA + 20%PSS
28	5.10	4.49	4.32	4.53	4.68

Table 4-15: Average Water Absorption of Group-II QCC mixes.

Period of Curing, Days	Water Absorption				
	50%C + 5%SF + 30%NP + 15%BHD	50%C + 5%SF + 30%NP + 15%CKD	50%C + 5%SF + 25%NP + 20%Clay	50%C + 5%SF + 25%NP + 20%LSP	50%C + 5%SF + 25%NP + 20%PSS
28	4.94	4.69	4.68	4.70	4.79



The water absorption in quaternary cement concrete specimens replacing 50% cement with 5% silica fume (SF), 30% fly ash (FA) and 15% bag house dust (BHD) and the three control mixes is plotted in Figure 4.51. Incorporation of silica fume (SF) in plain cement concrete decreased the water absorption while in the other mixes, the water absorption increased with cement replacement level. The water absorption of the QCC specimens was the highest. After 28 days of curing, the water absorption of plain, 95% OPC with 5% SF, 70% OPC with 30% FA and 50% OPC with 5% SF + 30% FA + 15% BHD was 4.61, 4.33, 4.48 and 5.10 % respectively.

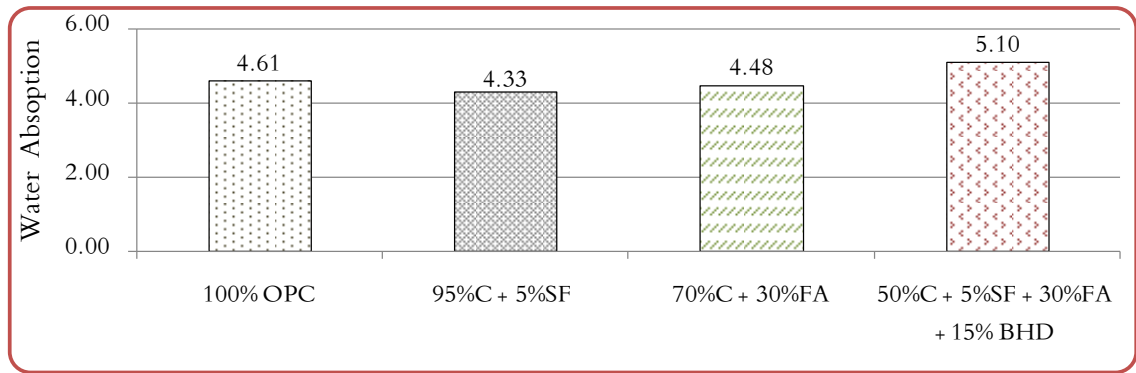


Figure 4-51: Water Absorption of QCC specimens with 15% BHD after 28 days of curing.

The water absorption in quaternary cement concrete specimens replacing 50% cement with 5% silica fume (SF), 30% fly ash (FA) and 15% cement kiln dust (CKD) and the three control mixes is plotted in Figure 4.52. Incorporation of silica fume (SF) in plain cement concrete decreased the water absorption while in the other mixes, the water

absorption increased with cement replacement level, though the absorption differential was not that significant. The water absorption of the QCC specimens was the highest. After 28 days of curing, the water absorption of plain, 95% OPC with 5% SF, 70% OPC with 30% FA and 50% OPC with 5% SF + 30% FA + 15% CKD was 4.61, 4.33, 4.48 and 4.49 % respectively.

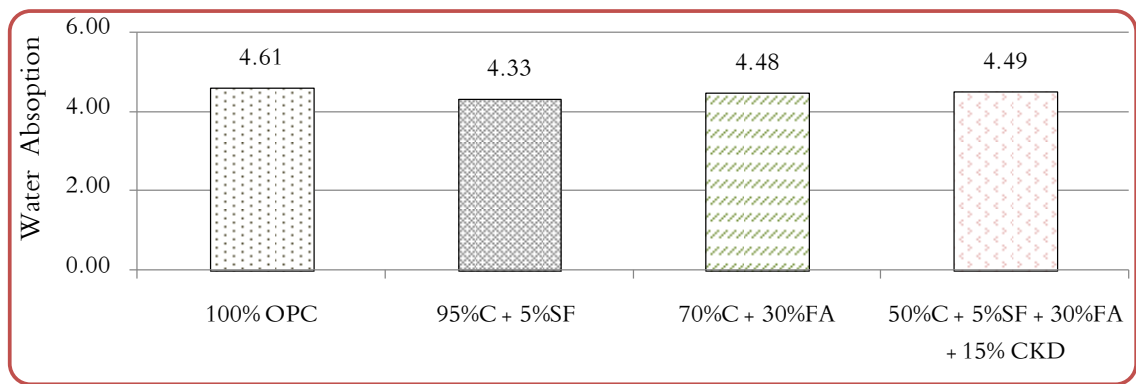


Figure 4-52: Water Absorption of QCC specimens with 15% CKD after 28 days of curing.

The water absorption in quaternary cement concrete specimens replacing 50% cement with 5% silica fume (SF), 25% fly ash (FA) and 20% clay (Clay) and the three control mixes is plotted in Figure 4.53. Incorporation of silica fume (SF) in plain cement concrete decreased the water absorption while in the other mixes, the water absorption increased with the cement replacement level, though the absorption differential was not that significant. After 28 days of curing, the water absorption of plain, 95% OPC with 5%

SF, 75% OPC with 25% FA and 50% OPC with 5% SF + 25% FA + 20% Clay was 4.61, 4.33, 4.52 and 4.32 % respectively.

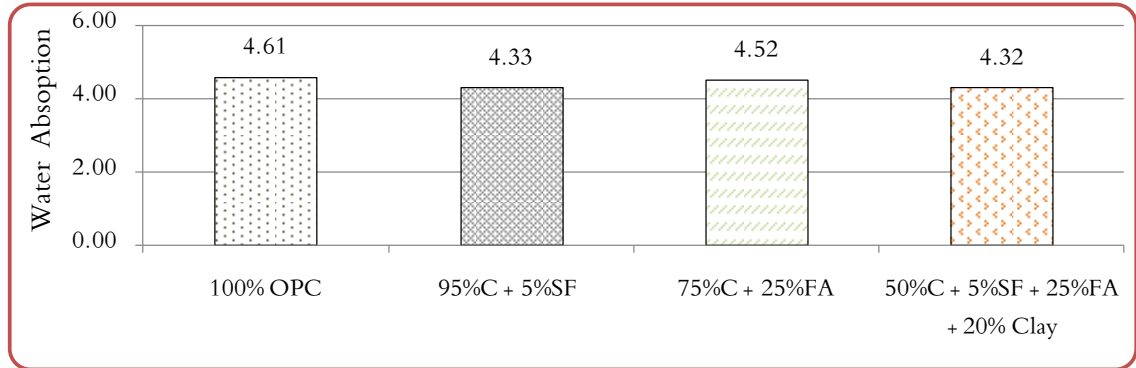


Figure 4-53: Water Absorption of QCC specimens with 20% Clay after 28 days of curing.

The water absorption in quaternary cement concrete specimens replacing 50% cement with 5% silica fume (SF), 25% fly ash (FA) and 20% lime stone powder (LSP) and the three control mixes is plotted in Figure 4.54. The water absorption of SF, FA and QCC specimens was less than that of plain cement concrete. After 28 days of curing, the water absorption of plain, 95% OPC with 5% SF, 75% OPC with 25% FA and 50% OPC with 5% SF + 25% FA + 20% LSP was 4.61, 4.33, 4.52 and 4.53 % respectively.

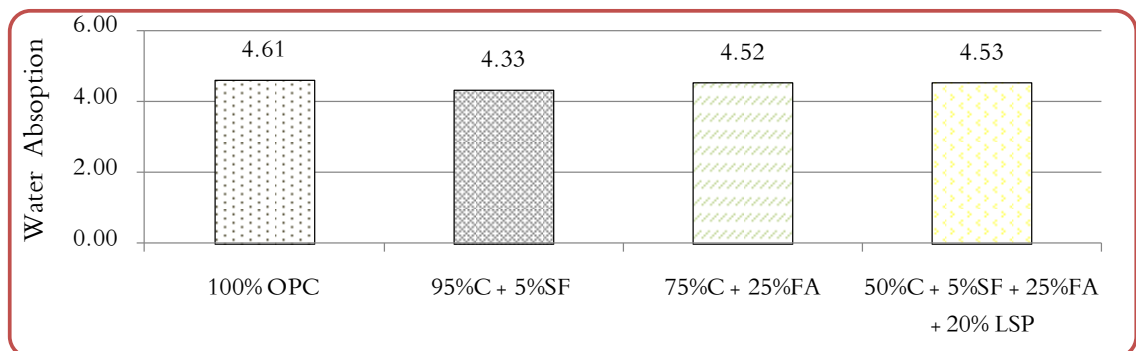


Figure 4-54: Water Absorption of QCC specimens with 20% LSP after 28 days of curing.

The water absorption in quaternary cement concrete specimens replacing 50% cement with 5% silica fume (SF), 25% fly ash (FA) and 20% pulverized steel slag (PSS) and the three control mixes is plotted in Figure 4.55. Minimum water absorption was noted in the SF cement concrete specimens. However, there was not much difference in the absorption. After 28 days of curing, the water absorption of plain, 95% OPC with 5% SF, 75% OPC with 25% FA and 50% OPC with 5% SF + 25% FA + 20% PSS was 4.61, 4.33, 4.52 and 4.68 % respectively.

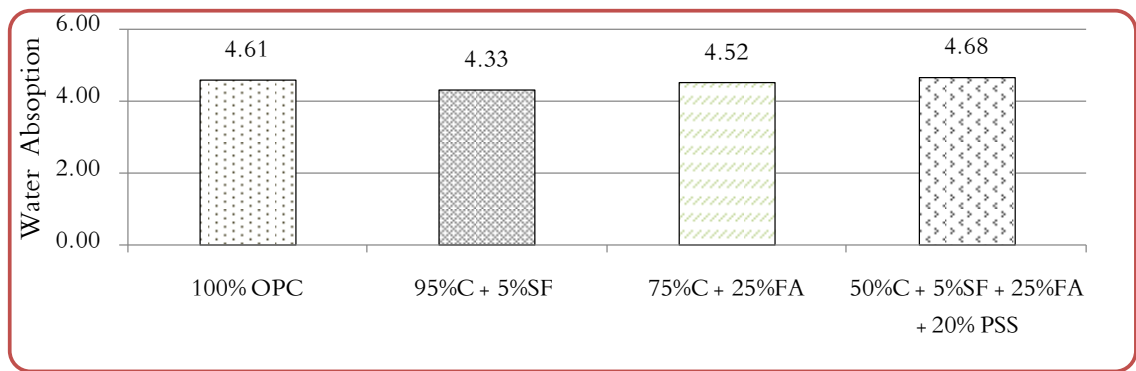


Figure 4-55: Water Absorption of QCC specimens with 20% PSS after 28 days of curing.

The water absorption in quaternary cement concrete specimens replacing 50% cement with 5% silica fume (SF), 30% natural pozzolan (NP) and 15% bag house dust (BHD) and the three control mixes is plotted in Figure 4.56. Incorporation of silica fume (SF) in plain cement concrete decreased the water absorption while in the other mixes, the water absorption increased with the cement replacement level. The water absorption of the QCC specimens was the highest. After 28 days of curing, the water absorption of plain,

95% OPC with 5% SF, 70% OPC with 30% NP and 50% OPC with 5% SF + 30% NP + 15% BHD was 4.61, 4.33, 4.57 and 4.94 % respectively.

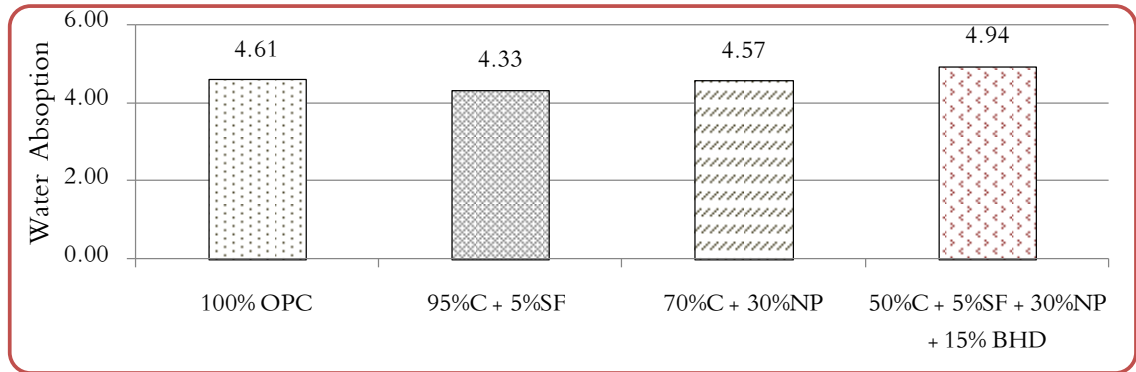


Figure 4-56: Water Absorption of QCC specimens with 15% BHD after 28 days of curing.

The water absorption in quaternary cement concrete specimens replacing 50% cement with 5% silica fume (SF), 30% natural pozzolan (NP) and 15% cement kiln dust (CKD) and the three control mixes is plotted in Figure 4.57. Incorporation of silica fume (SF) in plain cement concrete decreased the water absorption while in the other mixes, the water absorption increased with the cement replacement level. The water absorption of the QCC specimens was the highest. After 28 days of curing, the water absorption of plain, 95% OPC with 5% SF, 70% OPC with 30% NP and 50% OPC with 5% SF + 30% NP + 15% CKD was 4.61, 4.33, 4.57 and 4.69 % respectively.

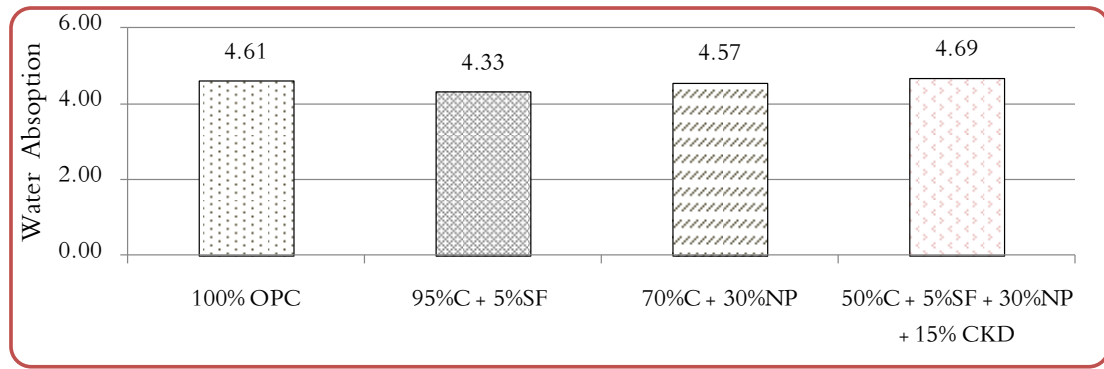


Figure 4-57: Water Absorption of QCC specimens with 15% CKD after 28 days of curing.

The water absorption in quaternary cement concrete specimens replacing 50% cement with 5% silica fume (SF), 25% natural pozzolan (NP) and 20% clay (Clay) and the three control mixes is plotted in Figure 4.58. Incorporation of silica fume (SF) in plain cement concrete decreased the water absorption while in the other mixes, the water absorption increased with the cement replacement level. The water absorption of the QCC specimens was the highest. After 28 days of curing, the water absorption of plain, 95% OPC with 5% SF, 75% OPC with 25% NP and 50% OPC with 5% SF + 25% NP + 20% Clay was 4.61, 4.33, 4.54 and 4.68%, respectively.

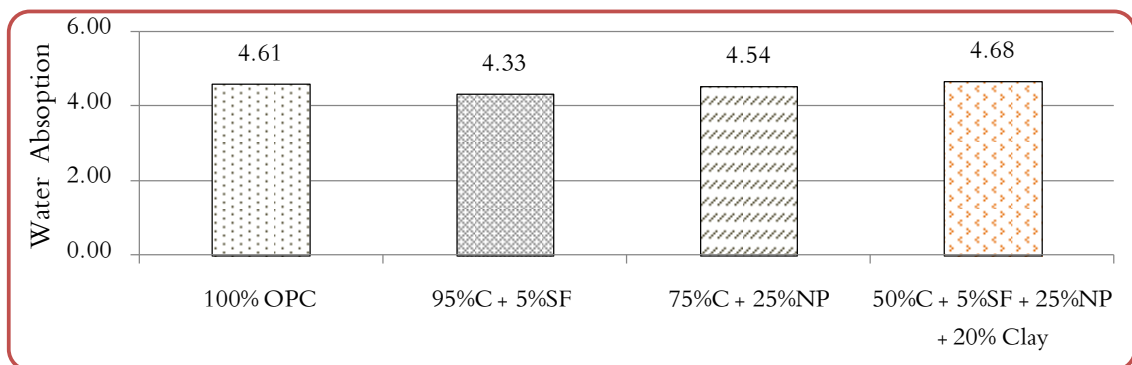


Figure 4-58: Water Absorption of QCC specimens with 20% Clay after 28 days of curing.

The water absorption in quaternary cement concrete specimens replacing 50% cement with 5% silica fume (SF), 25% natural pozzolan (NP) and 20% lime stone powder (LSP) and the three control mixes is plotted in Figure 4.59. Incorporation of silica fume (SF) in plain cement concrete decreased the water absorption while in the other mixes, the water absorption increased with the cement replacement level. The water absorption of the QCC specimens was the highest. After 28 days of curing, the water absorption of plain, 95% OPC with 5% SF, 75% OPC with 25% NP and 50% OPC with 5% SF + 25% NP + 20% C was 4.61, 4.33, 4.54 and 4.70%, respectively.

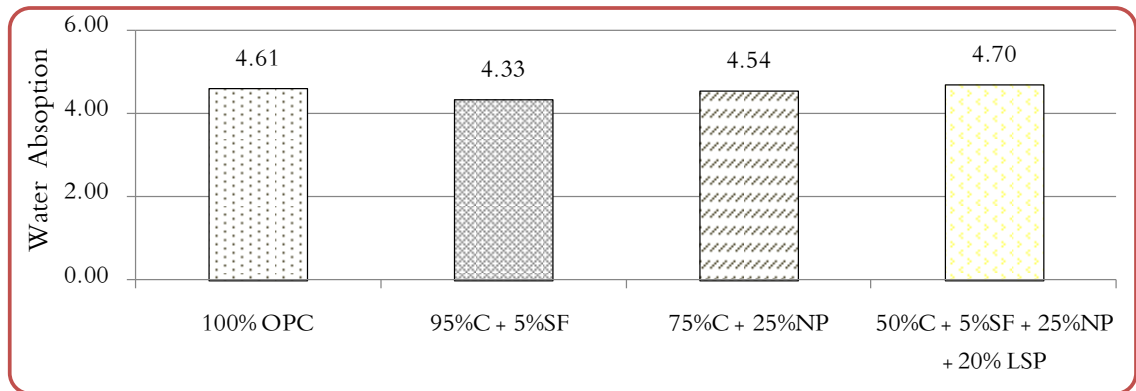


Figure 4-59: Water Absorption of QCC specimens with 20% LSP after 28 days of curing.

The water absorption in quaternary cement concrete specimens replacing 50% cement with 5% silica fume (SF), 25% natural pozzolan (NP) and 20% pulverized steel slag (PSS) and the three control mixes is plotted in Figure 4.60. Incorporation of silica fume (SF) in plain cement concrete decreased the water absorption while in the other mixes, the

water absorption increased with the cement replacement level. The water absorption of the QCC specimen was the highest. After 28 days of curing, the water absorption of plain, 95% OPC with 5% SF, 75% OPC with 25% NP and 50% OPC with 5% SF + 25% NP + 20% C was 4.61, 4.33, 4.54 and 4.79%, respectively.

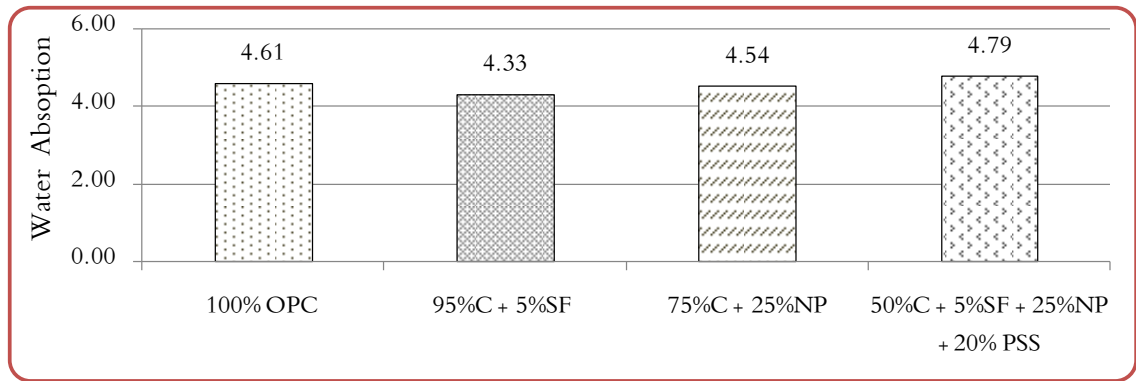


Figure 4-60: Water Absorption of QCC specimens with 20% PSS after 28 days of curing.

## 4.7 Setting Time

The initial and final setting time of quaternary cement concrete specimens is presented in Tables 4.16 through 4.17. The results have been grouped into two categories:

- (i) QCC specimens produced by replacing 50% cement with 5% silica fume, 25–30% fly ash and 15–20% by a locally available material (BHD, CKD, Clay, LSP or PSS) i.e. Mix 7, 8, 9, 10 and 11; (ii) QCC specimens produced by replacing 50% cement with 5% silica fume, 25–30% natural pozzolan and 15–20% by a local material (BHD, CKD, Clay, LSP or PSS), i.e. Mix 12, 13, 14, 15 and 16.



Table 4-16: Setting Time of Group-I QCC mixes.

Mix	50%C + 5%SF + 30%FA + 15%BHD	50%C + 5%SF + 30%FA + 15%CKD	50%C + 5%SF + 25%FA + 20%Clay	50%C + 5%SF + 25%FA + 20%LSP	50%C + 5%SF + 25%FA + 20%PSS
Initial setting	3 hrs 32 mins	2 hrs 57 mins	3 hrs 16 mins	2 hrs 43 mins	3 hrs 4 mins
Final setting	5 hr 17 mins	4 hrs 21 mins	4 hrs 49 mins	4 hrs 1 min	4 hrs 36 mins

Table 4-17: Setting Time of Group-II QCC mixes.

MIX	50%C + 5%SF + 30%NP + 15%BHD	50%C + 5%SF + 30%NP + 15%CKD	50%C + 5%SF + 25%NP + 20%Clay	50%C + 5%SF + 25%NP + 20%LSP	50%C + 5%SF + 25%NP + 20%PSS
Initial setting	3 hrs 51 mins	3 hrs 10 mins	3 hrs 28 mins	3 hrs 5 mins	3 hrs 17 mins
Final setting	5 hr 55mins	4 hrs 42 mins	5 hrs 19 mins	4 hrs 25 min	4 hrs 58 mins

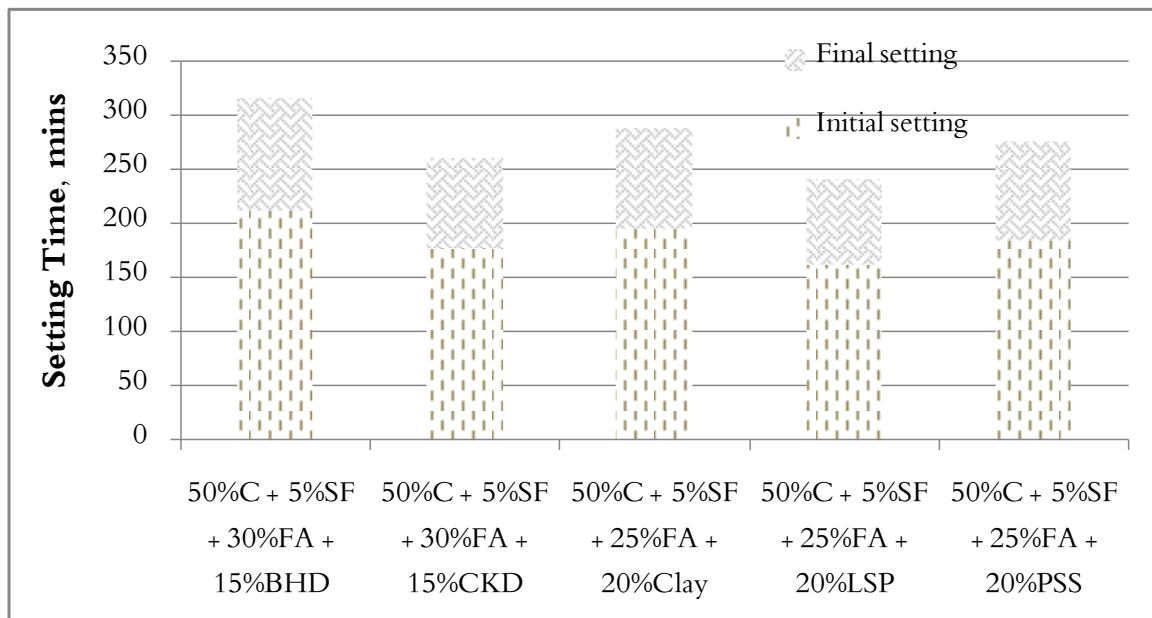


Figure 4-61: Setting Time of Group-I QCC specimens.

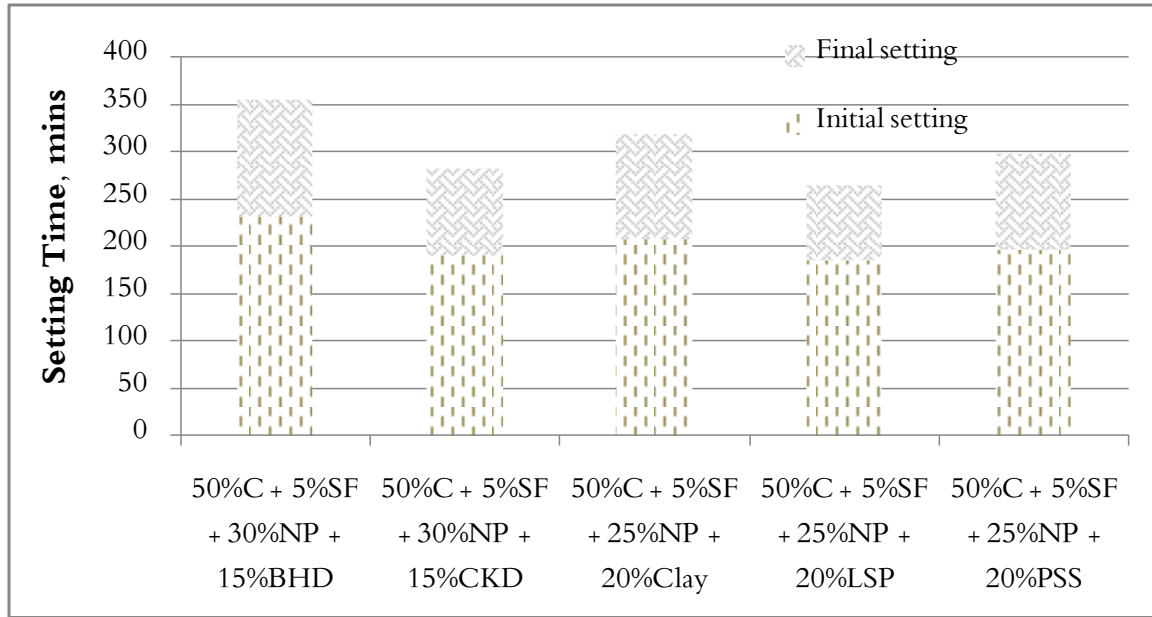


Figure 4-62: Setting Time of Group-I QCC specimens.

The initial and final setting times of all the QCCs were within the ASTM C150 limits.

## CHAPTER 5

# CONCLUSIONS AND RECOMMENDATIONS

### 5.1 Conclusions

This research was conducted to assess the mechanical properties and durability of Quaternary Cement Concrete (QCC) produced by replacing 50% cement with 30–35% supplementary cementing materials (FA, NP or SF) and 15–20% of the selected local material (BHD, CKD, Clay, LSP or PSS). The following conclusions can be drawn based on the data developed in this study:

- The compressive strength of QCC was generally less than that of OPC and binary cement concretes. However, the strength values were around 40 MPa.
- The water absorption in the QCC was comparable with the OPC and binary cement concretes.

- The drying shrinkage of some of the QCC specimen was more than that of OPC and binary cement concretes. However, the shrinkage in all the QCC specimens at seven days was less than 500  $\mu\text{m}$ .
- Drying shrinkage of QCC with NP and Clay/CKD/LSP was less than that of SF concrete and OPC.
- The setting time of QCC met the ASTM C 150 criteria.
- The chloride permeability of QCC specimens was generally less than that of OPC.
- The time to corrosion initiation in the QCC was generally the same or more than that of OPC and binary cement concretes.
- The corrosion current density on steel in most of the QCC specimens was less than that on steel in the OPC specimens.

## 5.2 Recommendations

The avenues for usage of QCC are summarized in the following tables.

QCC	$f_c'$ (MPa)	$I_{corr}$ ( $\mu\text{A}/\text{cm}^2$ )	Applications
50%C + 5%SF + 30%FA + 15%BHD	33.34	0.17	Medium strength structural concrete with high durability requirements.
50%C + 5%SF + 30%FA + 15%CKD	44.77	0.30	High strength structural concrete with moderate durability requirements.
50%C + 5%SF + 25%FA + 20%Clay	42.00	0.10	High strength structural concrete with high durability requirements.
50%C + 5%SF + 25%FA + 20%LSP	42.55	0.24	High strength structural concrete with high durability requirements.
50%C + 5%SF + 25%FA + 20%PSS	38.03	0.19	Medium strength structural concrete with high durability requirements.

50%C + 5%SF + 30%NP + 15%BHD	36.62	0.229	Medium strength structural concrete with moderate durability requirements.
50%C + 5%SF + 30%NP + 15%CKD	40.89	0.277	Medium strength structural concrete with moderate durability requirements.
50%C + 5%SF + 25%NP + 20%Clay	38.78	0.196	Medium strength structural concrete with high durability requirements.
50%C + 5%SF + 25%NP + 20%LSP	36.69	0.322	Medium strength structural concrete with moderate durability requirements.
50%C + 5%SF + 25%NP + 20%PSS	36.69	0.313	Medium strength structural concrete with moderate durability requirements.

## REFERENCES

1. Mehta, P.K. and P.J.M. Monteiro, *Concrete: structure, properties, and materials*. 1993: Prentice Hall.
2. Wang, C.K.S., C.G., *Reinforcement Concrete Design*. Sixth Edition. ed. 1998
3. Program, S.H.R., *Concrete and Structures: Progress and Products Update*. 1989: National Research Council, Strategic Highway Research Program.
4. Skalny, J.P., *Concrete Durability: An Issue of National Importance*. ACI, Detroit, 1987. **Special Publication-100**: p. 265-279.
5. R.K. Dhir, M.R.J., E.A. Byars, I.G. Shaabun, *Predicting Concrete Durability From its Absorption*. V.M. Malhotra (Ed.), *Durability of Concrete*, CANMET/ACI, ACI 1994. **Special Publication-145**.
6. Wallbank, E.J., *The performance of concrete in bridges: a survey of 200 highway bridges*. 1989, Great Britain. : H.M.S.O.
7. Al-Gahtani, A.S., *An Investigation of Corrosion of Reinforcement in Concrete in the Eastern Province of Saudi Arabia*. 1981, King Fahd University of Petroleum and Minerals, Dhahran.
8. Almusallam, A.A., Maslehuddin, M., Waris, A., Dakhil, F. H. and Al-Amoudi, O. S. B., *Plastic shrinkage cracking of blended cements in hot weather*. Magazine of Concrete Research, August 1999. **51**(4): p. pp. 241-246.
9. Maslehuddin, M., Saricimen, H., Al-Mana, A. I., and Shamim, M., *Performance of Concrete in A High Chloride-Sulfate Environment*. ACI, 1990. **Special Publication-122**: p. 469-494.
10. Maslehuddin, M., Rasheeduzzafar, Page, C. L. Al-Mana, A. I., *Influence of Some Parameters Relevant to Arabian Gulf Environment on Reinforcement Corrosion*. Arabian Journal for Science and Engineering: Theme Issue on Corrosion and its Prevention, April 1995: p. 239-257.
11. Rasheeduzzafar, A.-M., A. I., Haneef, M., and Maslehuddin, M., *Effect of Cement Replacement, Content and Type on the Durability Performance of Fly Ash Concrete in the Middle East*. ASTM Journal of Cement, Concrete, and Aggregates, Winter 1986: p. 86-96.
12. Maslehuddin, M., Saricimen, H., and Al-Mana, A. I., *Effect of Fly Ash Addition on the Corrosion Resisting Characteristics of Concrete*. ACI Materials Journal, January-February, 1987: p. 42-51.
13. Maslehuddin, M., Al-Mana, A. I., Shamim, M., and Saricimen, H., *Effect of Sand Replacement on the Early Age Strength Gain and Long-term Corrosion-Resisting Characteristics of Fly Ash Concrete*. ACI Materials Journal, January-February 1989: p. 58-62.

14. Almusallam, A.A., Waris, M. A., Maslehuddin, M. and Al-Gahtani, A. S., *Placing and shrinkage at extreme temperatures*. Concrete International, January 1999: p. 75-79.
15. Almusallam, A.A., Maslehuddin, M., Waris, M. A., Al-Amoudi, O. S. B. and Al-Gahtani, A. S., *Plastic shrinkage of concrete in hot and arid environments*. The Arabian Journal for Science and Engineering, Theme issue on Concrete Repair, Rehabilitation and Protection, December 1998. **23**(2C): p. 57-72.
16. Al-Amoudi, O.S.B., Maslehuddin, M., and Abiola, T. O., *Effect of type and dosage of silica fume on plastic shrinkage of concrete exposed to hot weather*. Construction and Building Materials, 2004. **18**(1): p. 737-743.
17. Administration, U.S.E.I., *Emission of Greenhouse Gases Report*. December 2009., U.S. Department of Energy.
18. Thomas, C.S., *Some Economics of Global Warming*. The American Economic Review, March 1992. **82**( 1): p. 1-14.
19. Development, W.B.C.f.S., *The Cement Sustainability Initiative: Progress Report*. June 2002, Switzerland.
20. Mahasen, N., Smith, S., and Humphreys, K., *The Cement Industry and Global Climate Change: Current and Potential Future Cement Industry CO<sub>2</sub> Emissions*, in *Greenhouse Gas Control Technologies - 6th International Conference*. 2003. p. 995–1000.
21. Taylor, H., *Cement chemistry*. 2nd ed. Thomas Telford. 2000: p. 289–90.
22. *European Construction in Service of Society ECOserve NETWORK. Cluster 2: production and application of blended cements*.
23. Lynsdale, C.J.a.K., I. M. *Chloride and oxygen permeability of concrete incorporating fly ash and silica fume in ternary systems*. in *Proceedings 5th CANMET/ACI International Conference on Durability of Concrete*. 2000. Barcelona.
24. Malolepszy, J.a.P., Z. *Effect of metakaolin on strength and chemical resistance of cement mortars*. in *Proceedings 5th CANMET/ACI International Conference on Durability of Concrete*. 2000. Barcelona.
25. Dehwah, H.A.F., Maslehuddin, M., Al-Amoudi, O. S. B., *Evaluation of Ternary Cements for Improving Concrete Durability in the Arabian Gulf - Final Report, submitted to Deanship of Scientific Research*. April 2009, King Fahd University Of Petroleum & Minerals.
26. Dehwah, H.A.F., Maslehuddin, M, Al-Amoudi, O. S. B. and Azhar, M. , *Mechanical Properties and Shrinkage Characteristics of Ternary Cement Concretes*.
27. Maslehuddin, M., Dehwah, H. A. F., Al-Amoudi, O. S. B., Shameem, M. and Azhar, M., *Sulfate Resistance and Permeability Characteristics of Ternary Cement Concretes*.
28. Al-Amoudi, O.S.B., Dehwah, H. A. F., Maslehuddin, M. and Azhar, M., *Corrosion Resistance of Ternary Cement Concretes*, King Fahd University of Petroleum and Minerals, Dhahran.
29. Menéndez, G., V. Bonavetti, and E.F. Irassar, *Strength development of ternary blended cement with limestone filler and blast-furnace slag*. Cement and Concrete Composites, 2003. **25**(1): p. 61-67.

30. Malhotra, V.M.E. *Fly Ash, Silica Fume, Slag, and Natural Pozzolans in Concrete*. in *Proceedings 2nd International Conference*, ACI SP 91, . 1986.
31. Malhotra, V.M.E. *Fly Ash, Silica Fume, Slag, and Natural Pozzolans in Concrete*. in *Proceedings, 3rd International Conference*, ACI SP 114. 1989. Trondheim, Norway.
32. Sivasundaram, V., Bouzoubaa, N., Bilodeau, A., Fournier, B., and Golden, D. M *Development of Ternary Blends for High-Performance Concrete*. ACI Materials Journal, January-February 2004. **101**: p. 19-29.
33. Jones, M.R., R.K. Dhir, and B.J. Magee, *Concrete containing ternary blended binders: Resistance to chloride ingress and carbonation*. Cement and Concrete Research, 1997. **27**(6): p. 825-831.
34. Hogan, F.J., *EFFECT OF BLAST FURNACE SLAG CEMENT ON ALKALI AGGREGATE REACTIVITY: A LITERATURE REVIEW*. Cement, Concrete and Aggregates, 1985. **7**(2): p. 100-107.
35. Thomas, D.A. and B.R. Establishment, *Review of the Effect of Fly Ash and Slag on Alkali-aggregate Reaction in Concrete*. 1996: Building Research Establishment.
36. Thomas, M.D.A., *Field Studies of Fly Ash Concrete Structures Containing Reactive Aggregate*. Magazine of Concrete Research, December 1996. **48**(177): p. 265-279.
37. Mehta, P.K., *Pozzolan and Cementitious Byproducts in Concrete- Another Look*. ACI 1989. **1**(Special Publication-114): p. 1-43.
38. Thomas, M.D.A., and Bleszynski, R. F., *The Use of Silica Fume to Control Expansion due to Alkali-Aggregate Reactivity in Concrete, A Review*. Material Science of Concrete (Ed J. Skanly and S. Mindess), 2000. **6**, **American Ceramics Society**.
39. Boddy, A.M., R.D. Hooton, and M.D.A. Thomas, *The effect of product form of silica fume on its ability to control alkali-silica reaction*. Cement and Concrete Research, 2000. **30**(7): p. 1139-1150.
40. Hooton, R.D., Bleszynski, R. F., and Boddy, A., *Issues Related to Silica Fume Dispersion in Concrete*. Materials Science of Concrete: The Sidney Diamond Symposium (Ed. M. Cohen, S. Mindess, J. Skanly), 1998: p. 435-446.
41. Najimi, M., Jamshidi, M., and Pourkhorshidi, A., *Durability of Concrete Containing Natural Pozzolan*. Proceedings of the Institution of Civil Engineers: Construction Materials, 2008. **161**(3): p. 113-118.
42. de Souza, C.A.C., Machado, A. T., Lima, L. R. P. A., Cardoso, R. J. C., *Stabilization of electric-arc furnace dust in concrete*. Materials Research, 2010. **13**: p. 513-519.
43. Maslehuddin, M., et al., *Properties of cement kiln dust concrete*. Construction and Building Materials, 2009. **23**(6): p. 2357-2361.
44. Dhir, R.K., Limbachiya, M. C., McCarthy, M. J., Chaipanich, A., *Evaluation of Portland Limestone Cements for Use in Concrete Construction*. Materials and Structures, 2007. **40**: p. 459-473.
45. Nehdi, M., *Ternary and Quaternary Cements for Sustainable Development*. Concrete International, 2001. **23**(No. 4): p. 34-42.



46. Thomas, M.D.A., Shehata, M. H., Shashiprakash, S. G., Hopkins, D. S., Cail, K., *Use of ternary cementitious systems containing silica fume and fly ash in concrete*. Cement and Concrete Research, 1999. **29**(8): p. 1207-1214.
47. Berry, E.E., *Strength development of some blended-cement mortars*. Cement and Concrete Research, 1980. **10**(1): p. 1-11.
48. Butler, W.B. *Durable Concrete Containing Three or Four Cementitious Materials*. in *Durability of Concrete, Proceedings, 4th CANMET/ACI International Conference*. 1997. Farmington Hills, Mich.: ACI, Special Publication-170, 2 : p. 309-330.
49. Popovics, S., *Portland cement-fly ash-silica fume systems in concrete*. Advanced Cement Based Materials, 1993. **1**(2): p. 83-91.
50. Bleszynski, R., *The Performance and Durability of Concrete with Ternary Blends of Silica Fume and Blast-furnace Slag [microform]*. 2003: University of Toronto, 2002.
51. Khatri, R.P., Gross, W., Baweja, D., and Stivivalnanon, V., *Performance Concretes for Coastal and Offshore Structures*, in *Concrete 95 Conference*. 1995: Brisbane, Australia.
52. Wang, S.S.a.K., *Development of "Green" Cement for Sustainable Concrete Using Cement Kiln Dust and Fly Ash*. International Workshop on Sustainable Development and Concrete Technology.
53. M.Maslehuddin, F.R.A., M.Shameem, M.Ibrahim, M.R.Ali, *"Effect of Electric Arc Furnace Dust on the Properties of OPC and Blended Cement Concretes*. Construction and Building Materials, 2011. **25**: p. 308–312.
54. Maage, M., *Service Life Prediction of Existing Concrete Structures Exposed to Marine Environments*. ACI Materials Journal, November/December, 1996: p. 603-608.
55. Carette, G.G., and Malhotra, V. M., *Mechanical Properties, Durability, and Drying Shrinkage of Portland Cement Concrete Incorporating Silica Fume*. Cement, Concrete, and Aggregate, 1983. **Vol. 5**(No. 1): p. 3-13.
56. Mehta, P.K., *Durability of Concrete in Marine Environment: A Review, Performance of Concrete in Marine Environment*. ACI Publication, 1986. **Special Publication-65**: p. 125-147.
57. Marzouk, H.M., and Hussein, A., *Properties of High-Strength Concrete at Low Temperatures*. ACI Materials Journal, 1990. **Vol. 87**(No. 2): p. 167-171.
58. Ballbaki, M., Sarker, S. L., Aitcin, P. C., *Properties and Microstructure of the HPC Containing Silica Fume, Slag, and Fly Ash*. ACI, Deteroit, 1992. **Special Publication-132**: p. 921-941.
59. Ozyildirim, C., *Durability of Concrete Bridges in Virginia*. ASCE Structures Congress XI Proceedings: Structural Engineering in Natural Hazards Mitigation, 1993: p. 996-1001.
60. M. Nehdi , M. Pardhanb, and S. Koshowskic, *Durability of self-consolidating concrete incorporating high-volume replacement composite cements*. Cement and Concrete Research, 2004. **34**.
61. Mehmet Gesoglu and E. Ozbay, *Effects of mineral admixtures on fresh and hardened properties of self-compacting concretes: binary, ternary and quaternary systems*. Materials and Structures, 2007. **40**: p. 923-937.

62. Mullick, A.K., *Performance of concrete with binary and ternary cement blends*. The Indian Concrete Journal, 2007.
63. Mehmet Gesoglu , Erhan Güneyisia, and E. Özbay, *Properties of self-compacting concretes made with binary, ternary, and quaternary cementitious blends of fly ash, blast furnace slag, and silica fume*. Construction and Building Materials 2009. **23**: p. 1847–1854.
64. P. Pipilikaki and M. Katsioti, *Study of the hydration process of quaternary blended cements and durability of the produced mortars and concretes*. Construction and Building Materials 2009. **23**: p. 2246–2250.
65. Ghrici, M., et al., *Some Engineering Properties of Concrete Containing Natural Pozzolana and Silica Fume*. Journal of Asian Architecture and Building Engineering, 2006. **5**(2): p. 349-354.
66. Bágel, L., *Strength and pore structure of ternary blended cement mortars containing blast furnace slag and silica fume*. Cement and Concrete Research, 1998. **28**(7): p. 1011-1022.
67. Lane, D.S. and C. Ozyildirim, *Preventive measures for alkali-silica reactions (binary and ternary systems)*. Cement and Concrete Research, 1999. **29**(8): p. 1281-1288.
68. Alexander, M.G., Streicher, P. E., *A Chloride Conduction in Silica Fume, Fly Ash and Blast-Furnace Concrete*. 1994: p. 752-764.
69. Wu, S., Naik, Tarun, R., *Chemically Activated Blended Cements*. ACI Materials Journal, September/October, 2003. **Vol. 100**(No. 5): p. 434-440.
70. Laldji, S.T.-H., Arezki *Properties of Ternary and Quaternary Concrete Incorporating New Alternative Cementitious Material*. ACI Materials Journal 2006. **103**(2): p. 83-89.
71. Laldji, S., Tagnit, H. A., *Properties of Ternary and Quaternary Concrete Incorporating New Alternative Cementitious Material*. ACI Materials Journal 2006. **103**(2): p. 83-89.
72. ASTM C 39, *"Standard Test Method for Compressive Strength of Cylindrical Concrete Specimens"*. Annual Book of ASTM Standards, Vol. 4.02, American Society for Testing and Materials, Philadelphia, 2005.
73. ASTM C 157, *"Standard Test Method for Length Change of Hardened Hydraulic-Cement Mortar and Concrete"* Annual Book of ASTM Standards, Vol. 4.02, American Society for Testing and Materials, West Conshohocken, 2005.
74. ASTM C 876, *"Standard Test Method for Half-cell Potentials of Uncoated Reinforcing Steel in Concrete"*. Annual Book of ASTM Standards, Vol. 4.02, American Society for Testing and Materials, West Conshohocken, 2005.
75. Stern, M. and A.L. Geary, *A Theoretical Analysis of the Slope of the Polarization Curves*. Journal of Electrochemical Society, 1957. **104**: p. 56.
76. ASTM C 191, *Standard Test Method for the Time of Setting of Hydraulic Cement by Vicat Needle*. Annual Book of ASTM Standards, 2005. **4.02**.
77. ASTM C 642, *Standard Test Method for Density, Absorption, and Voids in Hardened Concrete*. Annual Book of ASTM Standards, 2005. **4.02**.

# VITAE

## PERSONAL INFORMATION

Name : **Mohammed Khaja Moinuddin**  
Nationality : Indian  
Professional experience: **3 years**  
Languages known : Arabic, English, Hindi, Telugu, Urdu...  
E: mail address : [mkmoin@kfupm.edu.sa](mailto:mkmoin@kfupm.edu.sa)  
[mk\\_moin111@yahoo.com](mailto:mk_moin111@yahoo.com)  
Permanent address : 17-3A-278, SRT Colony, Yakuthpura  
Hyderabad, Andhra Pradesh, India  
Contact no : 0091-9032699689/9848591616  
Present address : Bldg-803/306, KFUPM, Dharan, KSA  
Contact no : 00966-533181693

## QUALIFICATIONS

Education : **MS Civil (Structures)**  
KFUPM (Saudi Arabia)  
**BE (Civil Engineering)**  
Osmania University (India)  
**Diploma (AutoCAD, STAAD.Pro)**  
Creative CADD Inc. (India)  
Softwares : ANSYS, AutoCAD, Fluent, Gambit,  
Primavera, STAAD.Pro.

Member of **ACI**

## EXPERIENCE

**Company** : **King Fahd University of Petroleum and Minerals**  
**Designation** : Research Assistant  
**Duration** : From Feb. 2010 to till date  
**Place** : Al-Dhahran, KSA  
**Company** : **SBF Engineering**  
**Designation** : Structural Engineer  
**Duration** : From June 2009 to Jan. 2010  
**Place** : Hyderabad, India